AD-766 494

# FUSED SILICA DESIGN MANUAL

VOLUME 1

GEORGIA INSTITUTE OF TECHNOLOGY

PREPARED FOR

NAVAL ORDNANCE SYSTEMS COMMAND

MAY 1973

DISTRIBUTED BY:

NTIS

National Technical Information Service
U. S. DEPARTMENT OF COMMERCE

AD 766494

# FUSED SILICA DESIGN MANUAL

## VOLUME I

May 1973

By

J. N. Harris
E. A. Welsh

Prepared under Contract N00017-72-C-4434

For

Naval Ordance Systems Command
Weapon Dynamics Division (Code ORD-035)
Department of the Navy

D D C
SEP 14 1973
E

By

Engineering Experiment Station
Georgia Institute of Technology
Atlanta, Georgia 30332

Reproduced by
NATIONAL TECHNICAL
INFORMATION SERVICE
US Department of Commerce
Springfield, VA. 22151

Approved for public release; distribution unlimited

151

Unclassified

Security Classification

## DOCUMENT CONTROL DATA - R & D

*Security classification of title, body of abstract and indexing annotation must be entered when the overall report is classified)*

1. ORIGINATING ACTIVITY (Corporate author)

Engineering Experiment Station
Georgia Institute of Technology
Atlanta, Georgia 30332

2a. REPORT SECURITY CLASSIFICATION

Unclassified

2b. GROUP

3. REPORT TITLE

FUSED SILICA DESIGN MANUAL, Volume I

4. DESCRIPTIVE NOTES (Type of report and inclusive dates)

5. AUTHOR(S) (First name, middle initial, last name)

Joe N. Harris, and Earle A. Welsh

6. REPORT DATE

May 1973

7a. TOTAL NO. OF PAGES

140

7b. NO. OF REFS

58

8a. CONTRACT OR GRANT NO.

N00017-72-C-4434

b. PROJECT NO.

c.

d.

9a. ORIGINATOR'S REPORT NUMBER(S)

Technical Report A-1403

9b. OTHER REPORT NO(S) (Any other numbers that may be assigned this report)

10. DISTRIBUTION STATEMENT

Approved for public release; distribution unlimited.

11. SUPPLEMENTARY NOTES

12. SPONSORING MILITARY ACTIVITY

Department of the Navy
Naval Ordnance Systems Command
Weapon Dynamics Division (ORD-035)
Washington, D. C. 20360

13. ABSTRACT

This manual provides a summary of the current status of the knowledge of designing radomes of slip-cast fused silica. It is intended to provide scientists and engineers designing and fabricating radomes and associated hardware a basic knowledge of the material and processing techniques as well as basic design information. Pages, figures, and tables have been numbered by chapters so that the manual can be easily expanded as additional information is developed. Subjects covered in this manual are: fused silica raw material preparation, size reduction and slip preparation, slip casting, drying and firing, room temperature and elevated temperature properties.

DD FORM 1 NOV 65 1473 (PAGE 1)

S/N 0101-807-6801



Unclassified

Security Classification

Unclassified

Security Classification

| 14 KEY WORDS | LINK A ROLE | LINK A WT | LINK B ROLE | LINK B WT | LINK C ROLE | LINK C WT |
|---|---|---|---|---|---|---|
| Fused Silica, Vitreous | | | | | | |
| Fused Silica, Slip-Cast | | | | | | |
| Slip Production | | | | | | |
| Slip Casting | | | | | | |
| Slip-Cast Fused Silica Processing | | | | | | |
| Fused Silica Properties | | | | | | |

DD FORM 1 NOV 65 1473 (BACK)

(PAGE 2)

ia

Unclassified

Security Classification

# FUSED SILICA DESIGN MANUAL
## VOLUME I

May 1973

By

J. N. Harris
E. A. Welsh

Prepared under Contract N00017-72-C-4434

For

Naval Ordnance Systems Command
Weapon Dynamics Division (Code ORD-035)
Department of the Navy

By

Engineering Experiment Station
Georgia Institute of Technology
Atlanta, Georgia 30332

Approved for public release; distribution unlimited.

## FOREWORD

The process of slip casting fused silica has been under development at Georgia Tech since 1956. Soon after the initial work with slip cast fused silica it was noted that this material exhibited a number of the desirable properties of transparent fused silica, such as a very low coefficient of thermal expansion and a dielectric constant and loss tangent which changed very little with changes in temperature and frequency. Other properties were considerably different such as opaqueness to radiation and lower thermal conductivity and dielectric constant than the transparent material. In addition, the slip casting process allowed the formation of large and intricate shapes which would be prohibitively expensive, if not impossible, using the conventional molten fused silica techniques.

Early in the work with this material it became apparent that slip-cast fused silica should be an ideal material for such hypersonic aerospace applications as radomes, EM windows and leading edges. In 1964 Georgia Tech published two handbooks: "Fused Silica Manual" by J. D. Fleming and "Slip-Cast Fused Silica" by J. D. Walton, Jr., and N. E. Poulos. The "Fused Silica Manual" was a compilation of available property data on transparent fused silica and slip-cast fused silica. "Slip-Cast Fused Silica" was primarily concerned with the fabrication, properties and environmental evaluation of slip-cast fused silica materials.

Since 1964 the quality control of commercially available fused silica slips has been considerably improved and a higher purity raw material has been used to make a far superior fused silica slip. For identification, the two available types of fused silica slip are referred to in this manual as (1) technical grade, and (2) high purity.

In addition to the improvement in fused silica slips since 1964, a considerable amount of work has been accomplished in developing design procedures. These procedures include mechanical, electrical, and thermal design and the design of attachment systems for radomes. Although the data presented in this manual can be used for general design purposes, they are collected and presented in such a way as to be of maximum value to the radome designer. This manual is prepared with the intent of providing the designer or engineer with the data and background necessary to specify the fused silica raw materials and the fabrication of the raw material into finished hardware, to design the radome and attachment system, and to qualify the finished radome for environmental or flight testing.

This manual has been divided into two volumes. Volume I describes the fused silica raw material, its processing into slip, the fabrication of hardware, including casting, drying and sintering, and the physical and mechanical properties of slip-cast material. The data in this volume can be of assistance in designing any item to be fabricated from slip-cast fused silica and is not limited to the design of radomes or other military hardware. Volume II provides information specifically for the design of radomes and attachments and data on rain erosion testing and rain erosion resistance of slip-cast fused silica. This volume is intended primarily for those interested in the design of radomes only.

VOLUME I

## ABSTRACT

This volume provides a summary of the current status of the knowledge of designing slip-cast fused silica hardware. It is intended to provide the user with a basic knowledge of the material and processing techniques as well as basic design information. Pages, figures and tables have been numbered by chapters so that the manual can be easily expanded as additional information is developed. Subjects covered in this volume are: fused silica raw material preparation, size reduction and slip preparation, slip casting, drying and firing and room temperature and elevated temperature properties.

TABLE OF CONTENTS


Page

CHAPTER I. INTRODUCTION. . . . . 1-1

1.1 Background. . . . . 1-1

1.2 Radome Materials. . . . . 1-4

1.2.1 Dielectric Properties . . . . . 1-5

1.2.2 Weight . . . . . 1-5

1.2.3 Thermal-Mechanical Response. . . . . 1-8

1.2.4 Thermal Shock . . . . . 1-9

1.2.5 Rain Erosion . . . . . 1-9

1.3 General Comparison of Slip-Cast Fused Silica Properties With Other Materials . . . . . 1-10

1.4 References for Chapter I. . . . . 1-13

CHAPTER II. RAW MATERIAL AND FUSED SILICA SLIP . . . . . 2-1

2.1 Raw Material. . . . . 2-1

2.2 Slip Production . . . . . 2-3

2.3 Properties of Fused Silica Casting Slips. . . . . 2-8

2.3.1 Chemical Analyses. . . . . 2-10

2.3.2 Physical/Chemical Properties . . . . . 2-13

2.3.3 Particle Size and Distribution . . . . . 2-13

2.4 Fused Silica Slip Specification . . . . . 2-13

2.5 Slip Storage and Handling . . . . . 2-17

2.6 Slip Aging . . . . . 2-17

2.6 References for Chapter II . . . . . 2-18

CHAPTER III. FABRICATION & PROCESSING . . . . . 3-1

3.1 Introduction . . . . . 3-1

3.2 Mold Fabrication . . . . . 3-1


(Continued)

Preceding page blank

TABLE OF CONTENTS (Continued)


Page

3.2.1 Master Model Preparation . . . . . 3-1

3.2.2 Mold Design . . . . . 3-2

3.2.3 Mold Preparation . . . . . 3-3

3.3 Slip Casting Fused Silica Parts . . . . . 3-5

3.3.1 Casting Rate . . . . . 3-5

3.3.2 Slip Casting . . . . . 3-9

3.4 Drying . . . . . 3-12

3.5 Sintering . . . . . 3-15

3.5.1 Effect of Chemical Purity on Sintering . . . . . 3-19

3.5.2 Effect of Time and Temperature on Sintering . . . . . 3-23

3.5.3 Effects of Atmosphere . . . . . 3-26

3.5.4 Effect of Particle Size on Sintering . . . . . 3-26

3.5.5 Selection of Sintering Conditions . . . . . 3-31

3.6 Machining of Slip-Cast Fused Silica . . . . . 3-46

3.7 Sealing of Blanks . . . . . 3-47

3.8 Other Forms of Fused Silica . . . . . 3-48

3.8.1 Glass Worked Fused Silica . . . . . 3-48

3.8.2 Fused Silica Foam . . . . . 3-49

3.9 References for Chapter III . . . . . 3-50

CHAPTER IV. SLIP-CAST FUSED SILICA PROPERTIES . . . . . 4-1

4.1 Introduction . . . . . 4-1

4.2 Mechanical Properties . . . . . 4-2

4.2.1 Room Temperature Properties . . . . . 4-2


(Continued)

TABLE OF CONTENTS (Concluded)


| | Page |
|---|---|
| 4.2.2 Elevated Temperature Properties | 4-12 |
| 4.3 Physical Properties | 4-20 |
| 4.3.1 Thermal Expansion | 4-20 |
| 4.3.2 Viscosity | 4-23 |
| 4.3.3 Thermal Conductivity | 4-23 |
| 4.3.4 Heat Capacity | 4-38 |
| 4.3.5 Enthalpy | 4-39 |
| 4.3.6 Thermal Diffusivity | 4-42 |
| 4.4 Electrical Properties | 4-42 |
| 4.4.1 Resistivity | 4-42 |
| 4.4.2 Dielectric Constant and Loss Tangent | 4-42 |
| 4.5 References for Chapter IV | 4-52 |
| APPENDIX I | A-1-1 |

LIST OF TABLES


Page

1-1. WEIGHT PARAMETER FOR RADOME MATERIALS . . . . . 1-8

1-2. SELECTED PROPERTIES OF FUSED SILICA AND OTHER CANDIDATE CERAMIC RADOME MATERIALS. . . . . 1-11

2-1. TYPICAL SPECTROGRAPHIC ANALYSES OF FUSED SILICA GRAIN FOR SLIP-MANUFACTURE. . . . . 2-2

2-2. SPECTROGRAPHIC ANALYSIS OF TECHNICAL AND HIGH PURITY FUSED SILICA SLIPS. . . . . 2-11

2-3. PROPERTIES OF TECHNICAL AND HIGH PURITY SILICA SLIPS. . . . . 2-13

4-1. SURFACE AND VOLUME EFFECTS ON MODULUS OF RUPTURE OF SLIP-CAST FUSED SILICA . . . . . 4-11

4-2. VOLUME EFFECTS ON TENSILE STRENGTH OF LARGE DIAMETER RINGS. . . 4-14

4-3. CONSTANTS FOR THE DENSITY FUNCTION FOR HIGH PURITY SCPS . . . . 4-34

4-4. CONSTANTS FOR THE THERMAL CONDUCTIVITY FUNCTION . . . . . 4-38

4-5. CONSTANTS FOR THE HEAT CAPACITY FUNCTION. . . . . 4-39

## LIST OF ILLUSTRATIONS


| | | Page |
|---|---|---|
| 1-1 | Viscosity of Fused Silica | 1-3 |
| 1-2 | Dielectric Constant versus Temperature for Candidate Radome Materials | 1-6 |
| 1-3 | Loss Tangent versus Temperature for Candidate Radome Materials | 1-7 |
| 2-1 | Partial Particle Size Distributions for High Purity Fused Silica Slip at Indicated Milling Times | 2-6 |
| 2-2 | Mean Particle Size versus Milling Time for High Purity Fused Silica Slip | 2-7 |
| 2-3 | pH versus Milling Time for High Purity Fused Silica Slip | 2-9 |
| 2-4 | Micrograph of Fused Silica Particles in Fused Silica Slip | 2-14 |
| 2-5 | Particle Size Distributions for Fused Silica Slips | 2-15 |
| 3-1 | Cast Wall Thickness versus Time of Casting for Fused Silica | 3-8 |
| 3-2 | Typical Pressure Casting Setup for Slip Casting Fused Silica Radome | 3-11 |
| 3-3 | Hypothetical Strengthening Processes in Slip-Cast Fused Silica | 3-17 |
| 3-4 | Cristobalite Content versus Sintering Time at 2200° F for Technical Grade and High Purity Slip-Cast Fused Silica | 3-19 |
| 3-5 | Bulk Density versus Sintering Time for High Purity and Technical Grade Fused Silica Slips Sintered at 2100° F, 2250° F, and 2400° F | 3-20 |
| 3-6 | Per Cent Porosity versus Sintering Time for High Purity and Technical Grade Fused Silica Slips Sintered at 2100° F, 2250° F, and 2400° F | 3-21 |
| 3-7 | Modulus of Rupture versus Sintering Time for High Purity and Technical Grade Fused Silica Slips Sintered at 2100° F, 2250° F, and 2400° F | 3-22 |
| 3-8 | Porosity as a Function of Sintering Time and Temperature for High Purity Slip-Cast Fused Silica with 7 Micrometer Mean Particle Diameter | 3-24 |


(Continued)

LIST OF ILLUSTRATIONS (Continued)


Page

3-9 Modulus of Rupture as a Function of Sintering Time and Temperature for High Purity Slip-Cast Fused Silica with 7 Micrometer Mean Particle Diameter. . . . . 3-25

3-10 Bulk Density of Technical Grade Slip-Cast Fused Silica Fired in Different Atmospheres at 2200° F. . . . . 3-27

3-11 Modulus of Rupture of Technical Grade Slip-Cast Fused Silica Fired in Different Atmospheres at 2200° F. . . . . 3-28

3-12 Dynamic Young's Modulus versus Sintering Time for High Purity Slip-Cast Fused Silica, with Mean Particle Diameters of 4, 7, and 17 Micrometers. . . . . 3-29

3-13 Bulk Density versus Sintering Time for High Purity Fused Silica Slips with Mean Particle Diameters of 4 and7 Micrometers Sintered at 2100°, 2250°, and 2400° F. . . . . 3-31

3-14 Per Cent Porosity versus Sintering Time for High Purity Fused Silica Slips with Mean Particle Diameters of 4 and 7 Micrometers Sintered at 2100°, 2250°, and 2400° F. . . . . 3-32

3-15 Modulus of Rupture versus Sintering Time for High Purity Fused Silica Slips with Mean Particle Diameters of 4 and 7 Micrometers Sintered at 2100°, 2250° and 2400° F. . . . . 3-33

3-16 Dynamic Young's Modulus versus Sintering Time for High Purity Slip-Cast Fused Silica Prepared from Slips with Mean Particle Diameters of 4 and 7 Micrometers Sintered at 2100°, 2250°, and 2400° F . . . . . 3-34

3-17 Bulk Density of Technical Grade Slip-Cast Fused Silica Fired in Air at One Atmosphere . . . . . 3-35

3-18 Porosity of Technical Grade Slip-Cast Fused Silica Fired in Air at One Atmosphere . . . . . 3-36

3-19 Modulus of Rupture of Technical Grade Slip-Cast Fused Silica Fired in Air at One Atmosphere . . . . . 3-37

3-20 Transient Heat Conduction in a Radome Initially at Temperature $T_i$, As External Surface is Held at Temperature $T_s$ While Internal Surface is Insulated. . . . . 3-40


(Continued)

LIST OF ILLUSTRATIONS (Continued)


Page

3-21 Transient Heat Conduction in a Cylindrical Test Bar, Initially at Temperature $T_i$, as the Surface is Held at Temperature $T_s$ . . . . . 3-41

3-22 Transient Heat Conduction in a Radome or Cylindrical Test Bar Initially at Temperature $T_i$, as the Surface is Raised to a Temperature $T_f$ at a Constant Rate . . . . . 3-42

4-1 Elastic Modulus versus Density for High Purity and Technical Grade Slip-Cast Fused Silica . . . . . 4-3

4-2 Elastic Modulus with Respect to Density for Slip-Cast Fused Silica from 30 to 139 $lb/ft^3$ . . . . . 4-4

4-3 Modulus of Rupture versus Density for High Purity Slip-Cast Fused Silica . . . . . 4-9

4-4 Modulus of Rupture versus Density for a Technical Grade Slip-Cast Fused Silica . . . . . 4-10

4-5 Compressive Strength of Slip-Cast Fused Silica with Respect to Bulk Density . . . . . 4-13

4-6 Flexural Modulus of Elasticity versus Temperature for Slip-Cast Fused Silica . . . . . 4-16

4-7 Modulus of Rupture versus Temperature for Slip-Cast Fused Silica . . . . . 4-17

4-8 Tensile Strength versus Temperature for Slip-Cast Fused Silica . . . . . 4-18

4-9 Compressive Strength versus Temperature for High Purity and Technical Grade Slip-Cast Fused Silica . . . . . 4-19

4-10 Poisson's Ratio of Slip-Cast Fused Silica . . . . . 4-21

4-11 Expansion Coefficient of Fused Silica . . . . . 4-22

4-12 Thermal Expansion of Slip-Cast Fused Silica Determined in a Graphite Dilatometer . . . . . 4-24

4-13 Variation of Viscosity with Time for Technical Grade Slip-Cast Fused Silica . . . . . 4-25


(Continued)

LIST OF ILLUSTRATIONS (Concluded)

Page

4-14 Variation of Viscosity with Time for High Purity Slip-Cast Fused Silica . . . . . 4-26

4-15 Cristobalite Levels in High Purity and Technical Grade Slip-Cast Fused Silicas after Viscosity Tests . . . . . 4-27

4-16 Thermal Conductivity of Slip-Cast Fused Silica at Various Porosity Levels . . . . . 4-29

4-17 Density of Slip-Cast Fused Silica versus Time at Temperature . . . . . 4-35

4-18 Thermal Conductivity of Slip-Cast Fused Silica . . . . . 4-37

4-19 Heat Capacity of Fused Silica . . . . . 4-40

4-20 Enthalpy of Fused Silica . . . . . 4-41

4-21 Thermal Diffusivity of Slip-Cast Fused Silica and Foamed Fused Silica . . . . . 4-43

4-22 Electrical Resistivity of Fused Silica. . . . . 4-44

4-23 Dielectric Constant of Slip-Cast Fused Silica versus Density Measured at X-Band. . . . . 4-45

4-24 Dielectric Constant of Slip-Cast Fused Silica as a Function of Density . . . . . 4-48

4-25 Dielectric Constant versus Temperature for Slip-Cast Fused Silica at 6 GHz . . . . . 4-49

4-26 Dielectric Constant and Loss Tangent for Fused Silica versus Temperature . . . . . 4-50

4-27 Dielectric Constant and Loss Tangent of High Purity Slip-Cast Fused Silica Measured with Focused Microwave Beam Apparatus . . . . . 4-51

# CHAPTER I

# INTRODUCTION

## 1.1 Background

Silica (silicon dioxide, $SiO_2$) exists in several crystalline forms in nature. The most abundant forms are quartz sand and quartz crystals. Fused silica is an amorphous (non-crystalline) form of silica and is usually prepared by the flame or arc fusion of quartz sand. If a very high purity fused silica product is desired, high purity quartz crystals or synthetic $SiO_2$ are the materials fused.

Another crystalline form of $SiO_2$ which is important to the discussion of fused silica and its properties is cristobalite. Fused silica begins to convert to cristobalite at high temperatures beginning at about 1600° F and continuing to the melting point. The rate of formation of cristobalite is dependent on many factors including the presence of other crystalline forms of $SiO_2$, impurities, atmosphere, time and temperature. Cristobalite exists in two crystalline forms: $\alpha$-cristobalite below about 400 to 500° F and $\beta$-cristobalite above this temperature. The transformation (inversion) from one form to the other is accompanied by a large volume change with resultant stresses developed within the fused silica structure. Hence, if cristobalite is present in excessive amounts the inversion will weaken or completely destroy a fused silica article.

Probably the single most attractive property of fused silica is its high resistance to thermal shock. This resistance is due primarily to its extremely low coefficient of thermal expansion, $0.3 \times 10^{-6}$ in/in/°F. Because of this property, fused silica has long been used in applications where articles are subject to rapid changes in temperature, such as high intensity lamps and

laboratory ware. It has also found use where high dimensional stability is required, in such as telescope mirrors and other precision optical products.

One of the reasons that the use of fused silica has not been more widespread is the difficulty of working it. Fused silica cannot be said to have a true melting point in the sense that there is an abrupt change in viscosity at a certain temperature. Figure 1-1 shows the viscosity of fused silica with respect to temperature from 1400° to 4400° F. ASTM C338 defines the softening point of a glass as a temperature at which a uniform fiber 0.55 to 0.75 mm in diameter and 23.5 mm in length, elongates under its own weight at a rate of 1 mm per minute when the upper 10 cm of its length is heated in a specified furnace at the rate of 5° C per minute. For a glass of the density of fused silica, this temperature corresponds to a viscosity of $10^{7.6}$ poises. Examination of Figure 1-1 shows this to be at a temperature of approximately 3100° F. This is the number normally quoted as the melting point of fused silica. However, to work a glass properly the viscosity must be on the order of $10^4$ poise. Examination of Figure 1-1 shows that this viscosity is not reached until a temperature of approximately 4500° F. Working at these high temperatures makes fused silica articles very costly, especially for large sizes.

In 1956 the Georgia Institute of Technology began working with a rebonded form of fused silica. This technique involved the process of slip casting. It provided fabrication techniques for forming large and intricate shapes to close tolerances which would be prohibitively expensive using the conventional molten silica forming techniques. The rebonded fused silica shapes can be processed at temperatures from 1800° to 2400° F and can be produced with densities from 30 lb/ft$^3$ to densities approaching the 139 lb/ft$^3$ of the conventional fused silica.

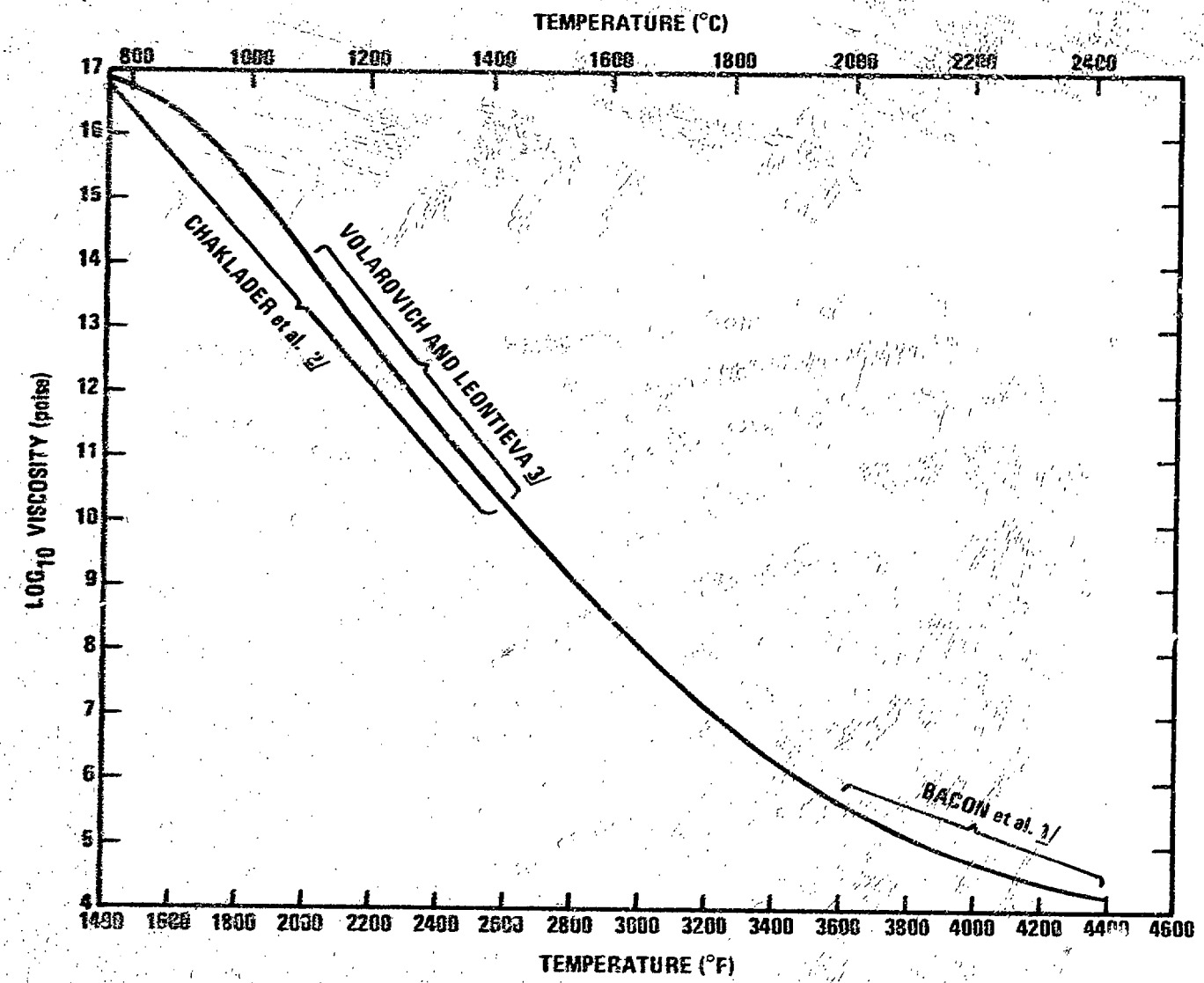


Figure 1-1. Viscosity of Fused Silica. (Reference 4, page 91.)

Some of the physical properties of the rebonded fused silica are considerably different from the conventional fused silica while some, such as thermal expansion and specific heat, are unchanged. As the properties of this new class of materials were investigated, it became apparent that rebonded fused silica had the properties required for use in aerospace applications such as leading edges, nose cones, and radomes. Since 1956 the majority of the structural work with slip-cast fused silica has been directed toward its application as a radome material. This was due primarily to the excellent electrical properties of this material. As requirements for radome materials have become increasingly more stringent, slip-cast fused silica has emerged as one of a very few non-composite materials which can meet present and future requirements. Since the majority of the current interest is in radome applications, this design manual is primarily directed at the design and fabrication of radomes. However, this does not preclude the use of slip-cast fused silica for other aerospace applications.

## 1.2 Radome Materials

Slip-cast fused silica is one of a very few materials that is suitable for use in radome and leading edge applications above Mach 5; however, as requirements for missile speeds increase, improvements are needed in ablation and rain erosion resistance of slip-cast fused silica. At the same time that improvements are sought in these two areas, every effort should be made to retain the other desirable physical and electrical attributes of slip-cast fused silica.

The selection of a hypersonic radome material is based on these criteria (1) dielectric properties, (2) weight, (3) thermal-mechanical response,

(4) thermal shock resistance, and (5) rain erosion resistance. The capabilities and limitations of slip-cast fused silica in each of these areas are as follows:

### 1.2.1 Dielectric Properties

The dielectric properties of importance in radome design are the dielectric constant and loss tangent and the change in these properties over the range of frequencies and temperatures for which the radome is being designed. In most cases the dielectric constant should be less than ten, with not more than 10 per cent variation in that value over the anticipated temperature range. In addition, the value for the loss tangent should be less than 0.01. Figure 1-2 shows the dielectric constant at 8 to 10 GHz as a function of temperature for a number of candidate radome materials. It can be seen that, compared to most other ceramics slip-cast fused silica has a low and relatively stable dielectric constant. A low dielectric constant is desirable since it allows a greater tolerance in the wall thickness of a radome. Figure 1-3 is a plot of loss tangent versus temperat for the same candidate radome materials. It can be seen that slip-cast fused silica and several others have an acceptable value of less than 0.01 at temperatures up to 2500° F.

### 1.2.2 Weight

The weight of a particular radome is a function of its shape and dielectric constant because of electrical and aerodynamic constraints. The relatively low dielectric constant of slip-cast fused silica results in thicker-walled radomes; however, the thicker wall does not present a weight problem because of the low density of slip-cast fused silica. The relative

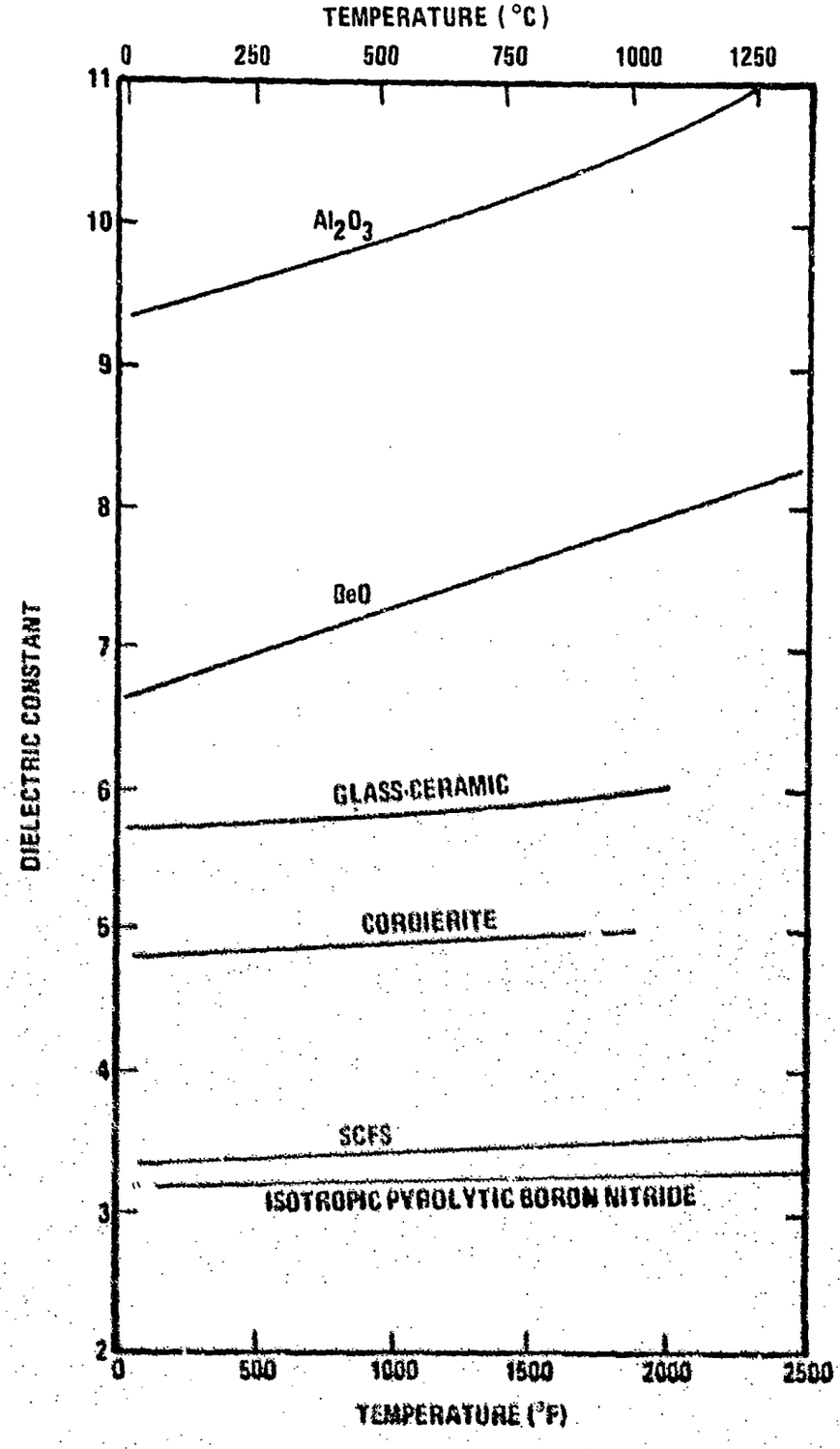


Figure 1-2. Dielectric Constant versus Temperature for Candidate Radome Materials.

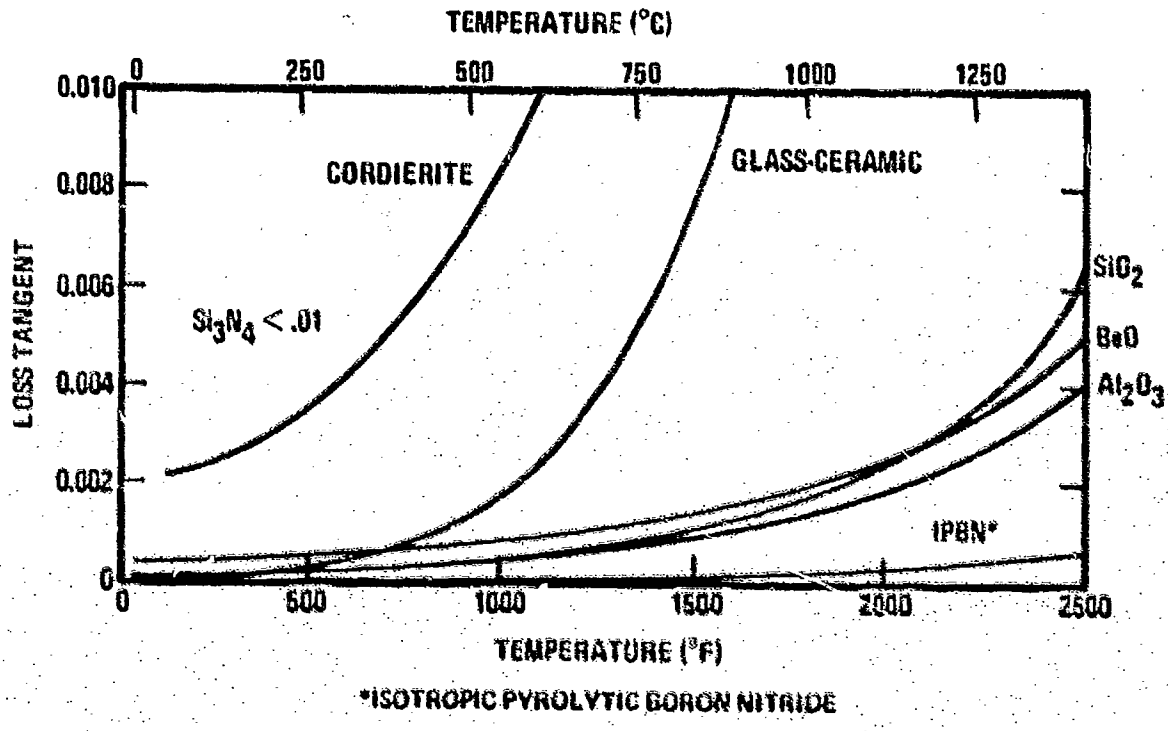


Figure 1-3. Loss Tangent versus Temperature for Candidate Radome Materials.

weight of slip-cast fused silica for a half-wave wall radome operating at X-band frequencies is compared with other ceramic radome materials in Table 1-1.

TABLE 1-1

WEIGHT PARAMETER FOR RADOME MATERIALS

| Material | Density ($\rho$) ($lb/in^3$) | Dielectric Constant ($\varepsilon$)* | Weight Parameter $\frac{\rho}{\sqrt{\varepsilon}}$ |
|---|---|---|---|
| $Al_2O_3$ | 0.137 | 9.60 | 0.044 |
| BeO | 0.105 | 6.60 | 0.041 |
| Cordierite Glass Ceramic | 0.094 | 5.60 | 0.040 |
| Vitreous Silica | 0.079 | 3.85 | 0.040 |
| Cordierite (Slip-Cast) | 0.085 | 4.80 | 0.039 |
| SCFS | 0.069 | 3.30 | 0.038 |
| $Si_3N_4$ | 0.086 | 5.60 | 0.036 |
| BN | 0.065 | 3.01 | 0.026 |

*Measured at 8 to 10 GHz.

### 1.2.3 Thermal-Mechanical Response

The relatively low tensile (2500 psi) and flexural (5000 psi) strength of slip-cast fused silica has been considered by some to be too low for radome applications. However, experience has shown that these strength levels are sufficient for aero-mechanical loads associated with hypersonic missile flight. With most other radome materials, high strength is required

to survive the thermal shock associated with such flight environments. However, the low thermal expansion of slip-cast fused silica results in low thermal stresses, and therefore, little strength is required to resist these stresses. Another property of SCFS which is attractive for high temperature applications is the fact that its strength increases with increasing temperature up to about 2000° F.

### 1.2.4 Thermal Shock

The thermal shock properties of slip-cast fused silica are well known, and the ability of this material to withstand thermal shock may be its single most attractive property. The low thermal expansion of this material gives slip-cast fused silica its unique resistance to thermal shock.

### 1.2.5 Rain Erosion

If slip-cast fused silica has a disadvantage when compared to other ceramic materials, it would be in rain erosion resistance. A ranking of rain erosion resistance of possible radome materials in order of decreasing rain erosion resistance would be in three general categories: good, fair and poor. In this grouping $Al_2O_3$ and BeO would be good, Cordierite glass ceramic and slip-cast cordierite fair, and slip-cast fused silica and IPM poor. At this time, the data necessary to classify $Si_3N_4$ as good or fair are not available. However, the very hard nature of $Si_3N_4$ (hardness ~ $Al_2O_3$ and BeO) and the high modulus of this material suggest that it should be superior to both forms of cordierite.

It should be pointed out in principle that the radome shape, as related to impact angle, can be designed to reduce the rain erosion damage to any material. Therefore, if a sufficiently small cone angle is used for the

forward portion of the radome, and if a protective tip is employed all candidate materials can survive encounter with rain at Mach 6. The intrinsic rain erosion resistance of the material used, however, will determine the allowable angle of attack and, therefore, the manueverability of the vehicle in rain.

It should be pointed out that the silica-based materials may exhibit improved rain erosion resistance at high temperatures. Preliminary experiments at Georgia Tech indicate that the impact damage mechanism in slip-cast fused silica produced by lead pellets from a 12-gauge shotgun undergoes considerable change between room temperature and 3000° F.

When slip-cast fused silica and dense fused silica glass were evaluated at Mach 3, it was found that the erosion resistance of the dense material was superior to the slip-cast 2/. When these materials were run at Mach 5, it was found that the dense material failed catastrophically, whereas, the slip-cast material merely increased in erosion rate over that of the Mach 3 environment 3/. It was also found that dense strong materials such as slip-cast cordierite also failed catastrophically at Mach 5 when the tip area was not protected. This reversal in merit suggests that strong dense materials may show relatively poor rain erosion resistance at hypersonic velocities.

## 1.3 General Comparison of Slip-Cast Fused Silica Properties With Other Materials

Table 1-2 compares properties of slip-cast fused silica with clear fused silica and several other ceramic materials. The properties that make slip-cast fused silica attractive for aerospace applications are its low thermal conductivity, thermal expansion, dielectric constant, loss tangent, and density. Disadvantages appear to be its low tensile and flexural strength

TABLE 1-2

SELECTED PROPERTIES OF FUSED SILICA AND OTHER CANDIDATE CERAMIC RADOME MATERIALS

| | Alumina ($Al_2O_3$) | Beryllia (BeO) | Fused Silica ($SiO_2$) | | | Boron Nitride (BN) | Silicon Nitride ($Si_3N_4$) | Major Phase-Cordierite ($2\ MgO \cdot 2\ Al_2O_3 \cdot 5\ SiO_2$) | |
|---|---|---|---|---|---|---|---|---|---|
| | High Purity | High Purity | Clear Glass | SCFS | Quartz-Silica Composite | IPBN | Reaction Sintered | Glass-Ceramic | Cordierite |
| Per cent major phase | 99-99.5 | > 99 | 99.9 | 99.8 | 99.8 | 99.9 | unknown | unknown | unknown |
| Density ($gm/cm^3$) | 3.7-3.9 | 2.85-2.95 | 2.2 | 2.1 | 1.68 | 1.25 | 2.4 | 2.6 | 2.45 |
| Per Cent Theoretical Density | 95-98 | 95-98 | 100 | 95 | 76 | 55 | 80 | 100 | 98 |
| Water Absorption Per Cent | 0 | 0 | 0 | 1-5 | 24 | 0 | <20 | 0 | 0 |
| Flexural Strength ($10^3$ psi) | 45 | 35 | 7* | 6.5 | 4.8 | 14 | 25 | 20* | 18 |
| Young's Modulus ($10^6$ psi) | 52 | 50 | 10.5 | 8.7 | 2.5** | 1.75 | 13 | 17.2 | 17 |
| Thermal Conductivity (Btu/ft-hr-°F) | 18 | 120 | 0.8 | 0.5 | 2.4 | 16 | 6 | 2.16 | ≈ 2 |
| Coefficient of Thermal Expansion ($10^{-6}$ in/in/°F) | 4.6 | 4.6 | 0.3 | 0.3 | 0.3 | 2.1 | 1.4 | 3.2 | 1.45 |
| Specific Heat (cal/gm-°C) | 0.27 | 0.26 | 0.17 | 0.18 | 0.246 | 0.29 | 0.2 | 0.18 | 0.19 |
| Poisson's ratio | 0.28 | 0.34 | 0.16 | 0.15 | unknown | 0.23 | unknown | 0.24 | 0.27 |
| Dielectric constant at 8-10 GHz | 9.5 | 6.6 | 3.85 | 3.4 | 2.9 | 3.01 | 5.6 | 5.65 | 4.8 |
| Loss Tangent at 8-10 GHz | 0.0001 | 0.0005 | 0.0002 | 0.0004 | 0.01 max | 0.0006 | 0.0005 | 0.0002 | 0.002 |

*Abraded surface.

**Calculated.

and its water absorption. However, the strength is sufficient for applied mechanical stress, and the low thermal expansion prevents thermal stresses from becoming a problem. Slip-cast fused silica is also unique in that it becomes stronger with increasing temperature. The problem of water absorption may be overcome by sealing with an organic coating.

## 1.4 References for Chapter I


1. Bacon, James F., et al., "Viscosity and Density of Molten Silica and High Silica Content Glasses," Phys. Chem. Glasses 1 90 (1960).

2. Chaklader, A.C.D., et al., "The Apparent Viscosity of Refractory Materials at High Temperatures," Refract. J. 36 292 (1960).

3. Volarovich, M. P. and A. A. Leontieva, "Determining Viscosity of Quartz Glass Within the Softening Range," Jour. Soc. Glass Tech. 20 139 (1936).

4. Fleming, J. D., Fused Silica Manual, Engineering Experiment Station, Georgia Institute of Technology, Atlanta, Georgia, September 1964, U.S. Department of Commerce OTS # 21312.

5. Ceramic Systems for Missile Structural Applications, Summary Report No. 1, Contract NOw-63-0143-d, for Bureau of Naval Weapons, Engineering Experiment Station, Georgia Institute of Technology, Projcet A-651, 31 October 1963, Appendix I, General Dynamics/Pomona, Tech Memo No. 6-223-571.

6. Harris, J. N. and J. D. Walton, Jr., Rain Erosion Sled Testing of Slip-Cast Fused Silica Radomes, Contract DA-01-021-AMC-14464(z), for U.S. Army Missile Command, Redstone Arsenal, Alabama, Engineering Experiment Station, Georgia Institute of Technology, Project A-925, October 1966, AD813521.

## CHAPTER II

## RAW MATERIAL AND FUSED SILICA SLIP

### 2.1 Raw Material

At present, two types of fused silica slip are available commercially. For convenience, these types will be referred to as technical grade and high purity. The major difference is in the chemical purity of the slip; the degree of purity results from differences in starting materials and milling techniques. High purity slips have lower alkali and alkaline earth content than technical grade materials.

The raw material for the technical grade fused silica is generally prepared by fusing a high quality quartz sand, either by electric arc melting or by flame fusion. The material generally retains some residual porosity and, in addition to the impurities present in the sand, may pick up further impurities from the graphite electrodes used in the arc fusion process. The resulting fused silica is translucent to opaque and ranges in color from off white to dark gray or even black, depending on the carbon and oxygen content. The slips produced from these materials range from off white to gray.

The raw material for high purity fused silica slip is a transparent high purity grade of fused silica and is produced in a number of ways. All commercially produced slips described in this manual were produced from transparent vitreous silica produced by the electric melting of selected high-purity quartz crystals in vacuum or low pressure inert gas. Such a method of production results in negligible hydroxyl content and virtually the same metallic impurities as in the starting quartz crystals. Table 2-1 gives spectrochemical analysis for a typical high purity and a typical technical

TABLE 2-1

TYPICAL SPECTROGRAPHIC ANALYSES

OF FUSED SILICA GRAIN FOR SLIP-MANUFACTURE

| Oxide | Technical Grade | High Purity |
|---|---|---|
| | % | % |
| $SiO_2$ (by difference) | 99.78 | 99.97 |
| $Al_2O_3$ | 0.140 | 0.018 |
| $Fe_2O_3$ | 0.001 | 0.0015 |
| CaO | 0.030 | 0.0025 |
| MgO | 0.022 | 0.0002 |
| $TiO_2$ | 0.021 | 0.0008 |
| $Na_2O$ | 0.002 | 0.0015 |
| $Li_2O$ | 0.002 | 0.0012 |
| $K_2O$ | 0.002 | 0.001 |

grade fused silica starting material. A second fusion method is the flame fusion of high purity quartz powder in an oxyhydrogen flame. The molten particles impinge on a heated surface, and build up a vitreous boule. The fused silica from this process contains from 0.015 to 0.04 weight per cent (w/o) hydroxyl from the flame, and is slightly lower in metallic contaminants than the starting quartz powder due to volatilization. The third method utilizes synthetic silicas which have lower metallic impurity levels than either of the two types above. The first of these is formed by vapor phase hydrolysis of a highly purified silica compound such as silicon tetrachloride, followed by fusion of the silica in an oxyhydrogen flame. This process yields high (up to 0.1 w/o) hydroxyl content but virtually no metallic contaminant. The material is produced by the oxidation of silicon tetrachloride and subsequent fusion of the silica in a "water free" flame such as an oxygen/argon plasma. The resulting silica contains virtually no impurities, either as hydroxyl or metals. At present there are no indications that any of these materials are not suitable for high purity fused silica slip production.

## 2.2 Slip Production

Fused silica is an unusual material in that casting slips can be prepared with this material without the aid of the acid treatment, deflocculants and suspension aids which are required with most other oxides. This is generally attributed to the fact that the silicon atoms in truncated tetrahedra at the surface of silica particles complete tetrahedral coordination by attaching a hydroxyl ion in place of the missing oxygen atom. This layer of bound hydroxyl promotes slip stability and controls the pH of the slip.

Milling must be carried out in water, as dry grinding followed by dispersion will not give the desired degree of hydration for a stable slip, even through the use of wetting agents. Also, it is doubtful that the particle size distribution produced by dry grinding would be as suitable for a slip as that provided by wet grinding. Standard porcelain-type mills are suitable for technical grade slips since the impurity level of the starting material is comparable to the level of alkali and alkaline earth impurities picked up from the mill lining. However, 85 per cent alumina mills and grinding media are recommended for technical grade slips and are mandatory for high-purity slips. The higher purity and density of the mill lining provides less contamination through mill wear and lower levels of harmful impurities in the material from the mill and grinding media. Ninety-nine per cent-plus alumina mills are not recommended because of their rapid wear rate and added cost.

When granular materials are used as mill feed they should be minus eight mesh. If the feed is in the form of tubing cullet or a thin flake material and will fracture readily, much coarser feed may be used. If the feed has been crushed in iron bearing crushers, some provision must be made for removing excess iron contamination. Magnetic methods are satisfactory for technical grade materials, but washing with concentrated hydrochloric acid diluted 3:1 may be necesary to obtain sufficient iron removal in a high-purity slip.

The following example is illustrative of the milling process for a one-gallon batch of high purity fused silica slip and shows the changes occurring during milling.

A one gallon batch of high purity fused silica casting slip was milled from cleaned transparent fused silica tubing cullet. The cullet was milled with deionized water in four 85 per cent alumina one-gallon mills with 85 per cent alumina grinding media in the form of 5/8-inch diameter spheres. The mill cavity was 8 inches in diameter. Each mill charge was as follows:

4600 gms - 85 per cent alumina grinding media

1380 gms - transparent fused silica tubing cullet

390 gms - deionized water

The mill charge was initially 82.6 w/o solids. The slip was ground at a mill speed of approximately 60 to 65 revolutions per minute, which is 60 per cent of critical speed for the mill. Critical speed, the speed at which the radial G forces on the grinding media cause them to ride the mill lining, is calculated from

$$\omega = \frac{54.19}{\sqrt{R}} \qquad (2\text{-}1)$$

where $\omega$ = critical speed, rpm, and

$R$ = mill inside radius, feet.

At intervals, 50 ml samples of slip were withdrawn from one of the mills and used for the determination of pH and particle size distribution. Particle size distributions were checked until mean particle diameter had been indicated, and in several cases the distributions were extended to finer particle fractions. Analysis was based on ASTM D422. Plots of the particle size distributions for various milling times are shown in Figure 2-1. Figure 2-2 is a plot of mean particle diameter as a function of milling

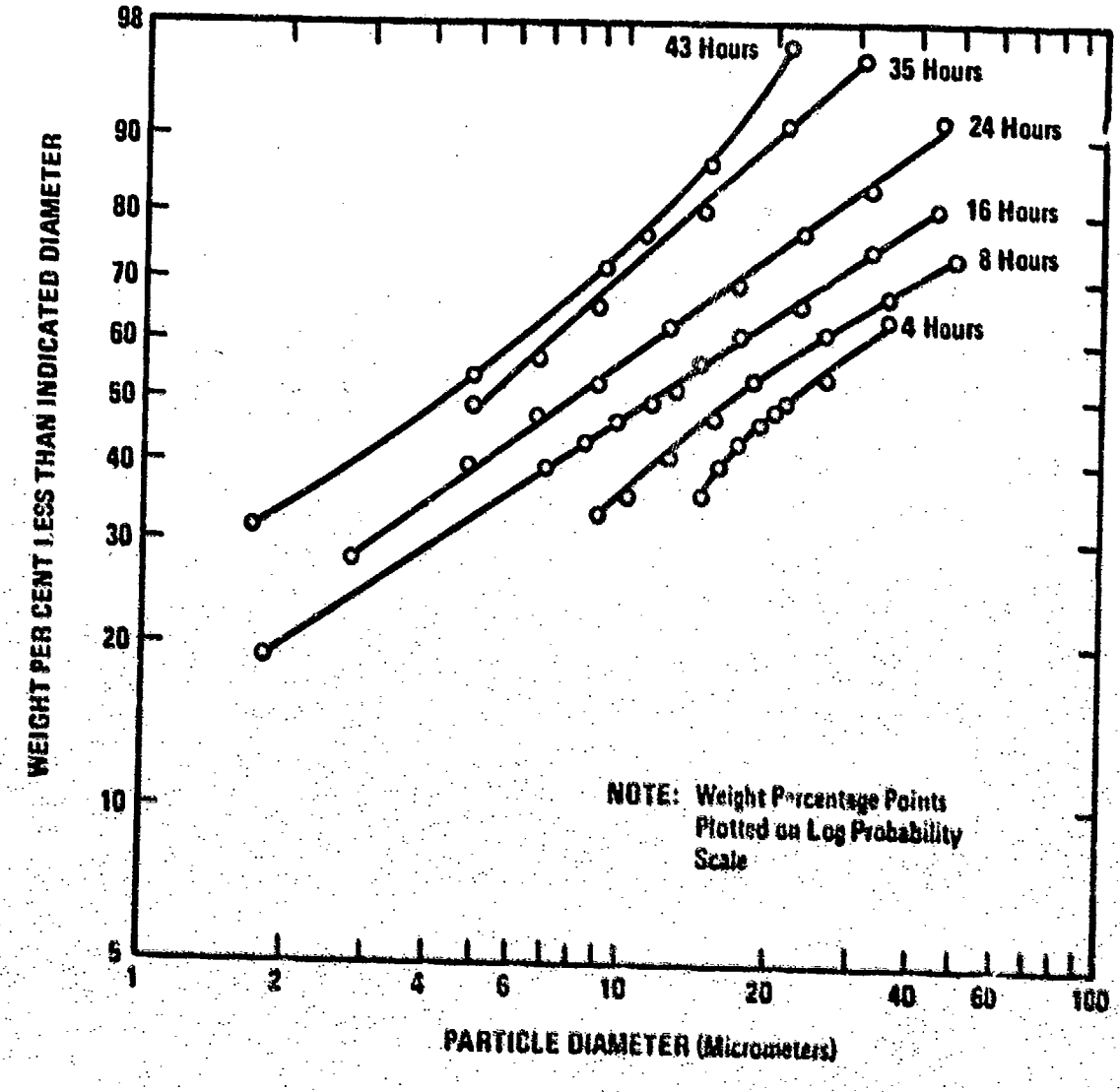


Figure 2-1. Partial Particle Size Distributions for High Purity Fused Silica Slip at Indicated Milling Times.

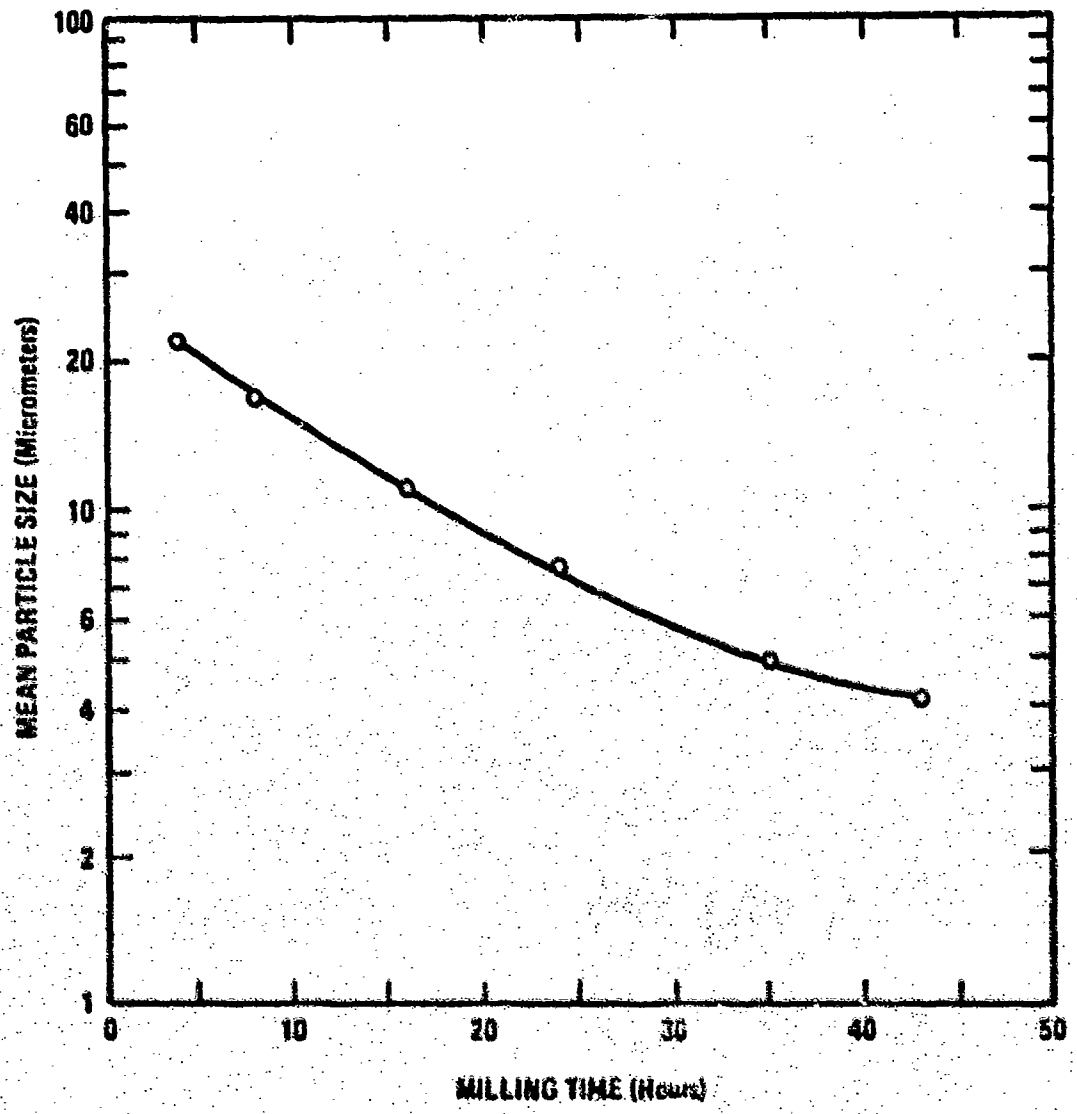


Figure 2-2. Mean Particle Size versus Milling Time for High Purity Fused Silica Slip.

time. All slips tended to settle badly until the mean particle diameter was brought down to approximately eight microns.

During milling, the particle size curves changed from an apparently bi-modal distribution at 4 and 8 hours (reflecting a remnant feed distribution) to the usual log normal distribution. As reported in the literature 3/, slips with 10 to 15 per cent of the particles larger than 60 μm diameter were unstable and tended to settle. After 24 hours of milling, this condition was no longer observed, and the slip was stable. With increased milling time, the pH of the slip shifted from neutral to acidic as seen in Figure 2-3. The pH appears to be a function of slip particle specific surface and the degree of hydration of the particles. The final mean particle diameter of the slip was finer than would be used for most hardware applications.

Unfortunately, it is not possible directly to scale-up ball and feed charges and milling times to production size mills. It is necessary to adjust these parameters experimentally for each mill.

## 2.3 Properties of Fused Silica Casting Slips

Many of the properties of fused silica slips were summarized by Murphy 2/ in 1968 in a study that compared fourteen technical grade slips and one high-purity slip. Since that time, high-purity slip has become available commercially, and technical grade slips have been improved to a more consistent level. As a result, much of the data previously reported are no longer applicable, particularly the spectrographic analyses. The following data were collected from slips produced from late 1968 to late 1971 and are more representative of currently available materials.

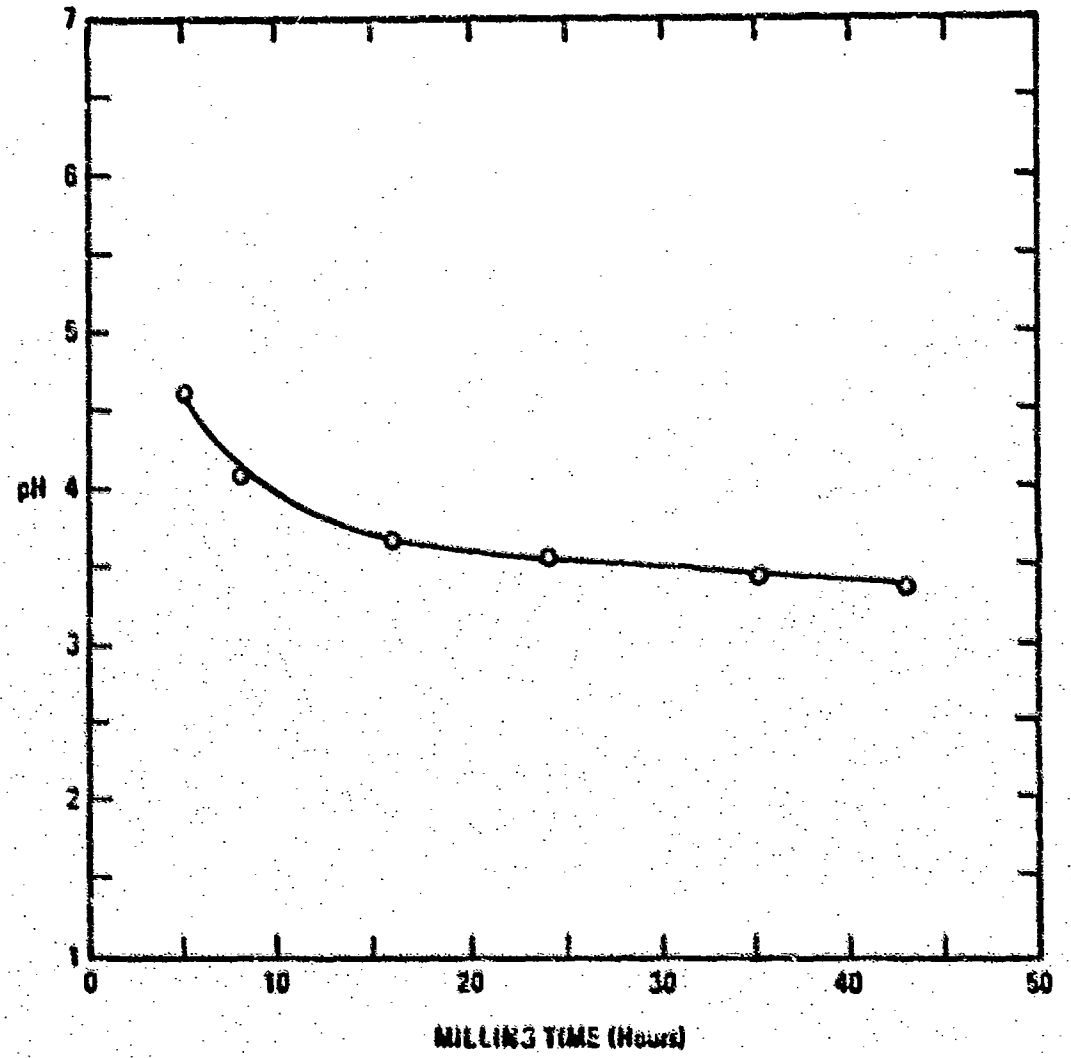


Figure 2-3. pH versus Milling Time for High Purity Fused Silica Slip.

### 2.3.1 Chemical Analyses

Analyses of two technical grade and nine high purity fused silica slips are shown in Table 2-2. Analyses were made by emission spectroscopy, with the exception of the alkalies, which were determined from flame photometry. From these results, it can be seen that the term "high purity" when used to describe the fused silica slip is somewhat of a misnomer. The milling process adds so many impurities that it becomes difficult to detect the difference in chemical analyses between the two types. In Table 2-1, there is an order of magnitude difference in the amounts of CaO and two orders of magnitude difference in MgO between the high purity and the technical grade fused silica mill feed. After milling, the difference in alkaline earth content as shown between the two types in Table 2-2 is considerably less. Based on the slips presented in Table 2-2, the minimum value for the alkaline earth oxide content in the technical grade material is 0.44 per cent, while the maximum for the nine high-purity slips is 0.33 per cent. While an empirical upper limit of 0.35 per cent alkaline earth oxide might be established as a boundary between technical grade and high-purity materials, it is believed that the rate of devitrification may be partially controlled by the location of the impurities. That is, the impurities located within the fused silica glass starting material may have a much more profound effect on devitrification than the same amount and type of impurities interspersed between the fused silica grains during the milling process.

Devitrification may also be partially controlled by remanent crystalline nuclei present in the technical grade material. Therefore, it is not possible to isolate fully the controlling factors in devitrification rate at this time.

TABLE 2-2

SPECTROGRAPHIC ANALYSIS OF TECHNICAL AND HIGH PURITY FUSED SILICA SLIPS

| | Technical | | High Purity | | | | | | | | |
|---|---|---|---|---|---|---|---|---|---|---|---|
| | $T_1$ | $T_2$ | $HP_1$ | $HP_2$ | $HP_3$ | $HP_4$ | $HP_5$ | $HP_6$ | $HP_7$ | $HP_8$ | $HP_9$ |
| $SiO_2$ | 99.57 | 99.51 | 99.61 | 99.60 | 99.58 | 99.54 | 99.66 | 99.73 | 99.66 | 99.59 | 99.69 |
| $Al_2O_3$ | 0.340 | 0.340 | 0.310 | 0.340 | 0.370 | 0.420 | 0.300 | 0.248 | 0.300 | 0.360 | 0.260 |
| $Na_2O$ | 0.008 | 0.002 | 0.008 | 0.005 | 0.008 | 0.001 | 0.001 | 0.004 | 0.001* | 0.001* | 0.001* |
| $K_2O$ | 0.001* | 0.010 | 0.001* | 0.001* | 0.001* | 0.001* | 0.001* | 0.003 | 0.001* | 0.001* | 0.001* |
| $Li_2O$ | 0.001* | 0.001* | 0.001* | 0.001* | 0.001* | 0.001* | 0.001* | --- | 0.001* | 0.001* | 0.001* |
| MgO | 0.014 | 0.011 | 0.011 | 0.008 | 0.009 | 0.006 | 0.001 | 0.014 | 0.011 | 0.016 | 0.016 |
| CaO | 0.030 | 0.050 | 0.022 | 0.010 | 0.004 | 0.015 | 0.015 | 0.003 | 0.007 | 0.017 | 0.010 |
| $Fe_2O_3$ | 0.027 | 0.056 | 0.017 | 0.027 | 0.021 | 0.008 | 0.010 | 0.001 | 0.010 | 0.010 | 0.009 |
| $TiO_2$ | 0.013 | 0.020 | 0.001 | 0.003 | 0.003 | 0.003 | 0.005 | 0.001 | 0.008 | 0.004 | 0.005 |

*Indicates limit of detection.

### 2.3.2 Physical/Chemical Properties

The physical and chemical properties of the same fused silica slips are summarized in Table 2-3. The pH is primarily a function of particle size and, therefore, surface area. More finely ground slips generally have lower pH values. The viscosity varies inversely with mean particle diameter and directly with the weight per cent solids. It should be pointed out that this holds true only for slips milled with no attempt to control pH. Earlier slips in some instances were made more viscous by shifting the pH by acid or base additions. Apparently the pH as a result of grinding results in a minimum viscosity, maximum stability slip.

### 2.3.3 Particle Size and Distribution

The particles in a fused silica slip will range from 50 to 60 μ on down to sub micron sizes. The particles are of irregular, angular shape, often occurring in thin flakes as shown in Figure 2-4. The particle size distribution is generally considered to be log normal and as a result will usually plot as a straight line on log probability as in Figure 2-1. The particle size distribution for the nine slips described above is shown in Figure 2-5 as plots of cumulative weight per cent undersize versus log diameter. These measurements were made by the sedimentation/hydrometer method as specified in ASTM D422 with the exception of $T_1$ and $HP_2$, which were made with a Coulter Counter. The distribution is quite similar, having approximately the same slope in the straight line portion and differing only in mean particle size.

## 2.4 Fused Silica Slip Specifications

A fused silica slip specification prepared at Georgia Tech 1/ is attached

TABLE 2-3

PROPERTIES OF TECHNICAL AND HIGH PURITY SILICA SLIPS

| | Technical | | High Purity | | | | | | | | |
|---|---|---|---|---|---|---|---|---|---|---|---|
| | $T_1$ | $T_2$ | $HP_1$ | $HP_2$ | $HP_3$ | $HP_4$ | $HP_5$ | $HP_6$ | $HP_7$ | $HP_8$ | $HP_9$ |
| pH | 6.0 | 5.5 | 5.1 | 4.8 | 4.7 | --- | 5.0 | 3.5 | 4.6 | 4.6 | 5.1 |
| Per Cent Solids | 82.5 | 82.2 | 82.2 | 83.1 | 83.3 | 82.6 | 83.3 | 84.3 | 82.6 | 83.4 | 83.4 |
| Mean Particle Size | 11.5 | 8.0 | 6.3 | 9.8 | 4.0 | 7.0 | 7.5 | 5.0 | 6.8 | 6.8 | 7.0 |
| Viscosity Centi-poise | 93 | 115 | 135 | 136 | 253 | 140 | 144 | --- | 122 | 151 | 110 |

1μ

Figure 2-4. Micrograph of Fused Silica Particles in Fused Silica Slip.

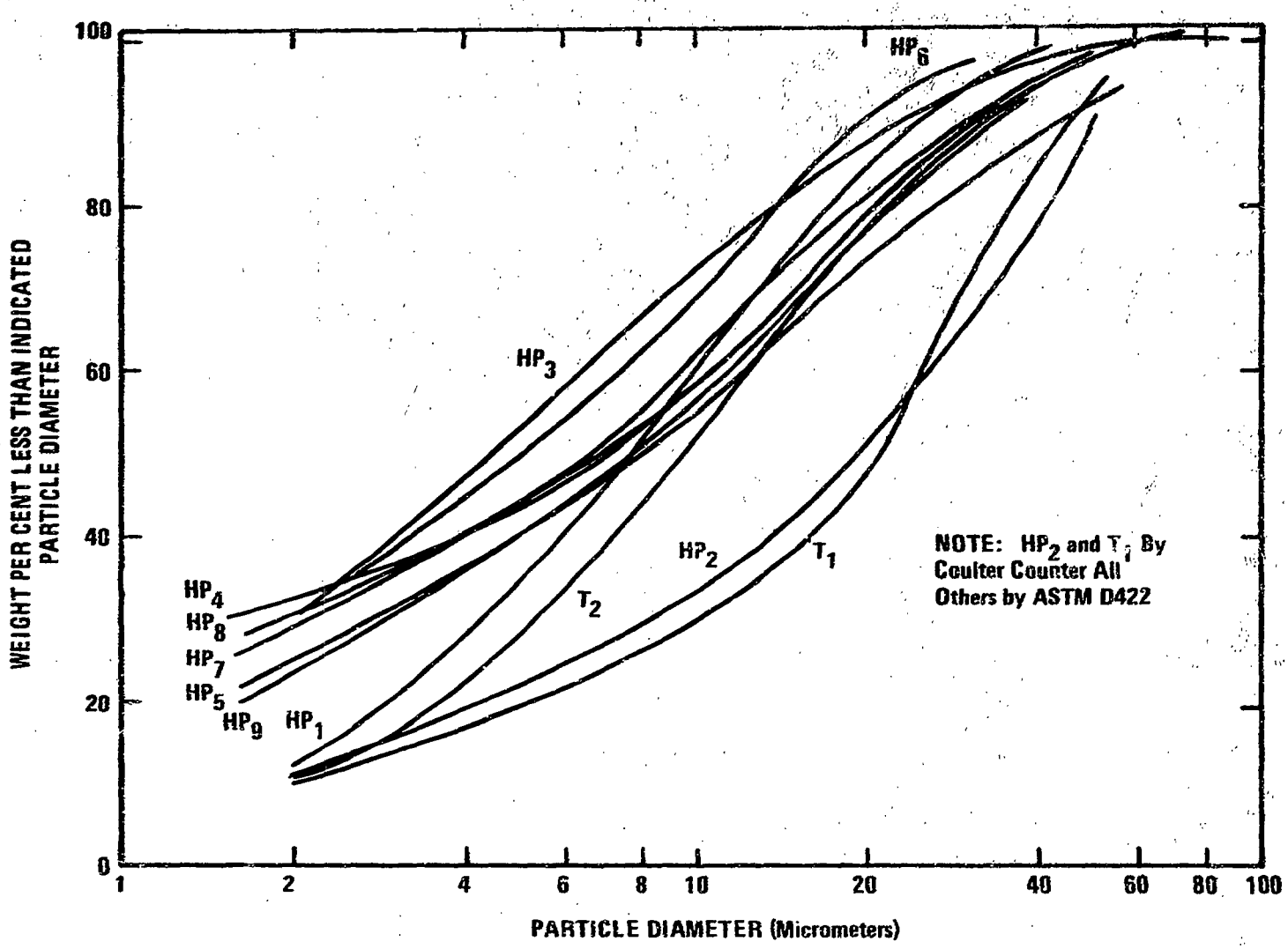


Figure 2-5. Particle Size Distributions for Fused Silica Slips.

as Appendix I. It should be noted that this specification applies only to high-purity slips. Briefly, the specification requires that the slip meet the following requirements.

1. A residue of not more than 5 weight per cent retained on a 325 mesh screen.

2. A minimum $SiO_2$ content of 99.5, with less than 50 ppm total alkali metals, (sodium, potasium lithium) and less than 300 ppm total alkaline earth oxides (calcium and magnesia).

3. No detectable crystalline silica in the slip.

4. Maximum water content of 18 weight per cent.

Mean particle size can be specified to suit individual needs. For example, thick shapes would require a larger mean particle diameter to avoid drying problems.

For technical grade slips, requirements are not as stringent, and the recommendations of Murphy 2/ are generally sufficient. The major requirements are:

1. Initial residual cristobalite content of less than 1 volume per cent.

2. Devitrification rate such that cristobalite content less than 15 v/o after 3-1/3 hours at 2200° F (Note: this is not to imply that 3-1/3 hours is a proper firing time for all slips, It provides a good compromise between density and cristobalite content, and serves merely as a basis for comparison of properties).

3. A minimum modulus of rupture of 3000 psi after 3-1/3 hours at 2200° F (In lieu of cristobalite measurements). This measurement may be used as a single requirement. In general, higher strengths can be obtained at longer sintering times, but optimum strength for some materials has been obtained in as little as 2-1/2 hours. Again, the requirement is merely a minimum value for useful hardware.

## 2.5 Slip Storage and Handling

Fused silica casting slip should be stored in polyethylene or similar polymeric containers or in polyethylene-lined metal drums. The slip should not be in contact with any metal. It is not necessary to keep the slip in suspension except prior to use. The containers should be continuously rolled or otherwise agitated for 48 hours for proper resuspension. Slip should not be allowed to freeze since this apparently precipitates silicic acid from the slip and prevents casting of a dense body. The slip generally contains a small portion of -4 +10 mesh material, which is slightly smaller than the interstices in the grinding media bed. This material should be screened, usually to -20 mesh, at the time the plaster mold is filled.

## 2.6 Slip Aging

For reasons not yet understood, some fused silica slips have undergone changes in viscosity, pH and sintering rate with age. The viscosity and pH have tended to increase and decrease slightly, respectively over a period of several months. The sintering rate however increased steadily over the first two to three weeks, after which it leveled off. Since the viscosity and pH changes present no particular difficulties in use, it is recommended that slips be used only after aging four weeks from date of manufacture.

## 2.6 References for Chapter II


1. Yu E. Pivinskii, F. T. Gorobets, "High Density Fused Silica Ceramics," Refractories, Russia 33, (8), 509-516, 1968.

2. Murphy, C. A., Characterization of Fused Silica Slips, Contract N00017-67-C-0053, Naval Ordnance Systems Command by Georgia Institute of Technology, Special Technical Report No. 2, April 1968.

3. Harris, J. N. and E. A. Welsh, Fused Silica Slip Requirements for Slip Casting Radomes, Contract N00017-70-C-4438, Naval Ordnance Systems Command, by Georgia Institute of Technology, Technical Report No. 1 to be published.

CHAPTER III

FABRICATION & PROCESSING

## 3.1 Introduction

A number of different fabrication techniques have been used to produce rebonded fused silica objects. Among these techniques are slip casting 1,2,3/, aggregate casting 4/, isostatic pressing 5,6/, hot pressing 7/, and electrodeposition 6/. Of all these techniques, slip casting provides a product with the highest strength, minimum cost and greatest ease of fabrication. With this technique, an aqueous suspension of finely ground particles (casting slip) is poured into a plaster mold which defines the shape of the object to be produced. Capillary action in the porous plaster draws water from the slip into the mold, increasing the solids content of the slip adjacent to the plaster forming a solid wall. The thickness of the wall increases with the time the slip is left in the mold. When sufficient thickness has built up, the excess slip is drained, leaving a dense but somewhat leathery shape in the mold.

After additional drying time, the shape becomes rigid and strong enough to be removed from the mold with careful handling. It is then further dried at an elevated temperature (150° to 300° F) and sintered to its final density. Sintering is usually accomplished at temperatures between 2100° and 2300° F.

## 3.2 Mold Fabrication

### 3.2.1 Master Model Preparation

The master model is a pattern from which the plaster mold is cast. It can be fabricated from virtually any impermeable material. For most

applications, aluminum has been the most satisfactory material, due mainly to its light weight in comparison with stainless steel and brass. For long production runs where durability is the main concern, stainless steel should be considered. Light weight fiberglass mandrels have been used, but these have required filling with plaster to gain the rigidity necessary for withstanding the rigors of pulling a large mandrel from the mold. Where weight requirements have eliminated even aluminum, a cellulose-lignin laminate has been successfully used. With both this mandrel and fiberglass mandrels, the surface has been varnished, sanded, and polished prior to use. With metal models, a high surface polish is necessary for use.

Since the drying and sintering shrinkage of slip-cast fused silica usually ranges from 1 to 2 per cent depending on the purity and the fineness of the slip, models should be made correspondingly oversize to compensate. The actual shrinkage should be determined from measurements of test bars sintered at varying time and temperature or, as an even better approximation of a radome shape, a cylinder with the top end closed. This data will normally be taken in conjunction with modulus of rupture and other property measurements used to determine optimum sintering conditions appropriate for the particular hardware end use.

### 3.2.2 Mold Design

Mold design should be kept as simple as possible. For instance, round bars can be drain-cast in an open-ended cylindrical mold with the bottom end resting on a glass plate. Disks can be cast by placing a short length of methyl-methacrylate or polycarbonate pipe on a flat plaster surface to form the mold cavity. For pressure casting, a fixture must be made to

hold a cover plate over the mold cavity, and the walls of the mold should be thick enough to withstand the internal pressure. For casting large shapes (up to 50-inch long radomes), a 3-inch minimum plaster wall thickness has been satisfactory for pressures up to 20 psi. The outer contour of the mold should conform as closely as possible to the inner or casting surface. For example, an ogive radome could be cast in a conical mold or even a mold with its outer surface formed by portions of two cones. The uniform wall thickness aids in obtaining a uniform wall thickness in the casting. The tendency toward thicker walls in the tip area of radomes has been attributed to the greater hydrostatic head at the tip when cast tip down. It is felt that this differential pressure, while a contributing factor, is insufficient to account for observed thickening. A larger mold volume/mold surface ratio at the tip could also cause this. A third possibility is that the thicker walls are due to a particle size gradient that develops during long-time casting. The larger particles settle toward the bottom and produce a coarser slip in this area. Experience has shown that coarser slips cast faster than finer particle slips.

### 3.2.3 Mold Preparation

Any good grade of commercial pottery plaster may be used. The mix is usually made up to 60 per cent consistency (40 parts water/50 parts plaster by weight). At this consistency approximately 1500 gms plaster and 1200 gms water are required for 100 $in^3$ of mold volume. A higher plaster-to-water ratio may be used to obtain greater mold durability, but this greater durability results in lower water absorption and lower casting rates. The effect of various variables such as slaking time, mix time, water content, etc.,

on strength and absorption of the mold has been summarized in references 8/ and 9/, while additional information is available from plaster manufacturers.

Briefly the steps in mold preparation are:

1) Accurately weigh plaster and water. Variations in composition can cause undesirable variations in casting properties of the mold.

2) Sift the plaster into the water and allow to slake (soak) for 3 to 4 minutes. Sifting breaks up lumps, and slaking allows thorough wetting of the plaster.

3) Mix the plaster until it begins to "cream" or thicken. Mixing should be thorough, but should not be vigorous enough to entrain air in the mix. Mixing usually requires 2 to 3 minutes.

4) Pour the plaster into the mold. If plaster is poured before it has thickened sufficiently, settling results in an inhomogeneous mold. If mixing is continued for too long a time, the plaster may "set" before the mold is filled completely.

5) When mold reaches maximum heat, remove dam and model. On some shapes there will be a tendency of the model to expand from the heat of hydration of the plaster, making removal difficult. Low expansion models, low thermal conductivity models, and models with provision for cooling are all possible remedies.

Mold variations can be held to a minimum by using water at the same temperature each time and by timing slaking and mixing carefully. Optimum

slake and mix time may have to be established for each mold configuration since, for example, large batches must be poured early to insure filling the mold completely.

Before use, the mold should be dried to a low moisture content. Drying temperatures should be kept below 120° F, particularly in the latter stages of drying, to prevent calcination of the plaster. Drying to a constant weight is the usual practice, although drying to a higher moisture content reduces the initial casting rate of the mold, a desirable feature under some circumstances.

## 3.3 Slip Casting Fused Silica Parts

### 3.3.1 Casting Rate

Slip casting is a filtration process and has been described in detail from this standpoint by Adcock and McDowell 10/. The wall thickness W varies directly with the square root of casting time, T

$$W = K\sqrt{T} \qquad (3\text{-}1)$$

where the proportionality constant K, is defined by

$$K = \frac{2\,PG\,E^3}{5\,Sp^2\,\eta\,(y-1)(1-E)^2} \qquad (3\text{-}2)$$

where K = proportionality constant

P = pressure drop across cast wall

E = void fraction in cast wall

Sp = Specific surface of solids (by permeability measurements)

$\eta$ = Viscosity of suspending medium

y = volume of slip containing volume (1-E) of solids

G = gravitational constant.

From this it follows that casting rates can be increased 1) by higher applied pressure, and 2) by using a slip with a larger mean particle diameter (lower specific surface). In the case where the driving process is only the capillary suction in the plaster, the casting process is referred to as drain casting. In cases where either pressure is applied to the slip or where the back face of the mold is under vacuum, the process is termed pressure or vacuum assited casting. As a rule-of-thumb, shapes with wall thicknesses under 1/2-inch are generally drain cast, while thicker shapes are pressure cast. Pressure casting helps reduce the amount of settling of slip in the mold cavity.

The simplest method of establishing the casting time for a given wall thickness is to make a trial casting under known conditions of pressure and mold moisture (molds are generally conditioned by drying to constant weight at temperatures under 120° F). From the trial wall thickness and casting time, a good value for the final casting time may be estimated from

$$\frac{W_1^2}{W_2^2} = \frac{\theta_1}{\theta_2} \qquad (3\text{-}3)$$

where $W_1$ = trial wall thickness

$W_2$ = required wall thickness

$\theta_1$ = trial casting time

$\theta_2$ = required casting time.

Fleming 11/ studied the casting rate of a 7.5μm mean particle diameter slip at applied pressures of from 0 to 60 psi. This work indicated that for drain casting, wall thickness could be expressed as

$$W = 0.048 \sqrt{\theta - 2.7} - 0.0207 \qquad (3\text{-}4)$$

where W = wall thickness (inches)

θ = casting time (minutes).

For pressure casting, the wall thickness can be approximated by

$$W = 0.012 \sqrt{\theta P} - 0.047 \qquad (3\text{-}5)$$

where P = gage pressure (psi).

This is an approximation, since the proportionality constant is not exactly a linear function of P. This has been attributed to two mechanisms. Adcock and McDowell 10/ indicate that the suction of the plaster increases with increasing pressure, while Fleming's data indicate that porosity in the cast wall increases with pressure. Both mechanisms would result in higher proportionality constants than would be expected.

Equations 3-4 and 3-5 are plotted in Figure 3-1. These curves provide a good basis for predicting trial casting times. When using these curves, one should remember that slips with mean particle diameter greater than 7.5 μm will usually cast at a rate higher than that shown, while more finely ground slips will cast more slowly. These curves are generally accurate to ± 10 per cent for slips with mean particle diameters from 7-5 μm.

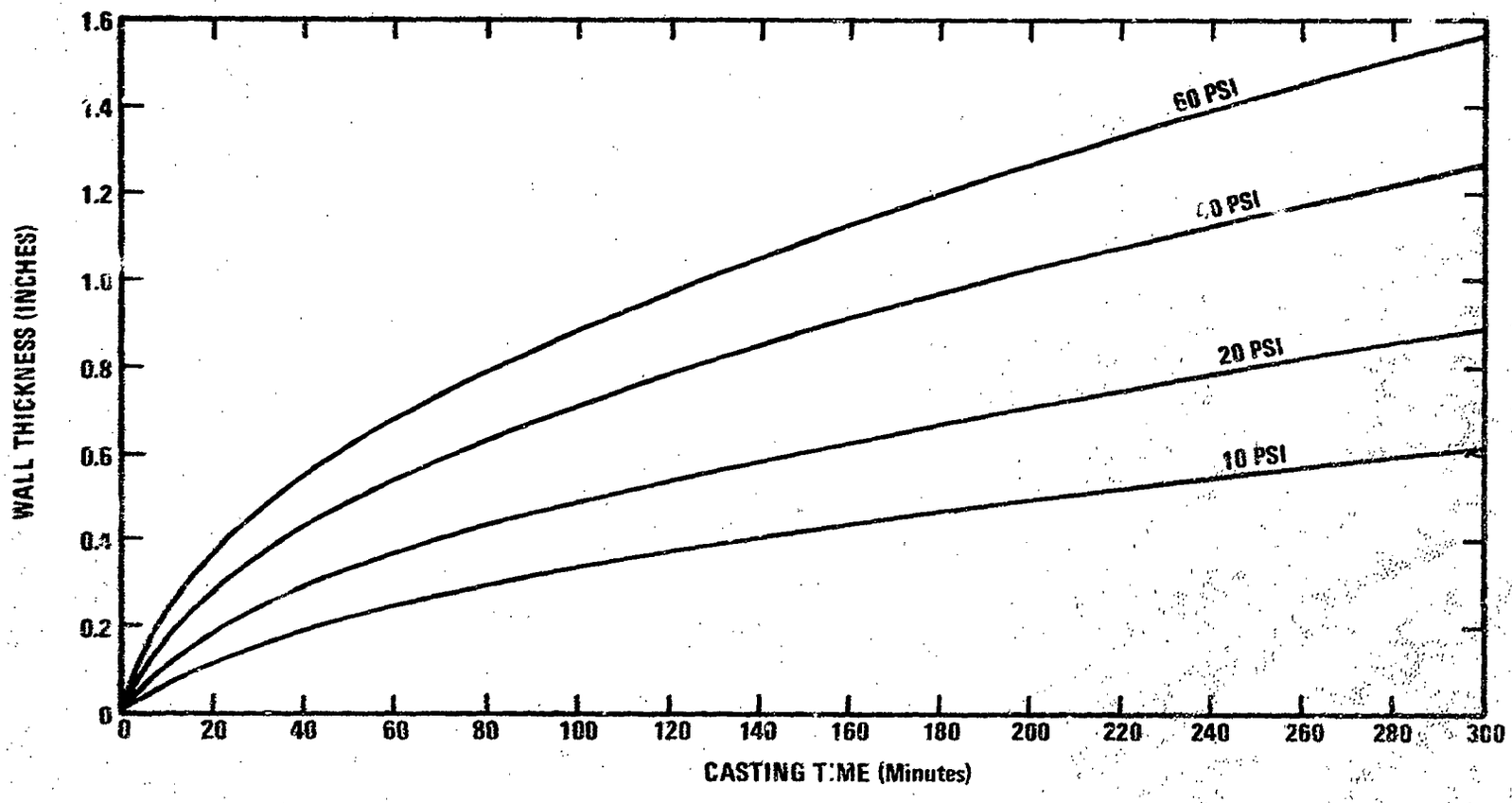


Figure 3-1. Cast Wall Thickness versus Time of Casting for Fused Silica. (Reference 11, page 42.)

Fleming 11/ studied the casting rate of a 7.5μm mean particle diameter slip at applied pressures of from 0 to 60 psi. This work indicated that for drain casting, wall thickness could be expressed as

$$W = 0.048\sqrt{\theta - 2.7} - 0.0207 \qquad (3\text{-}4)$$

where W = wall thickness (inches)

θ = casting time (minutes).

For pressure casting, the wall thickness can be approximated by

$$W = 0.012\sqrt{\theta P} - 0.047 \qquad (3\text{-}5)$$

where P = gage pressure (psi).

This is an approximation, since the proportionality constant is not exactly a linear function of P. This has been attributed to two mechanisms. Adcock and McDowell 10/ indicate that the suction of the plaster increases with increasing pressure, while Fleming's data indicate that porosity in the cast wall increases with pressure. Both mechanisms would result in higher proportionality constants than would be expected.

Equations 3-4 and 3-5 are plotted in Figure 3-1. These curves provide a good basis for predicting trial casting times. When using these curves, one should remember that slips with mean particle diameter greater than 7.5 μm will usually cast at a rate higher than that shown, while more finely ground slips will cast more slowly. These curves are generally accurate to ± 10 per cent for slips with mean particle diameters from 7-8 μm.

### 3.3.2 Slip Casting

At this point, the mold is ready for use. The slip, which has been thoroughly dispersed by rolling agitation for 48 hours or until all settled solids are back in suspension, is then poured through a 20 mesh screen or finer to remove large pieces of fused silica which are usually present. For drain casting, the slip is simply poured into the mold, and the mold is covered with a damp cloth to prevent formation of a skin on the liquid surface. For pressure casting, the slip is usually pumped into the mold from an outside reservoir. In casting hollow shapes such as cylinders or radomes, it is usually desirable to place a displacement mandrel in the center of the mold to reduce the mold cavity volume and thereby, the volume of slip required. After casting to the desired wall thickness, determined either from casting time or in pressure casting by measuring weight loss in the slip reservoir, the excess slip must be removed from the mold. With small shapes such as crucibles or 12 to 18-inch long radomes, this may be done by inverting the mold and pouring off the excess while holding the cast shape in the mold. With larger shapes, the slip is usually removed from the mold by siphoning or vacuum suction. The slip drained from the mold cavity after casting has been "scalped" of coarser particles, and reuse of this material will lead to drying problems. Small shapes can usually be removed from the mold and dried at room temperature overnight. Larger shapes, because of the leathery condition of the walls, should be dried in the mold until shrinkage ceases before removal from the mold.

The method of drain casting each radome varies with its size and wall thickness requirements, but the mold is usually rotated from a tip-up or tip-down position to the opposite position by turning the mold sometime

during the casting operation. A typical pressure casting set up to allow this is shown in Figure 3-2. In some cases, the mold rotation is simply for handling expediency in drying and removal of the radome from the mold. In other cases, the mold is rotated during the casting operation in attempts to minimize wall thickness gradients due to particle settling. Rotating the mold with a green radome can result in the green wall's pulling away from the mold when the long axis of the radome is horizontal to the floor. This problem can usually be eliminated by making certain that the radome mold is not rotated unless the mold is full of slip and under air pressure or unless the radome has thoroughly dried in the mold.

If the purpose of rotation is to minimize wall thickness gradients, filling of the mold may be accomplished in either a radome tip-down (as shown in Figure 3-2) or tip-up position depending on previous determinations as to what is the best position for entry of fill tubes into the mold. After filling, the mold is left in position for some specified period of time then rotated 180 degrees for another specified period of time. Rotation can be accomplished as often as necessary provided the mold remains full of slip and pressure (above atmospheric) is retained on the slip in the mold. The normal procedure is to end up with the mold in a tip down position. The excess slip is drained out through the tip (if the final shape requires a hole in the tip of the radome) or is pumped from the mold. The green casting is then allowed to dry thoroughly in the mold. During this drying period, the green radome is supported by the mold walls as it shrinks in drying. After this drying phase is completed, a firing base is attached to the open (base) end of the mold, and the mold is rotated to a tip up position. The maximum stress on the radome wall occurs when the long axis of the radome

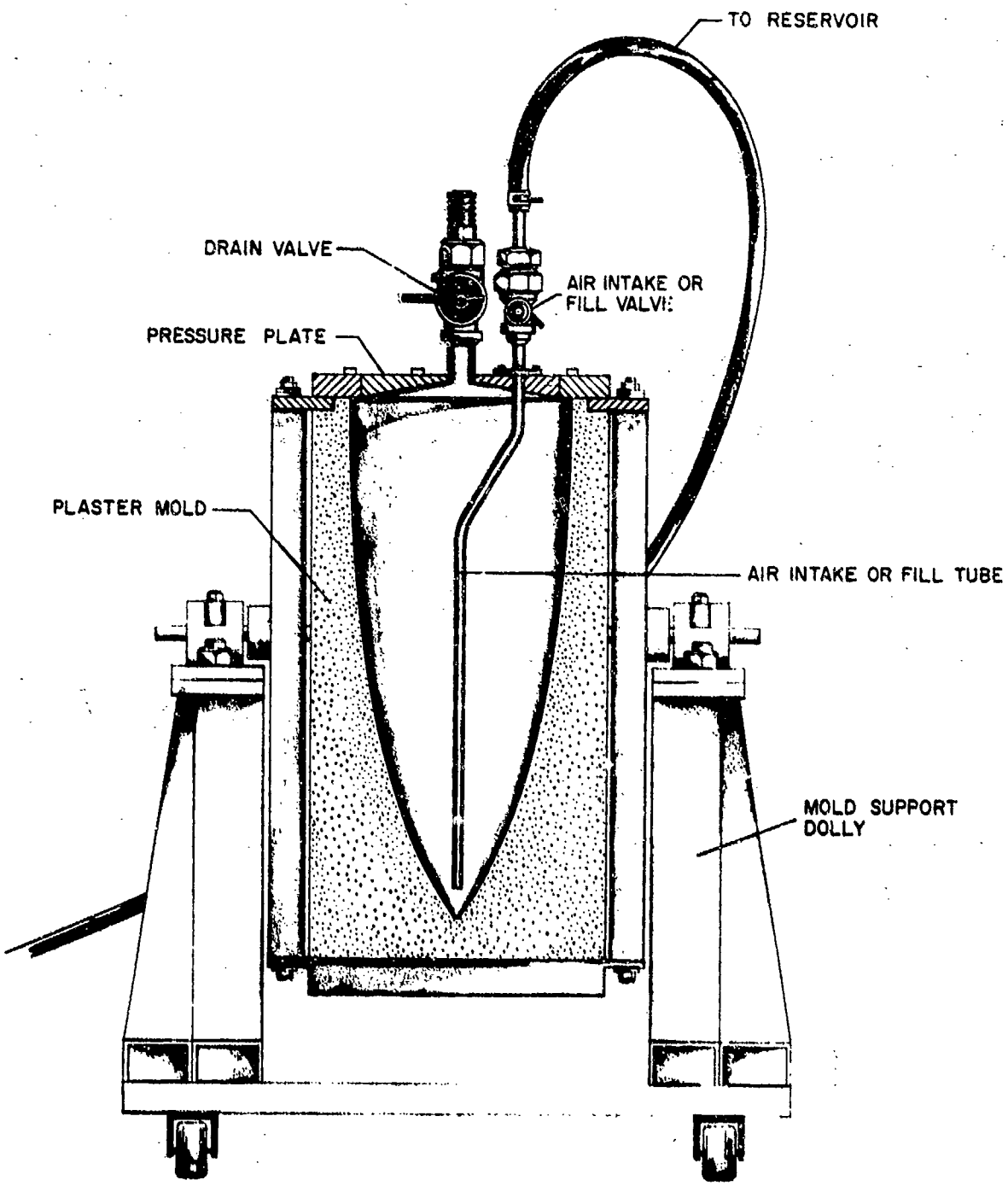


Figure 3-2. Typical Pressure Casting Setup for Slip Casting Fused Silica Radome.

and mold are in a horizontal position. It is assumed, however, that the dry radome has sufficient strength to withstand this stress. The mold is lifted away from the radome in preparation for further drying or firing.

In some cases due to radome geometry, wall thickness, and final tolerance requirements, it is desirable to move the freshly cast radome as little as possible so as to prevent any possibility of stressing the walls of the green casting. In this case the radome is cast, dried and fired with the tip up at all times. The radome mold is not moved from filling until the radome is dried. The main purpose of this technique is to eliminate any strains in the radome that might occur due to wall flexing during mold rotation. The mold is filled and drained from the base end. The radome remains in the mold until it has dried sufficiently to withstand movement without flexing its walls.

As soon as the excess slip is removed, the radome casting begins to dry and shrink away from the walls. The mold walls provide no support. Therefore, it is most important that the mold not be moved or vibrated in any manner for several hours. For satisfactory completion of drying and for removal of the radome from the mold, the pressure plate and internal displacement mandrel used in casting must be removed. Special handling tools and techniques are required to be sure the radome does not fall out of the mold during this operation.

## 3.4 Drying

Drying is a critical portion of the fabrication process, particularly for large shapes. At the end of casting, the pore spaces in the cast part are filled with water, and a thin film of water surrounds each particle.

Since the particles are not in direct contact but are cushioned by a water layer, the cast part has very little strength and will slump slightly if removed from the mold. At this point, castings from slips with 7 to 8 μm mean particle diameters will contain approximately 8.5 to 10 per cent water, depending on the packing efficiency of the particle size distribution.

As drying progresses, water is removed from the system, bringing the particles closer together until finally, at the "critical moisture content," the particles are in contact. Numerous studies have indicated that the bulk of the drying shrinkage occurs during this period. Measured values for drying shrinkage of castings from 7 to 8 μm mean particle diameter silica slips indicate drying shrinkages in the range from 0.05 to 0.1 per cent. Since these measurements were referenced to model size rather than actual mold size, the linear drying shrinkage is more probably in the range from 0.2 to 0.4 per cent, allowing for plaster mold setting expansion of approximately 0.2 per cent. This small shrinkage corresponds to a small moisture reduction on the order of 0.5 to 0.7 per cent. At this point, and certainly by the time 1.0 per cent moisture has been removed from the cast part, the part may be safely removed from the mold.

Thus the two most important points in drying large slip-cast fused silica shapes are:

(1) Drying should be carried out in the mold until the moisture content drops below the critical point (from 0.5 to 1 per cent loss).

(2) Drying rate during this time should be slow enough that moisture gradients across the cast wall are not large enough to cause

cracking from differential shrinkage. These conditions are difficult to estimate or define from existing data and must be determined by trial and error for the particular part and mold configuration used (drying rate is also restricted by mean particle diameter. More finely ground slips will form cast parts with smaller and, therefore, less permeable pores).

After the critical moisture content is reached, the part may be rapidly dried. Small shapes have been successfully dried at 350° F, but for most shapes it is recommended that drying temperatures be kept below 125° F. After the moisture content has been reduced to 1 or 2 per cent, the part should be dried to at least 250° and preferably 350° F before sintering.

The dried part must be handled with care as it has low strength. Fleming 11/ reports a dry strength of approximately 160 psi at a porosity of 17.8 per cent (~ 1.81 $gm/cm^3$), while Pivinskii and Gorobets 12/ report values from 425 to 1065 psi at bulk densities from 1.92 to 2.03 $gm/cm^3$ (Flemings values are more consistent with bulk densities achieved with commercially available slips). Harris, et al. 13/ reported dynamic Young's moduli from 4.2 to 5.6 x $10^5$ psi at bulk densities from 1.845 to 1.852 $gm/cm^3$.

The following are offered as examples of drying problems that have been encountered:

Example 1: In fabricating 18-inch diameter by 1-inch thick plates and 12 x 24 x 3/4-inch plates, drying warpage and cracking were severe. The warpage resulted from shrinkage on the face exposed to air. The problem was solved by two similar methods. First, the cast disk was sandwiched between two 1-1/2-inch thick slabs of plaster. Saturated kaolin wool fiber was used

to separate the part and plaster slabs. The part was allowed to dry through the plaster. The slow drying (up to 2 weeks) eliminated warpage and cracking. Similarly, the rectangular plate was left in the mold and covered with a layer of wet kaolin wool, followed by a wet plaster slab. Again, the resulting slow drying eliminated warpage and cracking.

Example 2: An 18-inch base diameter by 52-inch high radome shape cracked both in the mold and after removal from the mold. Cracking was eliminated by leaving the mold cavity sealed for 5 days. At this time the displacement mandrel could be removed without stressing the shape, and the shape could be safely removed and dried at room temperature. In this case, leaving the shape sealed in the mold and undisturbed for 5 days was sufficient to dry the shape past the critical moisture content.

Example 3: The shape described in the previous example, was cast from a slip exhibiting aging, by a radome manufacturer. A thinner walled shape, 18-inch base diameter by 40-inch in length was cast at Georgia Tech using slip from the same batch. In both cases drying had to be lengthened to three weeks. The drying conditions outside the mold were in the range 80° to 95° F and 30 to 50 per cent relative humidity. The extreme drying time suggested an abundance of sub-micron particles in the slip, but particle size analysis by sedimentation and scanning electron microscope failed to confirm this. Drying time less than three weeks resulted in longitudinal cracks in the radome wall on removal from the mold.

## 3.5 Sintering

Sintering is the further consolidation of the aggregate of fine particles

of amorphous silica upon heating. This heating is normally carried out at temperatures between 2100° and 2300° F.

During sintering, a mechanical bond is formed between the particles of the casting, increasing both density and mechanical properties. The sintering process is affected by a number of variables. Among them are chemical purity of the fused silica, time and temperature of sintering, sintering atmosphere, and particle size of the silica slip. Since many of the physical and mechanical properties of the sintered casting are somewhat interdependent, it is not possible to reach optimal property levels for all properties simultaneously. For example, maximum flexural strength is reached under conditions different from those necessary for minimum porosity. For this reason, sintering schedules must be determined by the end use of the casting.

During sintering, two competing processes are occurring as shown schematically in Figure 3-3. First, strengthening is occurring by an increase in the bond between particles and by a resulting increase in the density of the casting, both due to sintering. The second process is devitrification; at temperatures over 2000° F, vitreous silica crystallizes to form β-cristobalite. When the casting is cooled, the β-cristobalite changes to a higher density form α-cristobalite between 400° and 480° F (200 to 250° C). The accompanying 3 per cent volume shrinkage is sufficient to set-up microcracks in the structure and to weaken it noticeably. At some point in sintering, the strengthening effect of sintering is balanced by the weakening effect of cristobalite, and property values begin to fall. In this way, property values such as modulus of rupture, tensile strength, Young's Modulus, etc., all reach maximum values, followed by a decline in property levels as sintering continues.

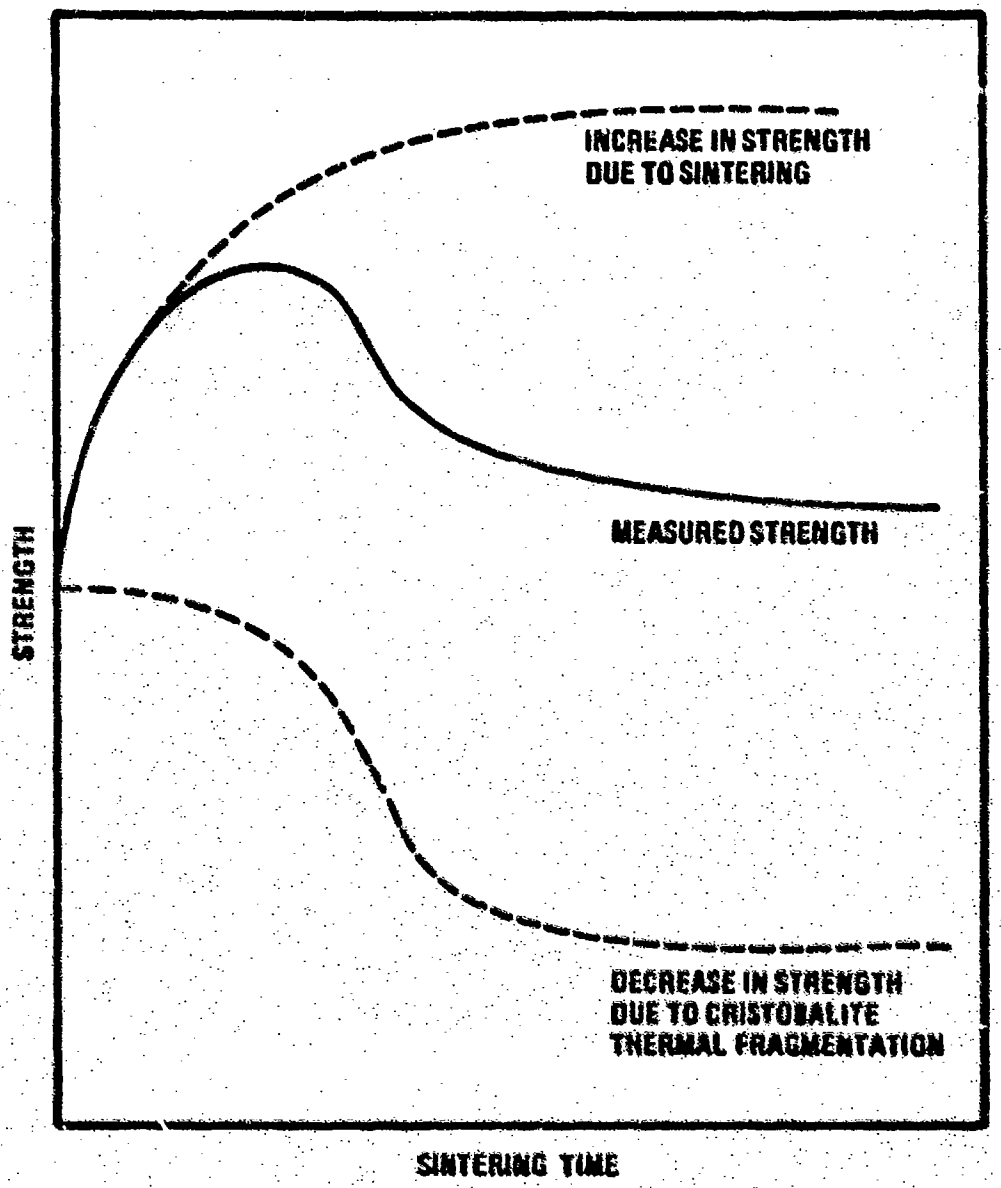


Figure 3-3. Hypothetical Strengthening Processes in Slip-Cast Fused Silica. (Reference 14, page 7.)

### 3.5.1 Effect of Chemical Purity on Sintering

Since the amount of cristobalite formed during sintering limits the amount of densification and strengthening during sintering, variations in the devitrification rate will determine limits on these properties. As discussed in Chapter 2, there are significant differences in the chemical analyses of technical grade and high purity slips. These differences are reflected in the devitrification rates of castings made from the two materials as shown in Figure 3-4. The curve for the technical grade material reflects data from a large number of technical grade slips produced over a period of 10 years. The currently available technical grade slips trend towards the right hand or lowest rate portion of the broad band. The high purity slips show a similar spread of values (distorted by the log scale), but the actual rates are much lower, permitting longer sintering times and higher values for modulus of rupture and bulk density, as well as lower values for porosity. Sintering properties of the two materials are compared in Figures 3-5, 3-6 and 3-7. The differences are not as pronounced at the lower temperature, but at 2400° F the differences are quite apparent. At 2250° F the technical grade slip goes through a porosity minimum while the high purity slip continues to decrease. At 2400° F the technical grade slip reaches a minimum porosity of around 10 per cent, and the high purity material sinters to less than one per cent porosity. Similar behavior is shown for bulk density. In both cases the reversal in the bulk density and porosity curves for the technical grade material is believed to result from excessive cristobalite formation, followed by the beginning of sintering at a much slower rate in the cristobalite. While the modulus of rupture curves reach similar maxima at the lower temperature, the maximum for the high purity material is much broader, offering more

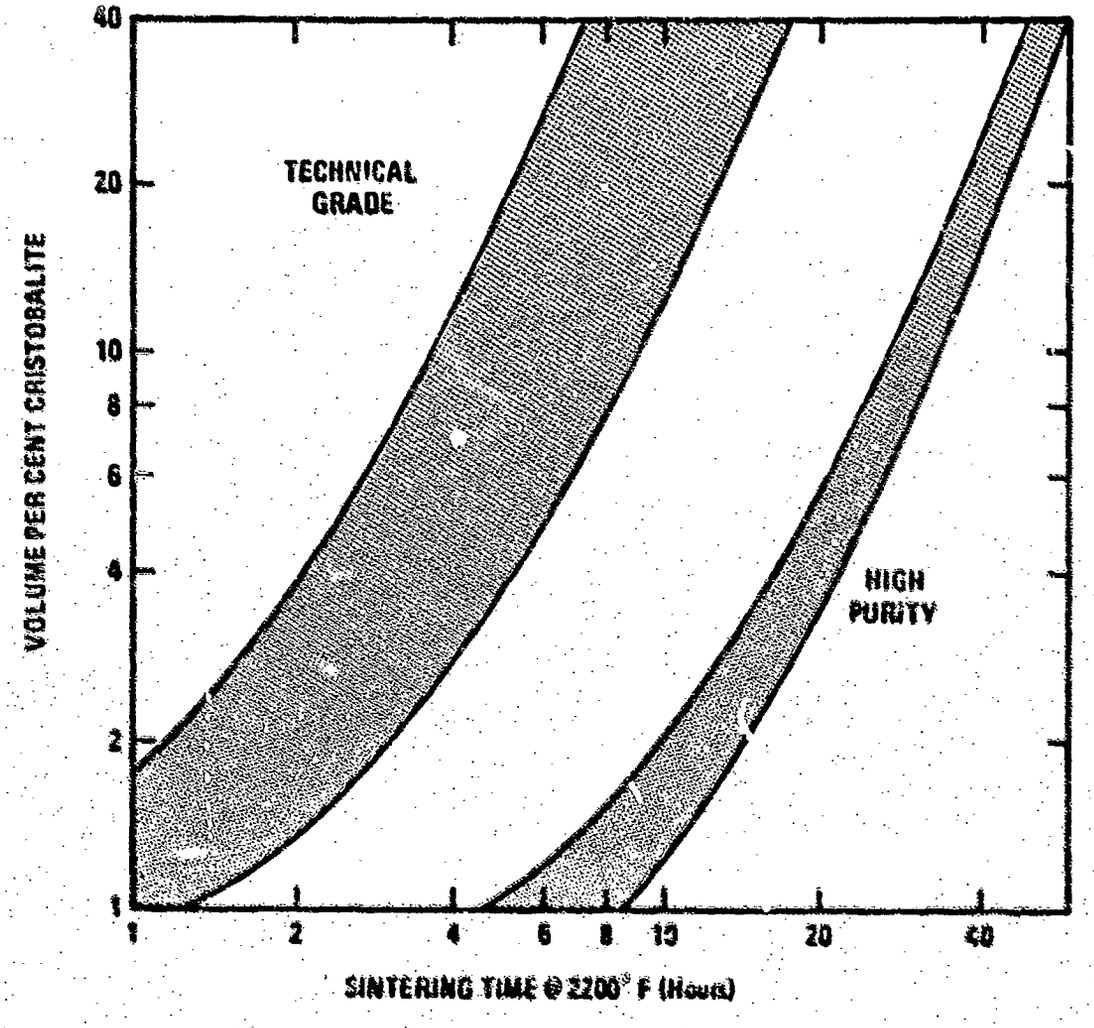


Figure 3-4. Cristobalite Content versus Sintering Time at 2200°F for Technical Grade and High Purity Slip-Cast Fused Silica. (Reference 15.)

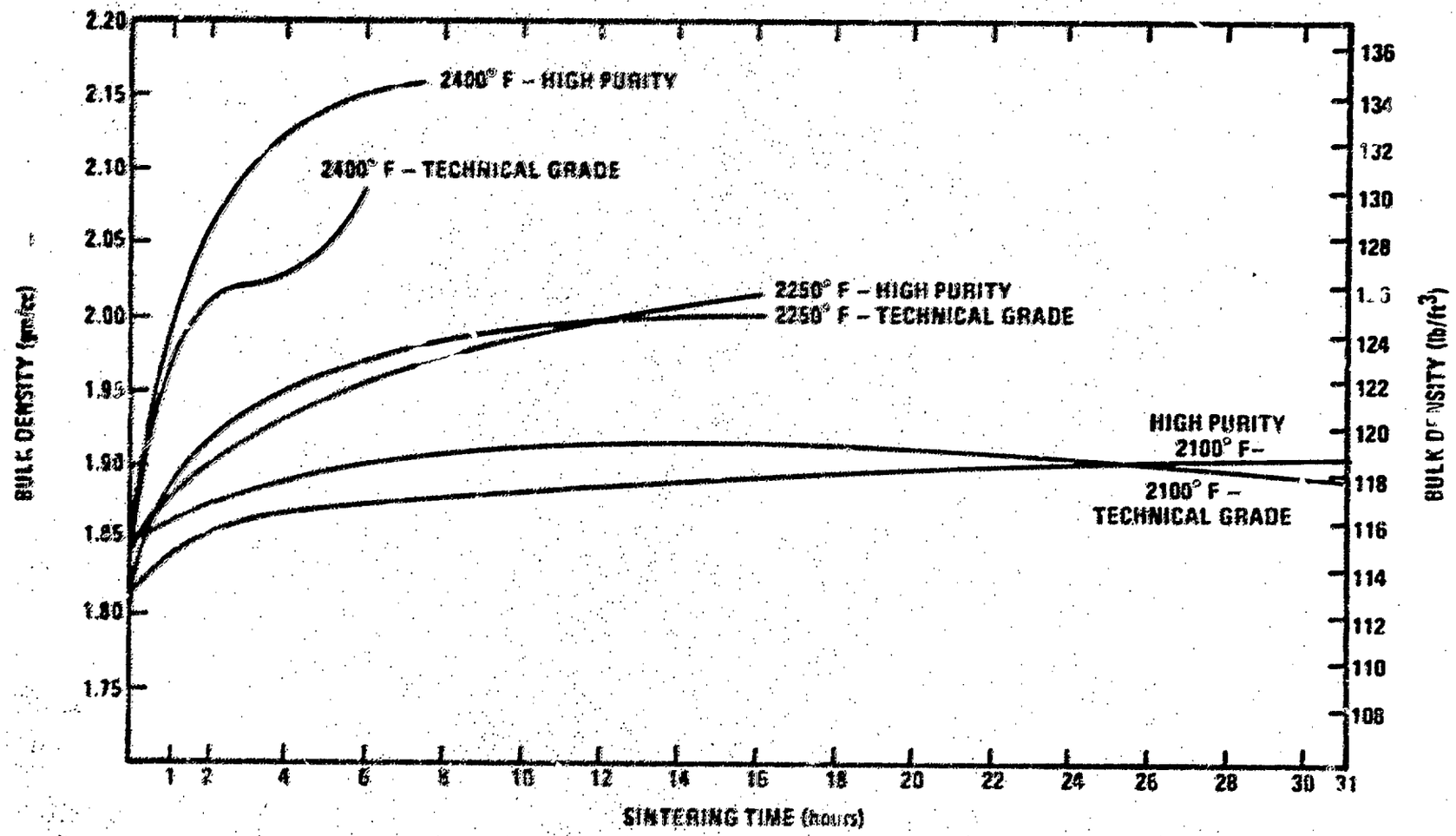


Figure 3-5. Bulk Density versus Sintering Time for High Purity and Technical Grade Fused Silica Slips Sintered at 2100°F, 2250° F, and 2400° F. (Reference 13, page 18.)

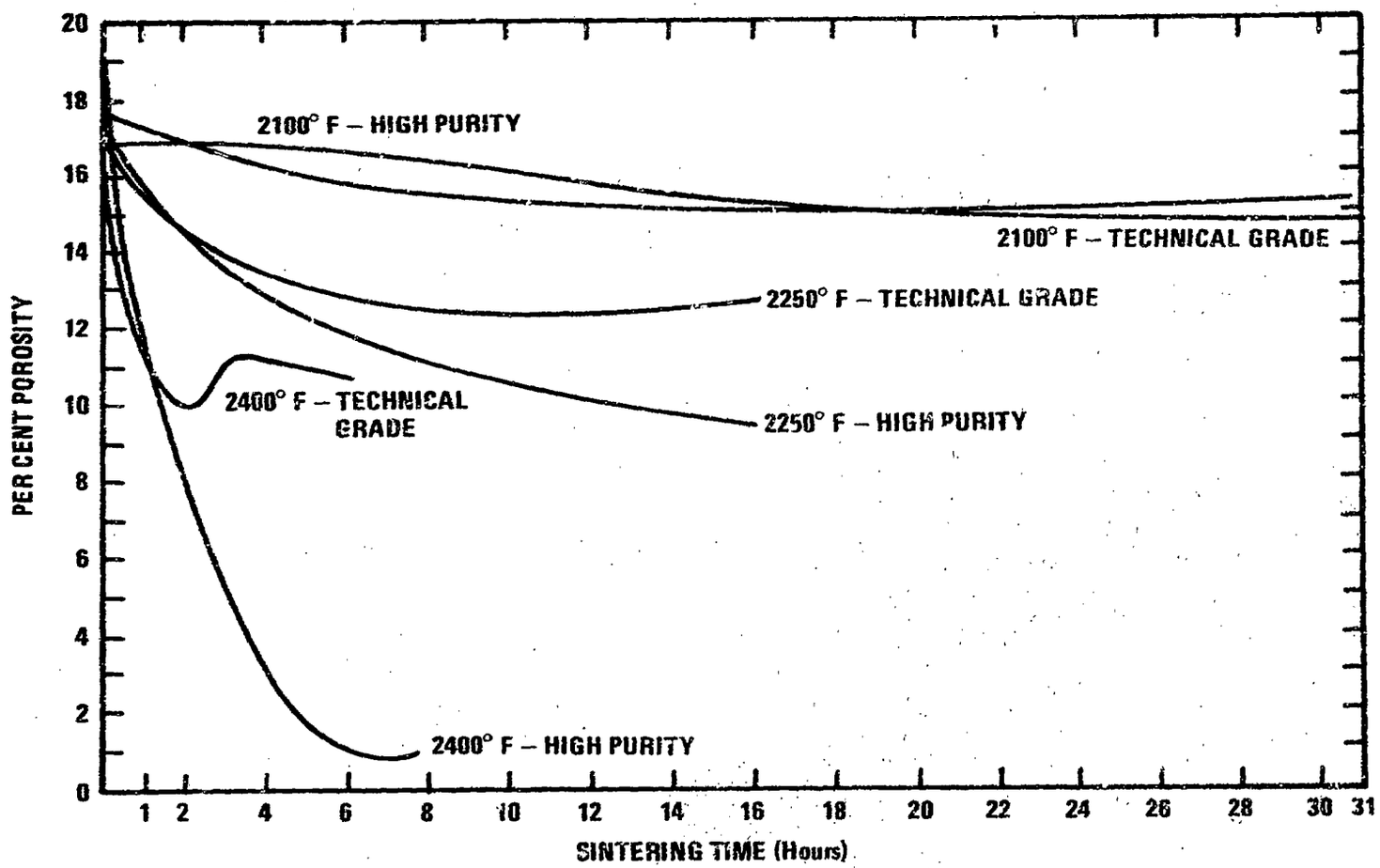


Figure 3-6. Per Cent Porosity versus Sintering Time for High Purity and Technical Grade Fused Silica Slips Sintered at 2100° F, 2250° F, and 2400° F. (Reference 13, page 17.)

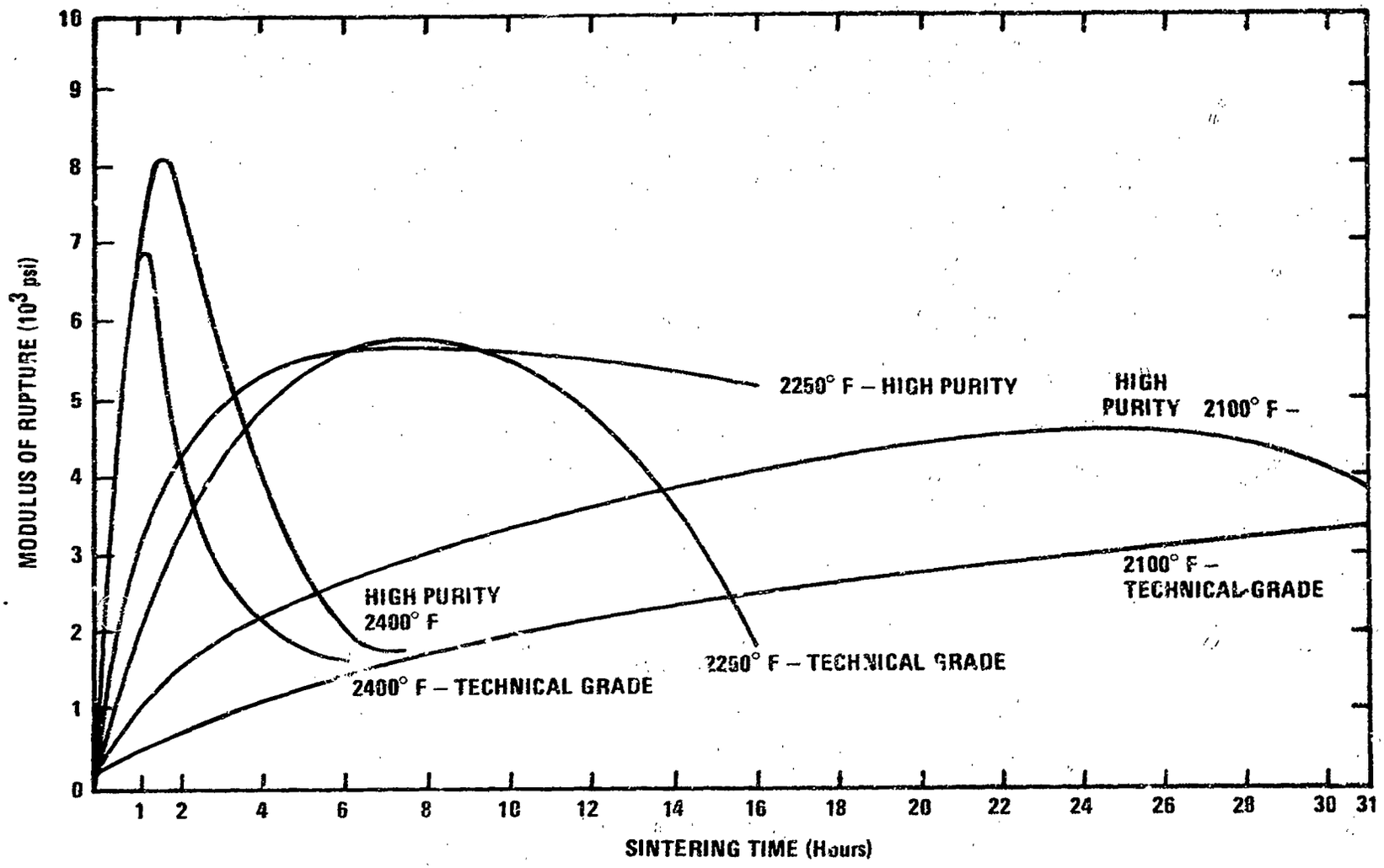


Figure 3-7. Modulus of Rupture versus Sintering Time for High Purity and Technical Grade Fused Silica Slips Sintered at 2100° F, 2250° F, and 2400° F. (Reference 13, page 16.)

easily controlled sintering. At the higher temperature, the high purity slip sinters to a higher modulus of rupture before excessive cristobalite formation occurs.

### 3.5.2 Effect of Time and Temperature on Sintering

Figures 3-8 and 3-9 show time-temperature-property level surfaces for porosity and modulus of rupture for a high purity slip with a mean particle size of 7 μm. Both figures show that by increasing temperature greater densification and strengthening is achieved. This result is due to the difference in activation energies for sintering and devitrification. Values for high purity slips were calculated as approximately 65 and 115 kcal/mole, respectively, by Harris and Theiling 13/. The higher activation energy for devitrification indicates that for a given increase in temperature the sintering rate will be increased more than the devitrification rate. In terms of Figure 3-3, the effect is to shift the maximum point further to the right.

For Figure 3-8, contours of porosity versus time at constant temperature are concave upward at low temperatures. As temperature increases, the curves become more linear until over a short interval a section with a concave-downward curvature is obtained. Such curvature is due to the beginning of formation of significant numbers of closed pores, which permit elimination of open porosity at bulk densities below theoretical density. Closed pores appear to be formed beginning at porosity levels of 9 to 10 per cent. This is in agreement with theoretical predictions 16/.

In Figure 3-9, contours of modulus of rupture versus time at constant temperature show a steady increase in maximum value and a corresponding

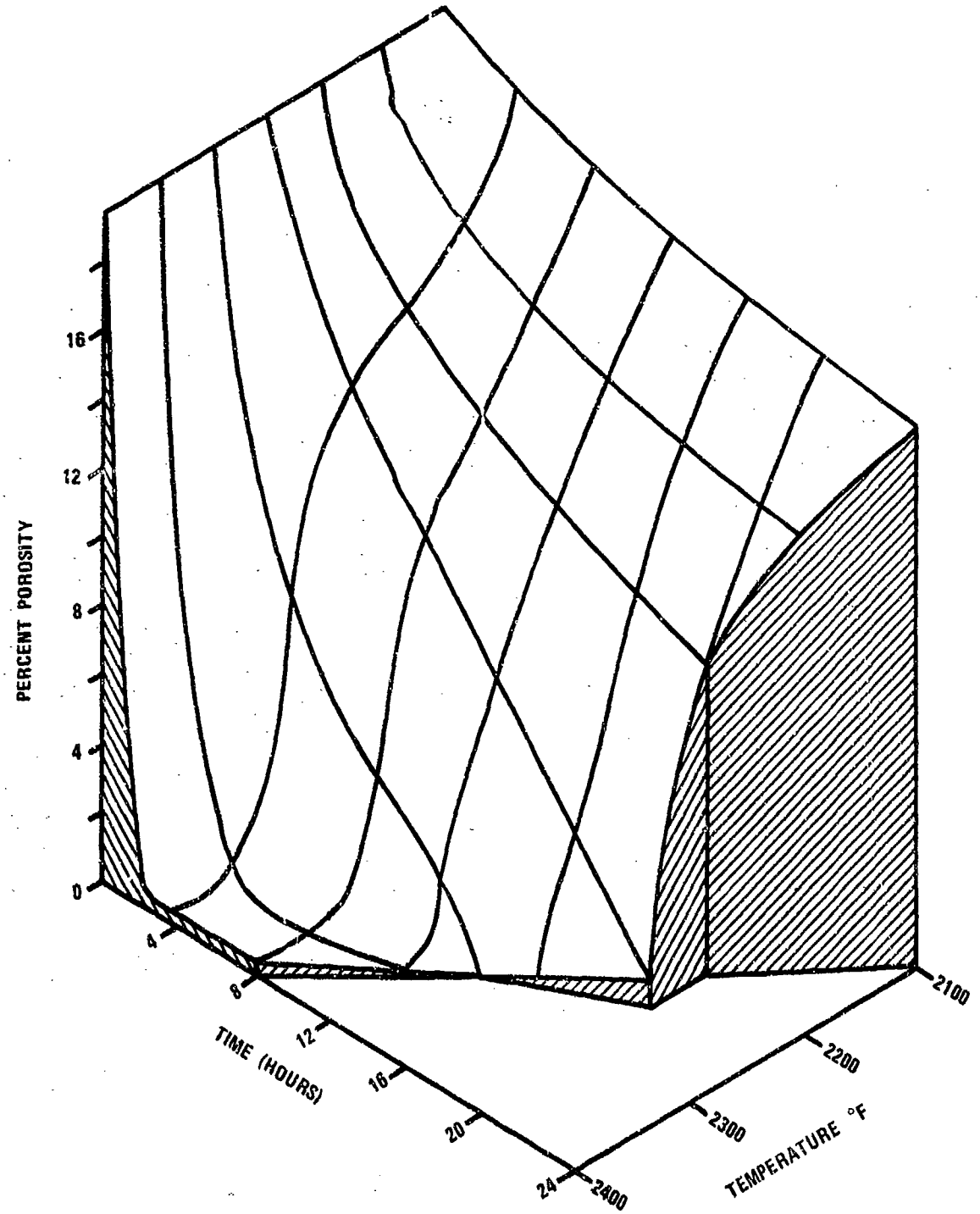


Figure 3-8. Porosity as a Function of Sintering Time and Temperature for High Purity Slip-Cast Fused Silica with 7 Micrometer Mean Particle Diameter.

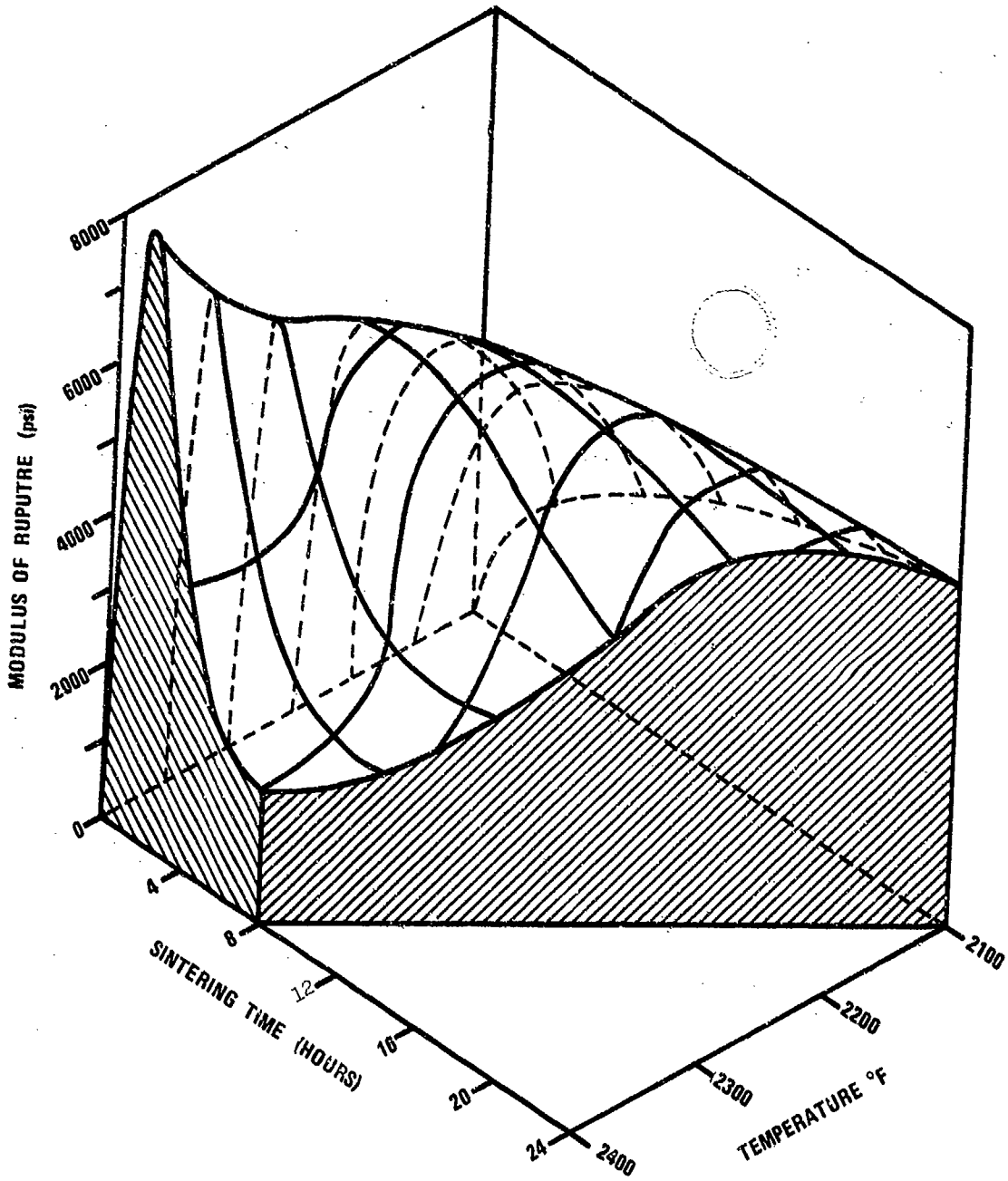


Figure 3-9. Modulus of Rupture as a Function of Sintering Time and Temperature for High Purity Slip-Cast Fused Silica with 7 Micrometer mean Particle Diameter.

decrease in peak breadth with increasing temperatures. At high temperatures, control of sintering time becomes increasingly critical, requiring a necessary trade-off of modulus of rupture and reproducibility of sintering conditions.

### 3.5.3 Effects of Atmosphere

The densification and devitrification rates for fused silica are affected by moisture and oxygen content of the surrounding atmosphere in much the same way as by temperature. A number of authors consider correct stoichiometry to be a prerequisite for devitrification 17,18,19/. In their view, most fused silicas, particularly the silicas produced by flame fusion processes, are oxygen deficient and must be oxidized in order for devitrification to proceed. By this view, water vapor serves as a source of oxygen. Another view is that the weakening effect of hydroxyl units in the silica glass structure catalyzes devitrification 18,20/. In either event, the effects are similar. Figures 3-10 and 3-11 show bulk density and modulus of rupture versus time for a 7-micron mean particle diameter technical grade slip. As expected, steam provides enhanced sintering, while argon retards sintering. Higher water partial pressure would be expected to provide further enhancement, while vacuum sintering would be expected to retard sintering further.

### 3.5.4 Effect of Particle Size on Sintering

Slips with lower mean particle diameters have greater specific surface area and a greater number of particle-particle contacts. This results in an increased sintering rate, particularly in the early stages of sintering. Figure 3-12 shows elastic modulus versus sintering time for three high purity slips with mean particle sizes of 4, 7 and 17 μm. The bulk density and

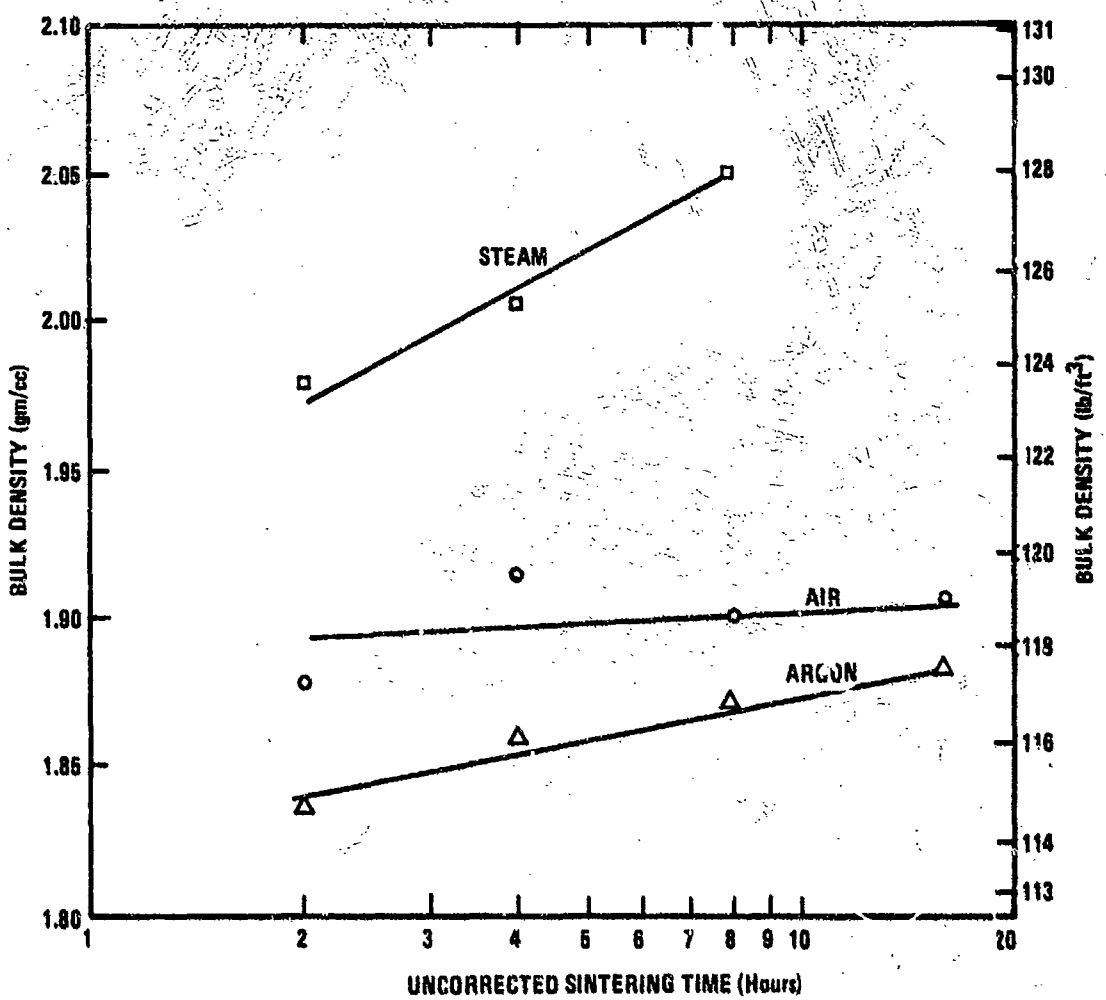


Figure 3-10. Bulk Density of Technical Grade Slip-Cast Fused Silica Fired in Different Atmospheres at 2200° F. (Reference 1, page 53.)

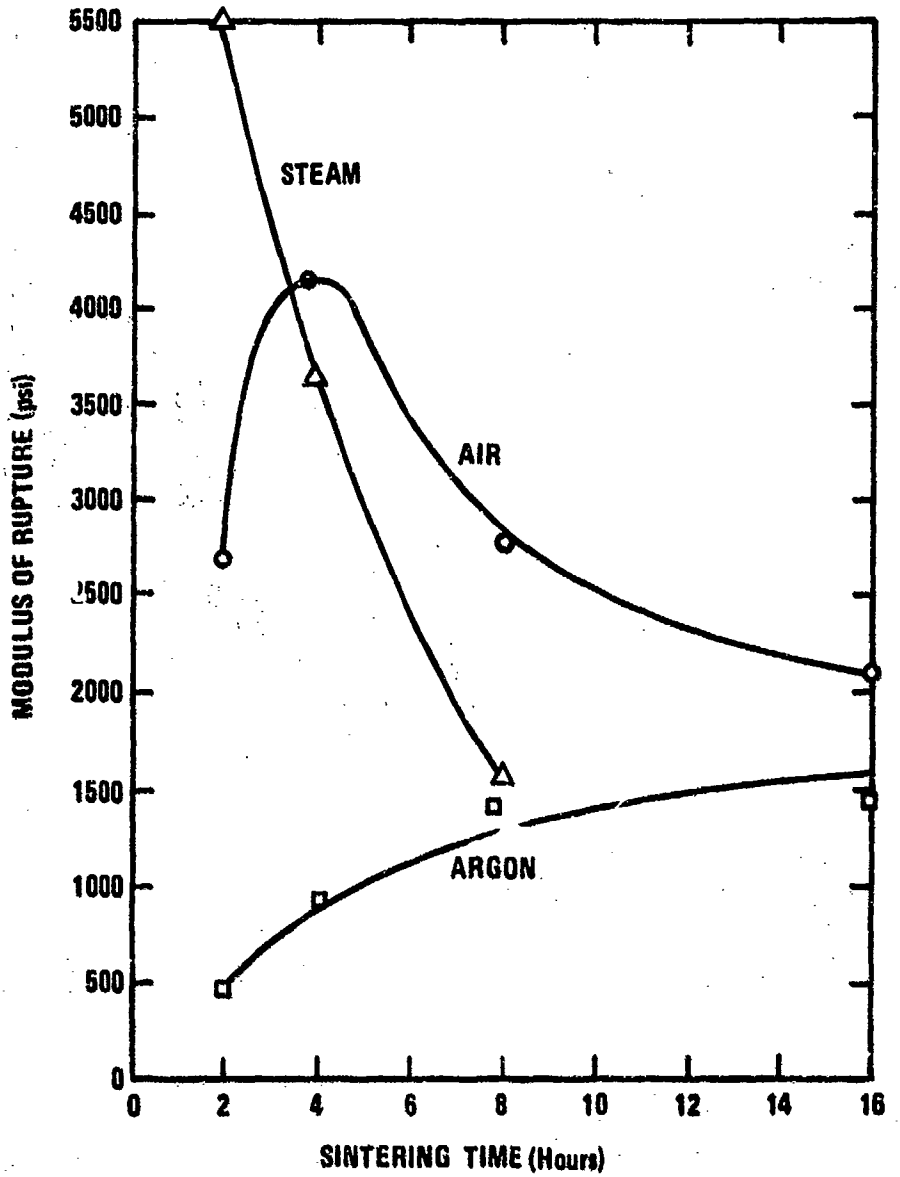


Figure 3-11. Modulus of Rupture of Technical Grade Slip-Cast Fused Silica Fired in Different Atmospheres at 2200° F. (Reference 11, page 54.)

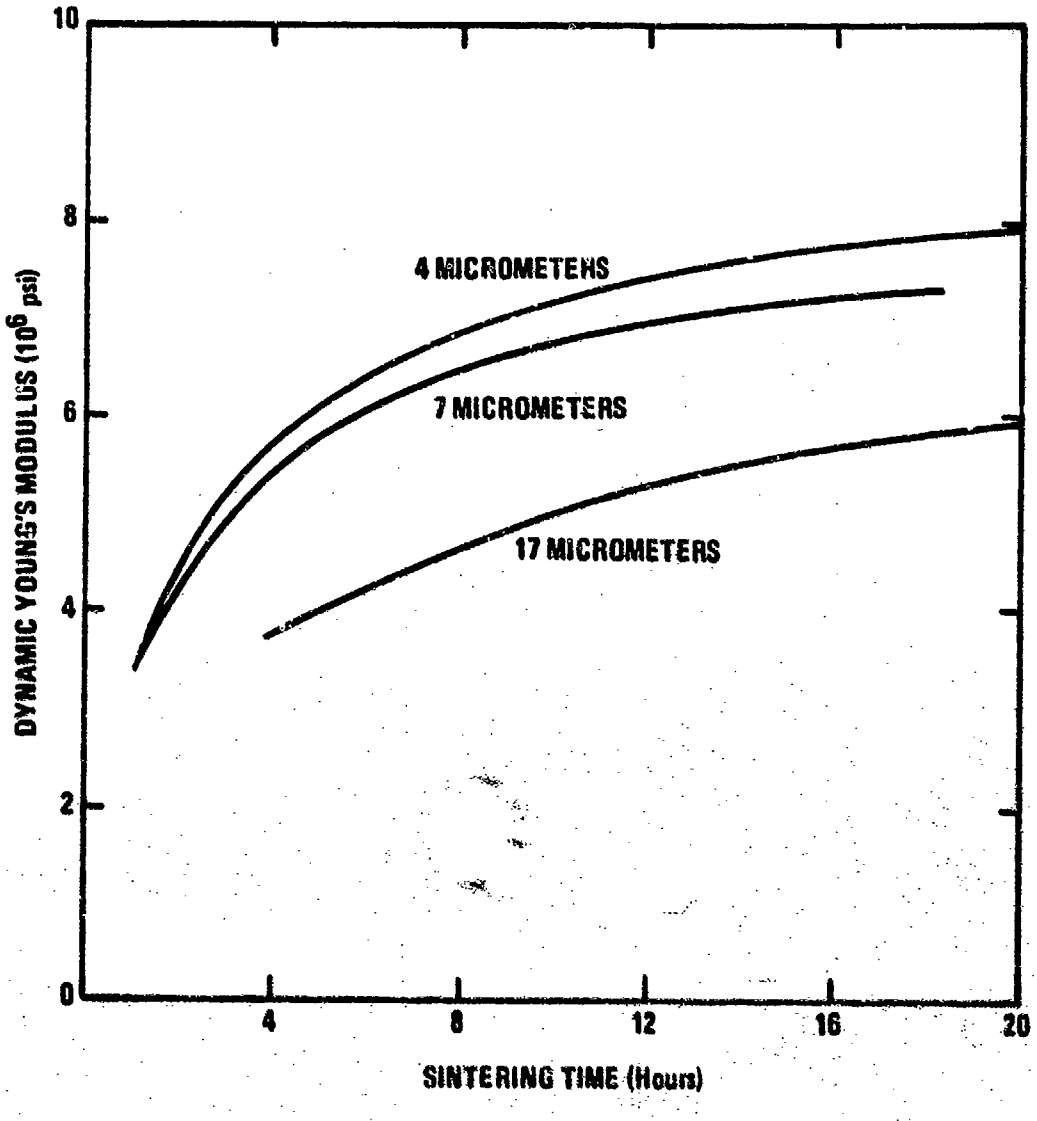


Figure 3-12. Dynamic Young's Modulus versus Sintering Time for High Purity Slip-Cast Fused Silica, with Mean Particle Diameters of 4, 7 and 17 Micrometers.

modulus of rupture curves show corresponding increases in slopes during the earliest portion of sintering. Despite the increased surface area of the more finely ground slips, no measurable effect of particle size on devitrification rate has been observed.

### 3.5.5 Selection of Sintering Conditions

The selection of sintering conditions must be dictated by the property requirements of the finished item, as well as by the capabilities of the fabricator's kilns. Figures 3-13 through 3-19 show room temperature values of bulk density, porosity, modulus of rupture and dynamic Young's modulus of elasticity for a technical grade slip and two high purity slips sintered at several temperatures for varying times. These illustrate the interdependence of several properties and can be used to establish tentative sintering schedules. Because of variations in temperature profiles and sintering characteristics in various fabricator's kilns, an actual sintering schedule must be determined by making trial firings with either the desired part or a similar shape. Radomes, for instance, may be replaced with closed-end cylinders for initial tests. The sintering temperature is again dependent on the actual hardware item. For example, one property which must be controlled in a radome is its dielectric constant. The dielectric constant is a function of the final bulk density. To insure a reproducible dielectric constant, as well as precise physical dimensions which will minimize machining, sintering should be carried out at temperatures from 2200° to 2250° F, where sintering rates are slow enough that sintering times can be controlled adequately. On the other hand, for a crucible application, where porosity should be minimal, the sintering temperatures should be in the range

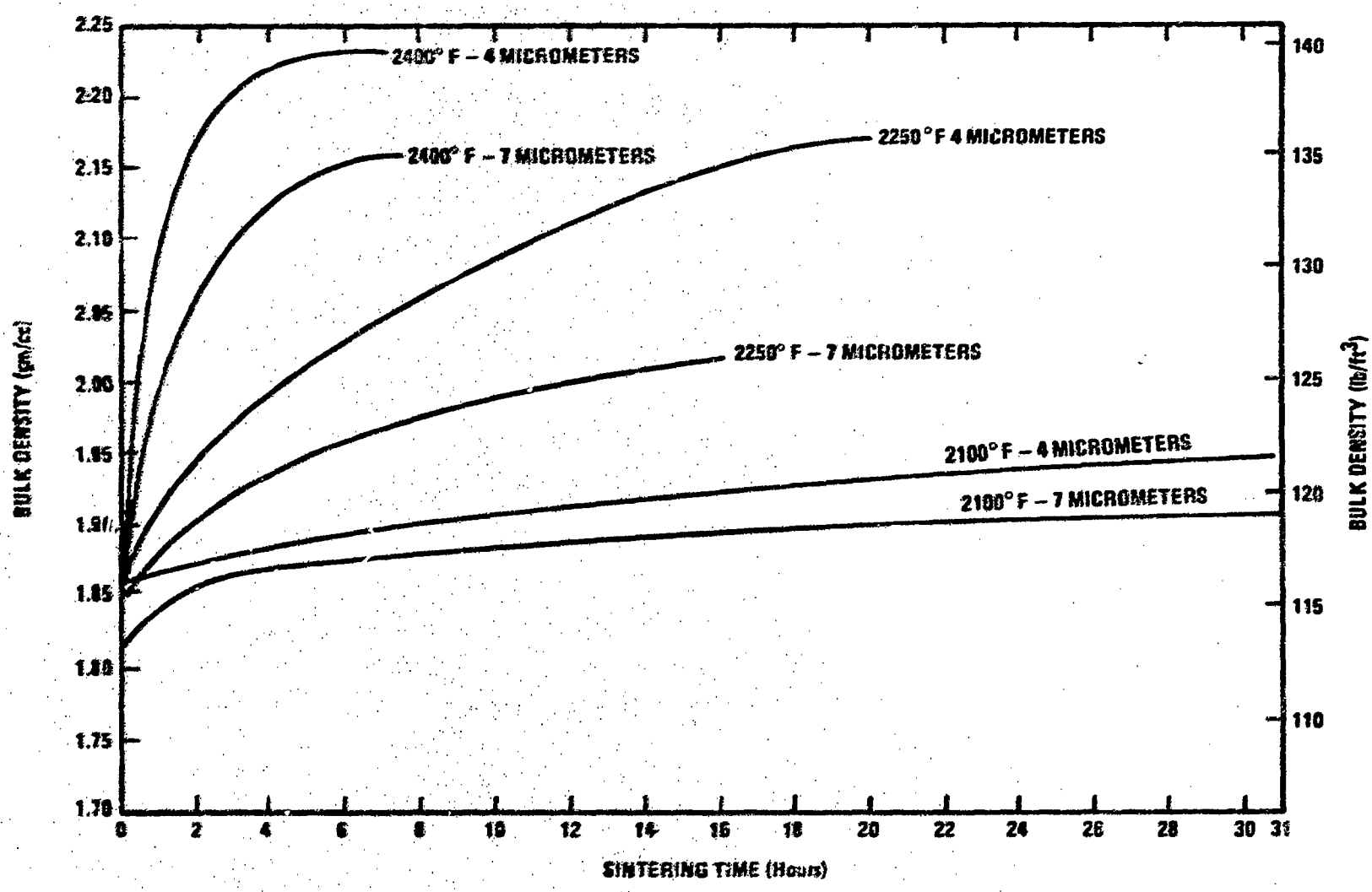


Figure 3-13. Bulk Density versus Sintering Time for High Purity Fused Silica Slips with Mean Particle Diameters of 4 and 7 Micrometers Sintered at 2100° F, 2250° F, and 2400° F. (Reference 13, page 18.)

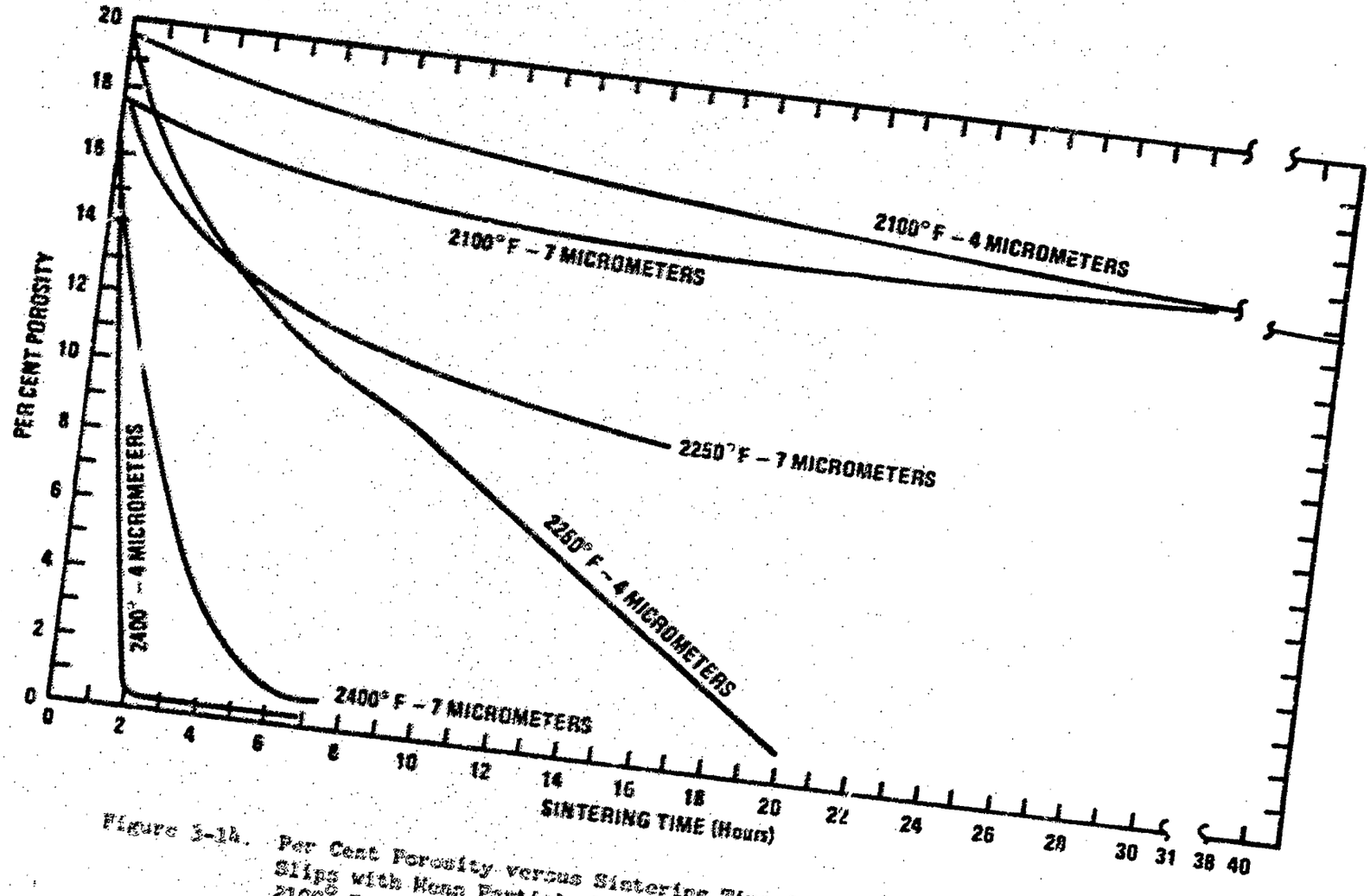


Figure 3-14. Per Cent Porosity versus Sintering Time for High Purity Fused Silica Slips with Mean Particle Diameters of 4 and 7 Micrometers Sintered at 2100° F, 2250° F, and 2400° F. (Reference 13, page 13.)

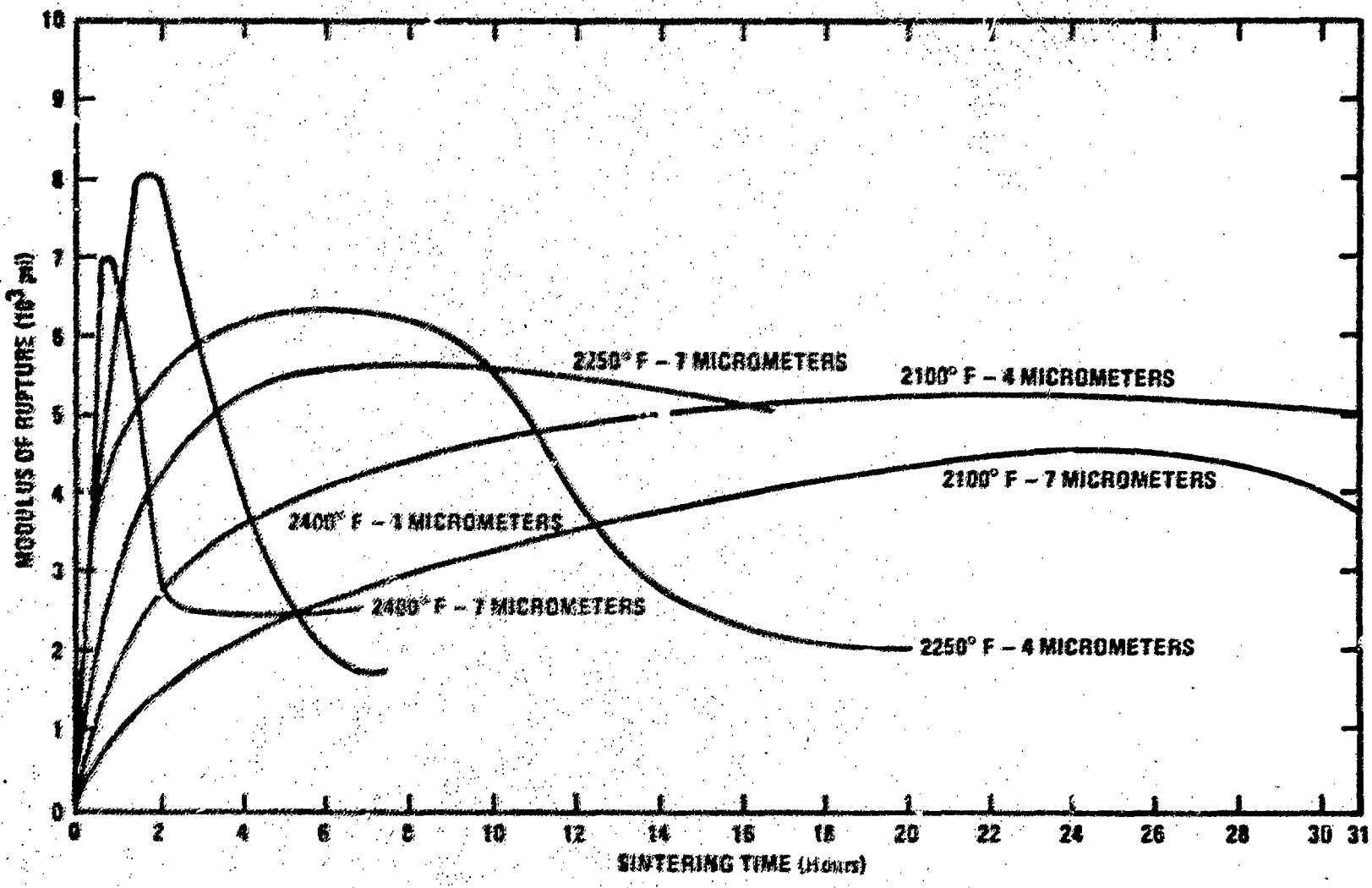


Figure 3-13. Modulus of Rupture versus Sintering Time for High Purity Fused Silica Slips with Mean Particle Diameters of 4 and 7 Micrometers Sintered at 2100° F, 2250° F, and 2400° F. (Reference 13, page 16.)

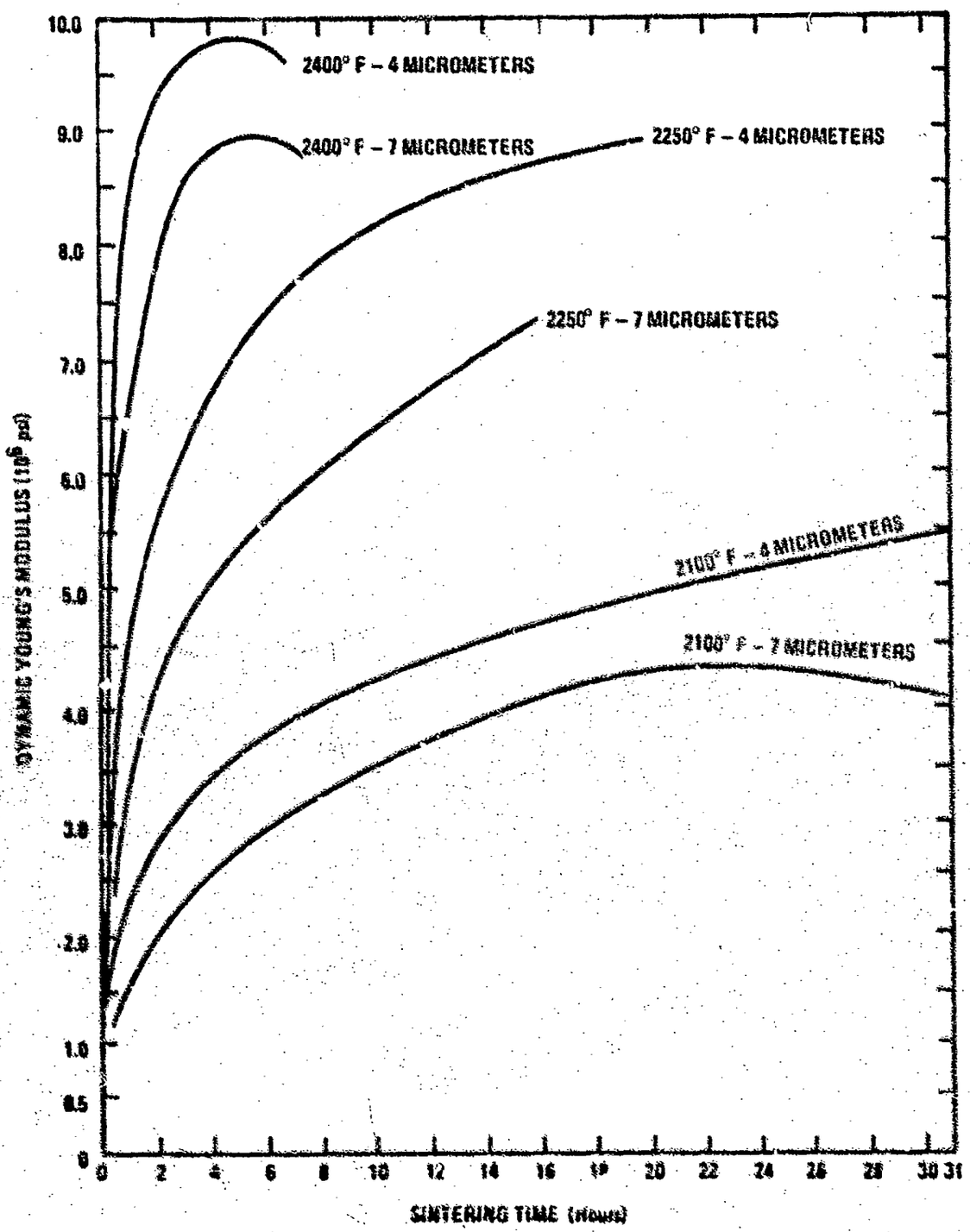


Figure 3-16. Dynamic Young's Modulus versus Sintering Time for High Purity Slip-Cast Fused Silica Prepared from Slips with Mean Particle Diameters of 4 and 7 Micrometers Sintered at 2100° F, 2250° F, and 2400° F. (Reference 15, page 18.)

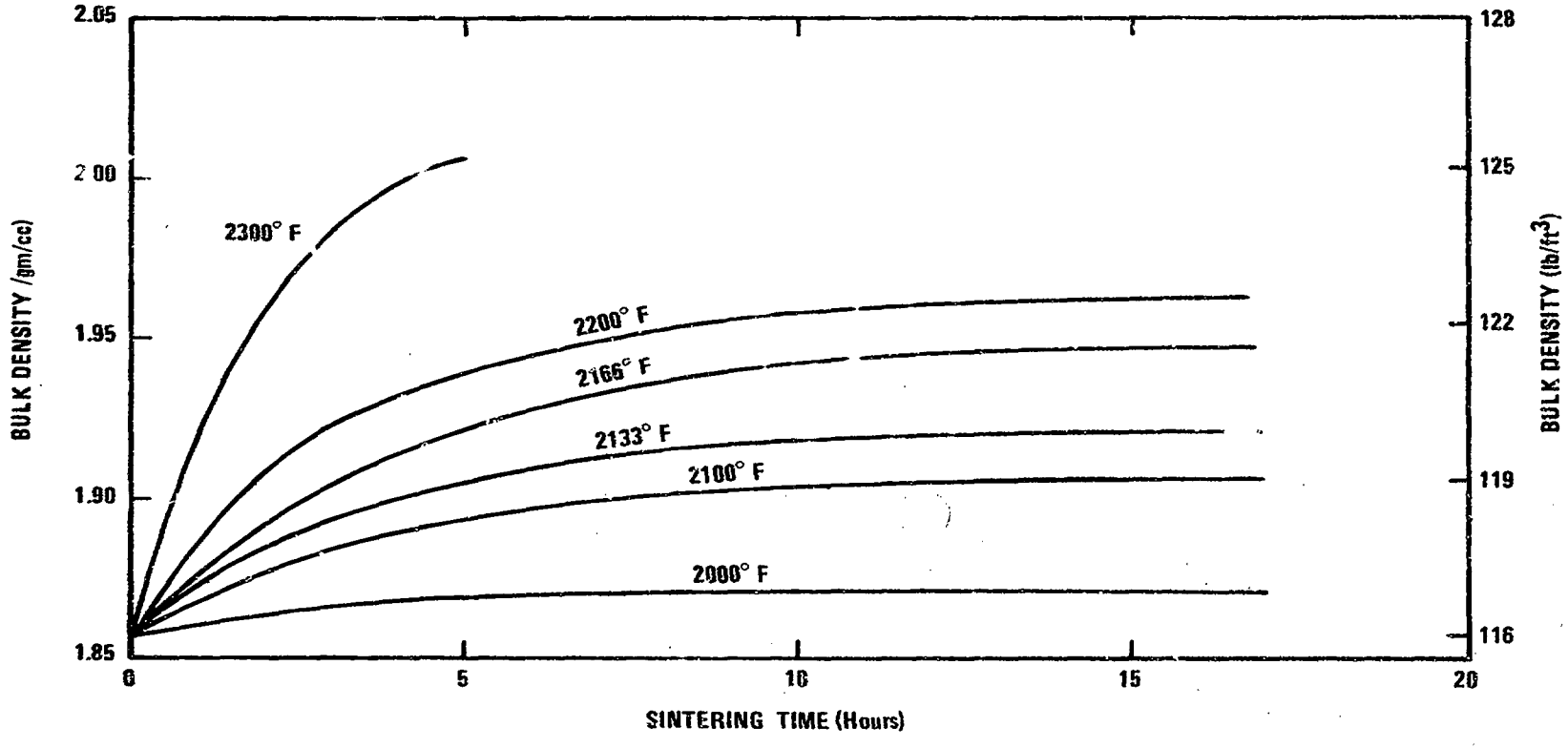


Figure 3-17. Bulk Density of Technical Grade Slip-Cast Fused Silica Fired in Air at One Atmosphere. (Reference 11, page 61.)

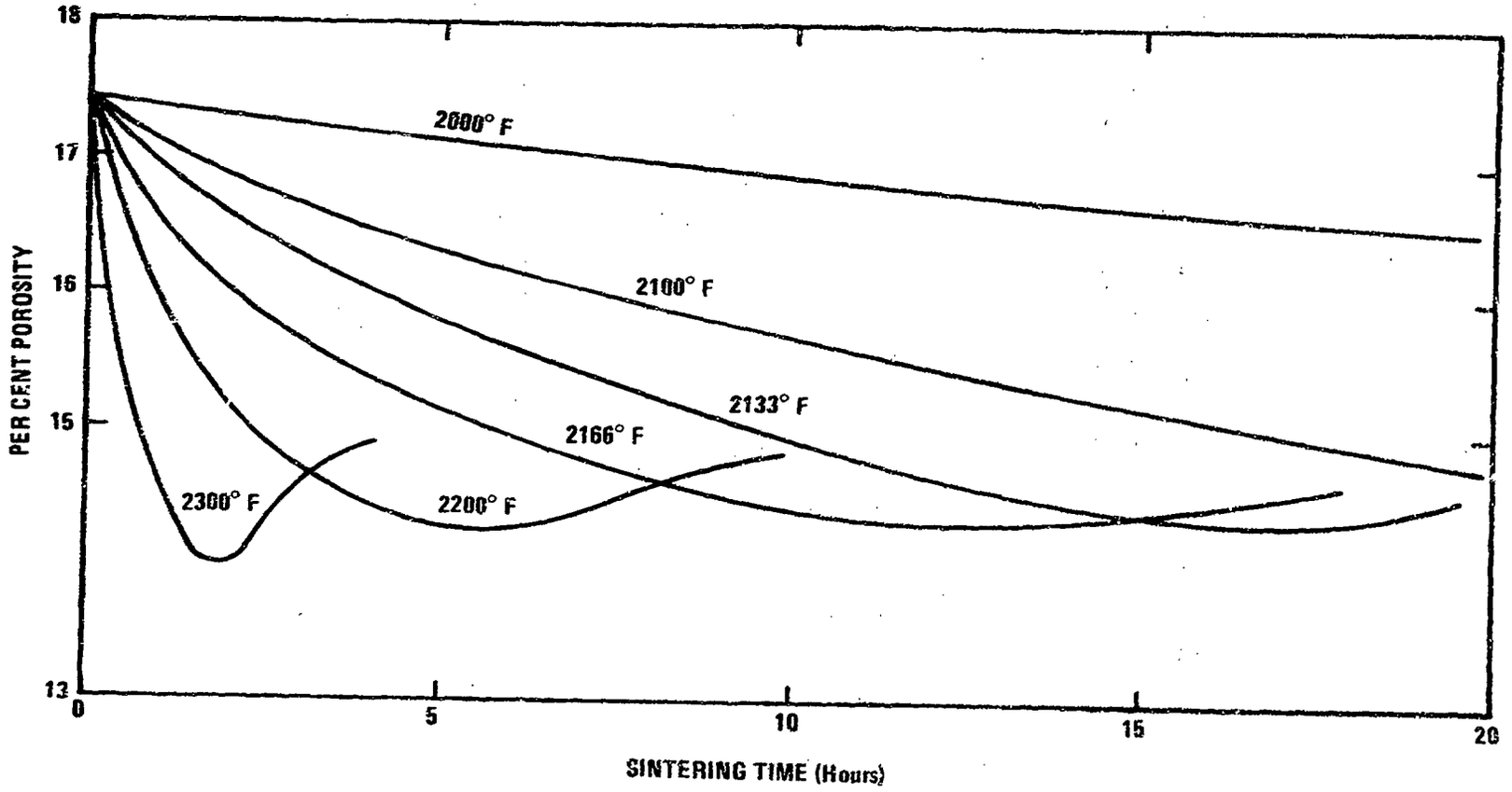


Figure 3-18. Porosity of Technical Grade Slip-Cast Fused Silica Fired in Air at One Atmosphere. (Reference 11, page 58.)

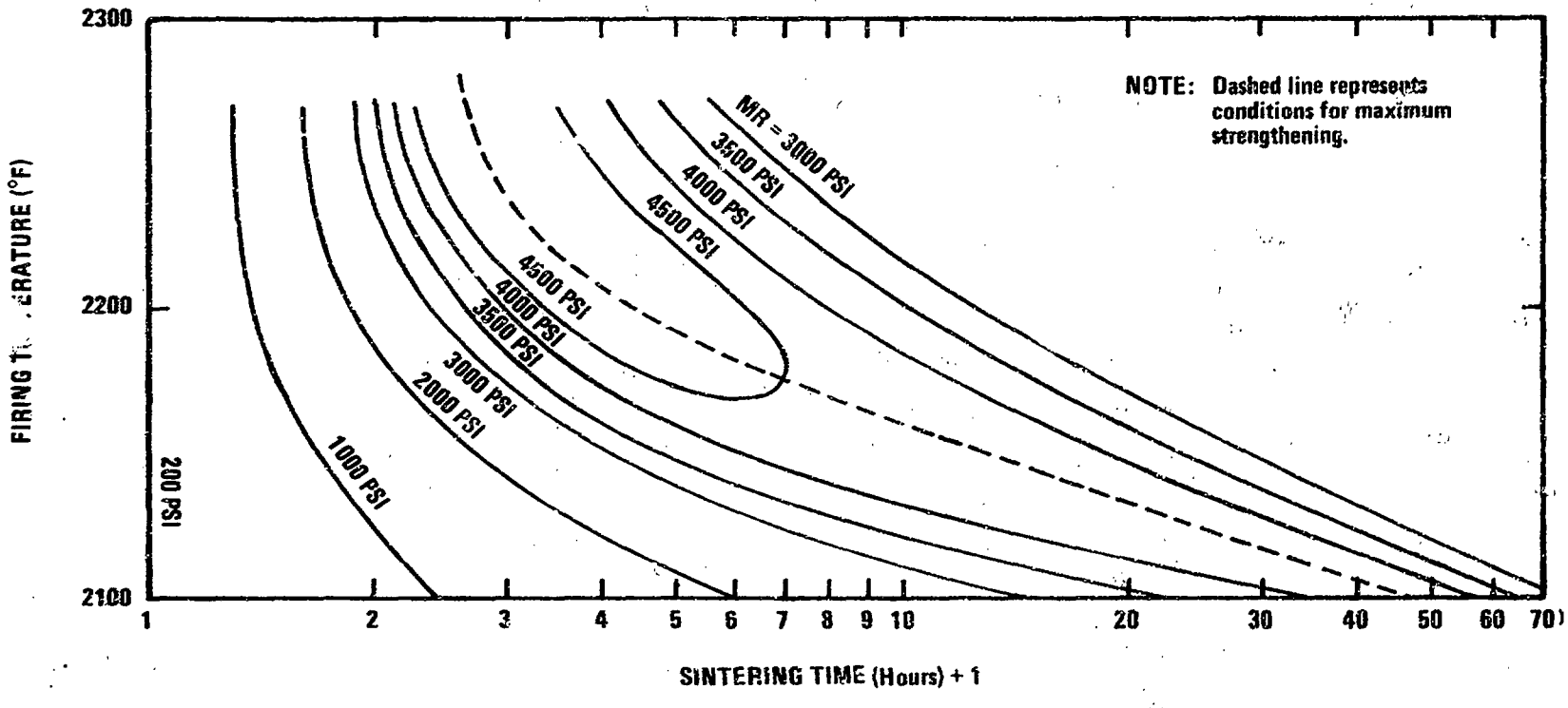


Figure 3-19. Modulus of Rupture of Technical Grade Slip-Cast Fused Silica Fired in Air at One Atmosphere. (Reference 11, page 55.)

of 2300° to 2500° F to insure an impervious part with some degree of mechanical strength.

With its low thermal expansion coefficient, it is virtually impossible to thermal shock a slip-cast fused silica part. Therefore, where bottom-loading kilns are available, thoroughly dried parts may be placed in a furnace preheated to the sintering temperature and removed and air quenched after sintering.

All of the data reported here were taken from slip-cast fused silica sintered in silicon carbide, electrical resistance heated kilns. Some commercial fabricators have used gas fired kilns, but it is felt that with the variations in flue gas moisture content and their effect on sintering more precise control is available with electrically heated kilns (see 3.5.3). PRECAUTIONARY NOTE: All of the data reported here for high purity fused silica slips were developed from non-aging slip, the material which has been used for the great bulk of high purity slip-cast fused silica. It is possible for slips which exhibit aging to exhibit a higher sintering rate than normal. Sintering times on the order of 60 to 70 per cent of the predicted terms have been observed. For this reason it should be emphasized that <u>SINTERING CONDITIONS SHOULD ALL WAYS BE VERIFIED WITH TRIAL FIRINGS BEFORE PRODUCTION HARDWARE IS SINTERED</u>, and sintering conditions should be rechecked periodically to insure that both material sintering rates and kiln conditions are remaining constant.

From a standpoint of minimizing property variations across the wall of a radome or other part, it is desirable to control heating rates at sintering temperatures so that the backside temperature remains within 10° F or so of the frontface temperature. To solve the necessary heat conduction

relationships, Boland 21/ has prepared a series of charts shown in Figures 3-20, 3-21 and 3-22. When using these charts, one calculates the value for the horizontal axis from the known temperature conditions. Once this value is obtained, the appropriate value of $\alpha\tau/R^2$ may be read off the vertical axis of the chart. From this time, heating rates may be calculated for the desired conditions. Examples of the type calculations that can be made are shown below.

Example 1

Property gradients can be minimized in slip-cast fused silica by minimizing the temperature differences in the silica whenever any part of the silica is at a temperature where the cristobalite growth rate is significant. Suppose a slip-cast fused silica radome with a wall thickness of 0.75 inch is to be fired at 2200° F. Cristobalite does not form rapidly at 2000° F or below, and the radome may be heated to 2000° F in almost any manner which is convenient. It would probably be most economical to heat the silica in the shortest possible time. Therefore, suppose the surface of the radome will be raised to 2000° F suddenly (as rapidly as possible), and then, after a suitable soak at 2000° F, the surface of the radome will be raised to 2200° F at a constant rate. How long should the radome be soaked at 2200° F?

Suppose the available experimental data indicate that the radome should be soaked at 2000° F until the backside temperature comes up to at least 1990° F.*

*A maximum allowable temperature differential of 10° F during initial heating has proven to be satisfactory at Georgia Tech for the firing of slip-cast fused silica components up to 0.75 inches in thickness.

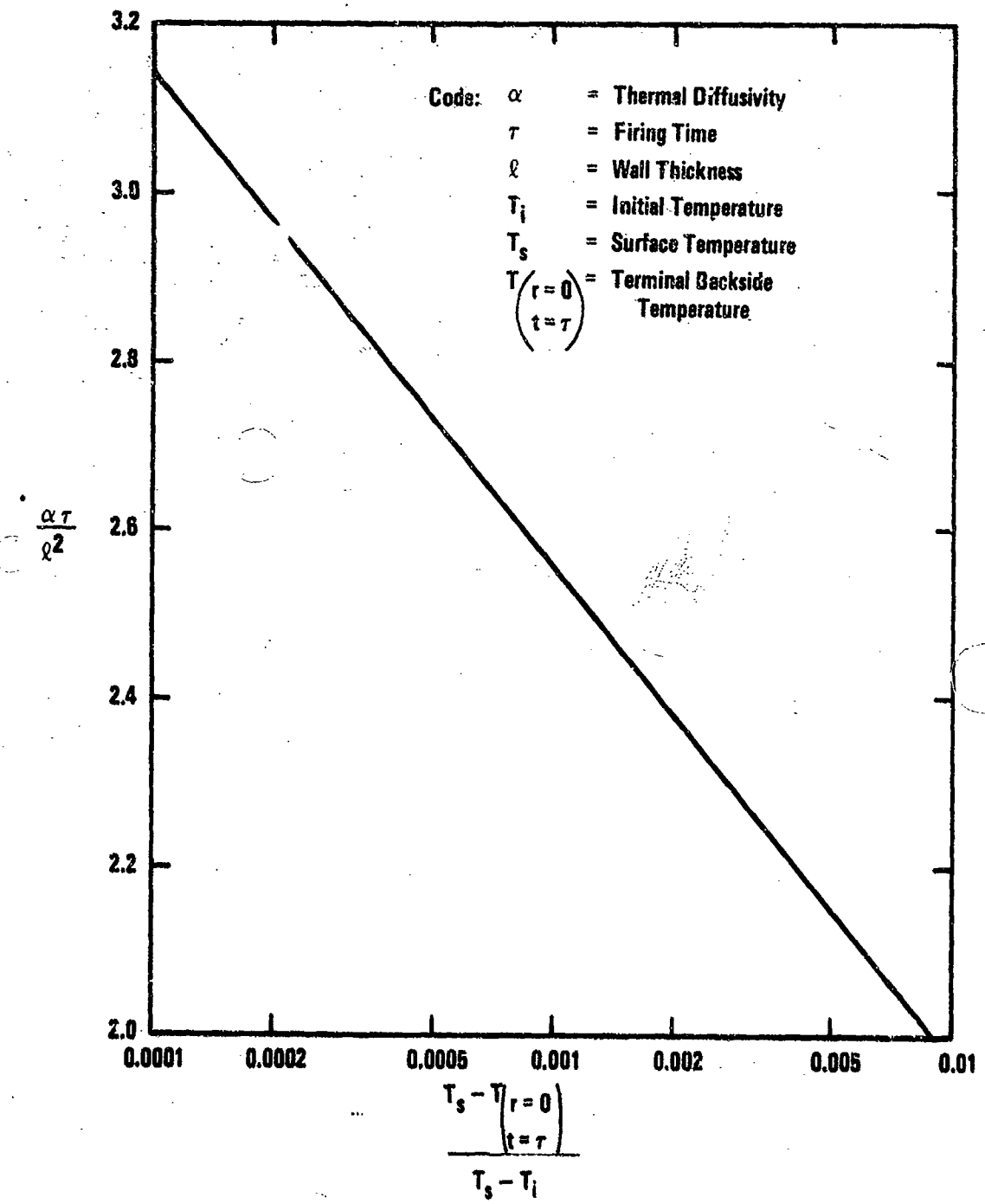


Figure 3-20. Transient Heat Conduction in a Radome Initially at Temperature $T_i$, as External Surface is Held at Temperature $T_s$ while Internal Surface is Insulated. (Reference 21, page 20.)

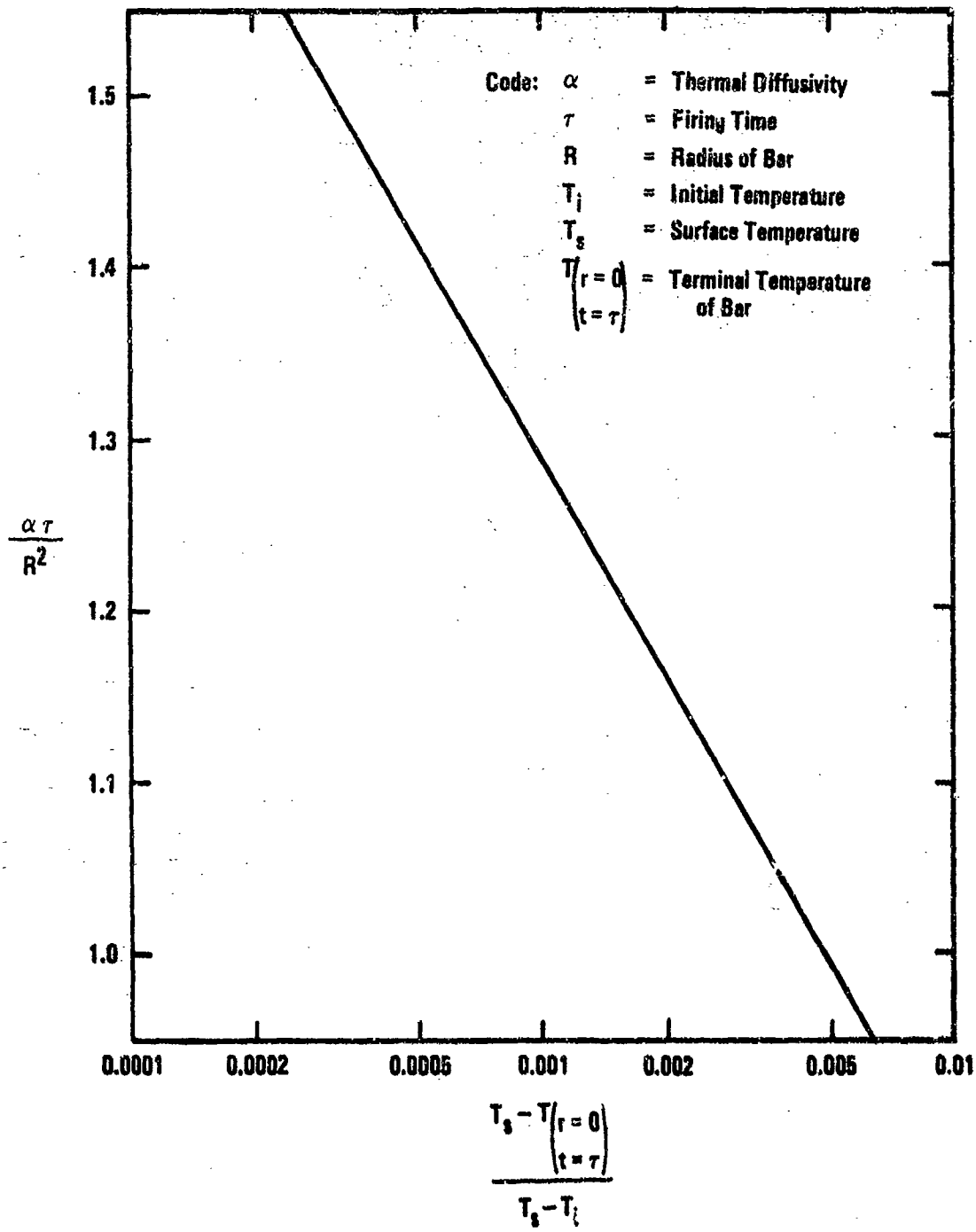


Figure 3-21. Transient Heat Conduction in a Cylindrical Test Bar, Initially at Temperature $T_i$, as the Surface is Held at Temperature $T_s$. (Reference 21, page 21.)

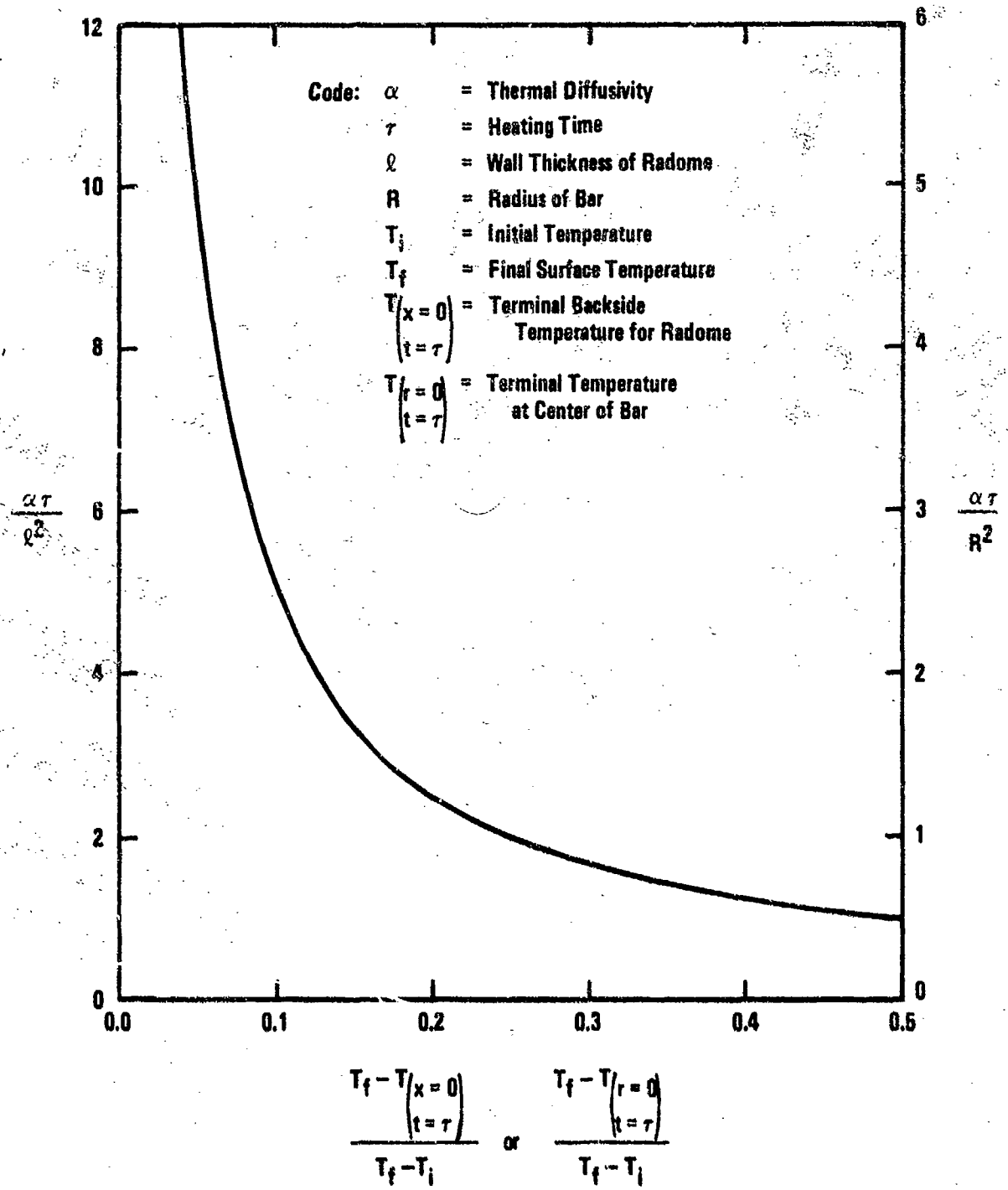


Figure 3-22. Transient Heat Conduction in a Radome or Cylindrical Test Bar Initially at Temperature $T_i$, as the Surface is Raised to a Temperature $T_f$ at a Constant Rate. (Reference 21, page 22.)

Then the question can be answered by referring to Figure 3-20:

$$T_s = 2000° \text{ F} \tag{3-6}$$

$$T_{\substack{x = 0 \\ t = \tau}} = 1990° \text{ F} \tag{3-7}$$

$$T_i = 70° \text{ F} \tag{3-8}$$

$$\frac{T_s - T_{\substack{x = 0 \\ t = \tau}}}{T_s - T_i} = \frac{10}{1930} \approx 0.00052 \tag{3-9}$$

$$\frac{\alpha \tau}{\ell^2} \approx 2.72 \text{ (from Figure 3-20)} \tag{3-10}$$

$$\tau \approx \frac{2.72\ \ell^2}{\alpha} \approx \frac{2.72\ (\frac{0.75}{12}\text{ ft})^2}{0.0114\ \text{ft}^2/\text{hr}} \approx 0.93 \text{ hr.} \tag{3-11}$$

The soak time at 2000° F need be only about 56 minutes. This number is conservative as the minimum value of the thermal diffusivity of the silica was used ($\alpha = 0.0114\ \text{ft}^2/\text{hr}$) 11/.

Example 2

How fast can the surface temperature of the radome, described in Example 1, be raised from 2000° to 2200° F, assuming the radome is initially at 2000° F uniformly?

Suppose the available experimental data indicate a maximum allowable

temperature differential of 20° F* in the radome while the temperature of the radome is, at any point, above 2000° F. Then the question can be answered by referring to Figure 3-22:

$$T_f = 2200° \text{ F} \tag{3-12}$$

$$T_{\begin{bmatrix} x = 0 \\ t = \tau \end{bmatrix}} = 2180° \text{ F} \tag{3-13}$$

$$T_i = 2000° \text{ F} \tag{3-14}$$

$$\frac{T_f - T_{\begin{bmatrix} x = 0 \\ t = \tau \end{bmatrix}}}{T_f - T_i} = 0.10 \tag{3-15}$$

$$\frac{\alpha \tau}{\ell^2} \approx 5.0 \text{ (from Figure 22)} \tag{3-16}$$

$$\tau \approx \frac{5\ \ell^2}{\alpha} \approx \frac{5\ (\frac{0.75}{12}\ \text{ft})^2}{0.0114\ \text{ft}^2/\text{hr}} = 1.71 \text{ hr.} \tag{3-17}$$

The surface temperature of the radome should be raised from 2000° F to 2200° F at a rate no faster than 200° F/1.71 hr $\approx$ 2° F/min.

Example 3

Suppose a cylindrical test bar of fused silica, initially at 2000° F

---

*A maximum allowable temperature differential of 20° F at temperatures above 2000° F appears marginal for slip-cast fused silica radomes 0.75 inches in thickness, based on experience at Georgia Tech using electric kilns.

uniformly, is heated to 2200° F in the same manner as the radome in Example 2. What size test bar would give rise to the same temperature differential as experienced by the radome (20° F)?

Referring to Figure 3-22

$$\frac{\tau\,\alpha}{R^2} \approx 2.5 \tag{3-18}$$

$$R = \sqrt{\frac{(1.71\ \text{hr})\ (0.0114\ \text{ft}^2/\text{hr})}{2.5}} \approx 0.088\ \text{ft.} \tag{3-19}$$

The radius of the test bar should be approximately 1.06-inch.

Example 4

Suppose the test bar in Example 3 was originally at room temperature (70° F), and suppose the bar was first heated by suddenly raising the surface temperature to 2000° F. How long must the bar be subjected to this condition before the center of the bar comes up to at least 1990° F?

Referring to Figure 3-21

$$T_s = 2000°\ F \tag{3-20}$$

$$T_{\begin{bmatrix} r = 0 \\ t = \tau \end{bmatrix}} = 1990°\ F \tag{3-21}$$

$$T_i = 70°\ F \tag{3-22}$$

$$\frac{T_s - T_{\begin{bmatrix} r = 0 \\ t = \tau \end{bmatrix}}}{T_s - T_i} = \frac{10}{1930} \approx 0.00052 \tag{3-23}$$

$$\frac{\alpha \tau}{R^2} \approx 1.42 \text{ (from Figure 3-21)} \qquad (3\text{-}24)$$

$$\tau \approx \frac{1.42\ R}{\alpha} \approx \frac{1.42\ (0.088\ \text{ft})^2}{0.0114\ \text{ft}^2/\text{hr}} \approx 0.96\ \text{hr} \qquad (3\text{-}25)$$

The soak time need be only about 58 minutes, which is only slightly longer than the soak time for the radome considered in Example 1 when subjected to the same conditions.

## 3.6 Machining of Slip-Cast Fused Silica

Although slip-cast fused silica parts can be match cast to fairly close tolerances, some degree of finish machining is often required. Such finishing should be carried out in a manner that will prevent contamination of the part. For this reason distilled water is the preferred coolant. In addition, tooling fixtures, particularly those parts in contact with the silica should be made from non ferrous materials. Diamond grinding with low (1000-2000 sfm) wheel speeds and low material feed rates has proven satisfactory, although some manufacturers report satisfactory results with dense silicon carbide wheels. Feed rates are limited by the thickness of the part, since comparatively low grinding pressure can cause tensile failure at the back side of the part. Conical shapes with 0.076-inch walls have been successfully machined, but it is felt that this approaches a lower limit on wall thickness. After machining, parts should be dried and, if size permits, leached with dilute (3:1) aqua regia to remove all traces of grinding wheel debris. Drying followed by heating to 1000° F is usually sufficient to remove most organic contaminants such as grease.

## 3.7 Sealing of Blanks

One of the major problems in using slip-cast fused silica for radome applications is the fact that it is a porous material, subject to water absorption. In the area of strengths and densities of concern for radome applications, this porosity may range from 3 to 12 volume per cent.

One method of sealing fused silica is to fuse the surface using an arc-plasma jet or oxyacetylene torch 22/. This produces a dense, glassy layer with no connected pores. This type of sealing has the advantage of producing a seal which will withstand the same temperatures as the radome itself. The disadvantages are that it is expensive, time consuming, and difficult if not impossible to seal the inner surface of a sharply pointed radome. Also, above Mach 3 the rain erosion resistance is decreased 23/ by the glassy surface.

Since densification shrinkage results in tensile stresses in the glaze layer, it is recommended that the part to be glazed be preheated to 2000° F, glazed, and annealed for 15 minutes at 2150° F, followed by slow (4° F per minute) cooling to 1900° F 22/. Due to the difficulty in obtaining a uniformly thick stress free glaze, this type of sealing is not recommended for radome applications.

Most radome applications are a one time use only, and the radome, along with the rest of the missile, is destructed at the end of the mission. For this type of application, the surface can be sealed using silicone resins 18/. These materials can be applied at room temperature and cured at moderate temperatures (475° F). Thin coatings are easily applied to the outside of the radome by spraying and to the inside by brushing or spraying. Thin coatings do not degrade the electrical characteristics of the radome, and the material will burn out at hypersonic velocities.

A coating of this type is Dow Corning 808® silicone resin. The resin is prepared for spraying by diluting three parts resin with one part xylene. The resin is sprayed on in several thin coats, allowing the solvent to evaporate between coats. The resin is cured a minimum of one hour at 475° F. Note: Since the resin does not dry tack free before cure, the coated part must be handled in such a manner as to avoid marring the coating.

A second method of sealing with silicone resin is to impregnate the slip-cast fused silica with a resin such as General Electric SR80®. A radome may be impregnated by inverting the radome and filling with resin. The resin is then allowed to soak through until the outside surface is wet. At this point the excess resin is drained and the part dried and cured as follows:

24 hours soak at 100 ± 25° F

6 hours increase from 100 to 300° F

3 hours soak at 300° F

5 hours increase from 300 to 485° F

5 hours soak at 485° F

3 hours cool to 200° F.

Both resin sealing methods have been found to produce no degradation in dielectric properties of sealed materials.

## 3.8 Other Forms of Fused Silica

Two other forms of fused silica mentioned throughout this manual are: (1) glass worked fused silica, and (2) fused silica foam.

### 3.8.1 Glass Worked Fused Silica

The terminology glass worked fused silica as used in this report refers to clear or translucent fused silica prepared by melting quartz under

extremely high temperatures and/or vacuum to remove air and give a dense transparent or translucent product. This type of product is used primarily for optical and chemical applications.

### 3.8.2 Fused Silica Foam

Two types of fused silica foam are commercially available. (1) Closed pore glassy foam can be prepared by carbonaceous forming of a silica melt. (2) Open pore foam is prepared by entraining air in fused silica slip at room temperature, following by drying and sintering. This type of open pore fused silica foam can be produced in a range of densities from 25 $lb/ft^3$ up to the density of slip-cast fused silica. It is available commercially in densities of 30 and 50 $lb/ft^3$. Property data given in this manual for fused silica of less than 115 $lb/ft^3$ density is for open pore fused silica foams.

## 3.9 References for Chapter III


1. Fleming, J. D., "Slip Casting of Fused Silica," Amer. Ceram. Soc. Bull. 40, (12), 748-750 (1961).

2. Pivinskii, Yu E., F. T. Gorobets, "High Density Fused Silica Ceramics," Refractories, Russia 33, (8), 509-516, (1968).

3. Schulle, Wolfgang, "Fabrication of Articles from Fused Silica Slip Casting and Sintering," Silikattechn 13, 282-284, 1962.

4. Pivinskii, Yu E., "Increase in the Packing Density of Powder Particles During the Molding of Semifinished Ceramic Particles," Glass and Ceramics, Russia, 26, (9), 538-542 (1969).

5. Harris, J. N., V. C. Theiling, W. C. Miiller, High Strength, Broadband, Lightweight Silicon Oxide Radome Techniques, AFAL-TR-70-114 (1970).

6. Harris, J. N., E. A. Welsh, High Strength, Broadband, Lightweight Silicon Oxide Radome Techniques, AFAL-TR-69-103, (1969).

7. Vasilos, Thomas, "Hot Pressing of Fused Silica," J. Amer, Ceram, Soc. 43, (10), 517-519 (1960).

8. Lambe, C. M., "Preparation and Use of Plaster Molds," in Ceramic Fabrication Processes, ed. W. D. Kingery, Technology Press and John Wiley & Sons, 1958.

9. Whiteside, E. L., "Quality Control in the Plaster Mold Shop," Amer. Ceram. Soc. Bull. 45, (11), 1022-1026 (1966).

10. Adcock, D. S. and I. C. McDowall, "The Mechanism of Filter Pressing and Slip Casting," J. Amer. Ceram. Soc. 40, 355-362.

11. Fleming, J. D., Fused Silica Manual, prepared for U.S.A.E.C., Contract No. AT-(40-1)-2483 by Georgia Tech Engineering Experiment Station, 1964.

12. Pivinskii, Yu E., F. T. Gorobets, "Some Features of Slip Casting Quartz," Glass and Ceramics, Russia 25, 285-288, (1968).

13. Harris, J. N., V. C. Theiling, et al., Ceramic Systems for Missile Structural Applications, Summary Report 3, prepared for Naval Ordnance Systems Command under Contract N00017-67-C-0053, by the Georgia Tech Engineering Experiment Station (1970).

14. Fleming, J. D., et al., Materials for High Temperature Nuclear Engineering Applications, Quarterly Report No. 4, TID-18891 (1963).

15. Welsh, E. A., "High Purity Slip-Cast Fused Silica," presented at the 73rd Annual Meeting, American Ceramic Society, Chicago, Illinois, 1970.

16. Budworth, D. W., "Theory of Pore Closure During Sintering," Trans Brit Ceram Soc 69 (1), 29-31 (1970).

17 Bcganov, A. G., V. S. Rudenko, G. L. Bashnina, "Cristallization Patterns and the Nature of Quartz Glass," Inorganic Materials 2, 312-322, (1965).

18. Wagstaff, F. E., S. D. Brown, I. B. Cutler, "The Influence of $H_2O$ and $O_2$ Atmospheres on the Crystallization of Vitreous Silica," Phys Chem Glasses 5, (3), 76-81, 1964.

19. Wagstaff, F. E., K. F. Richards, "Preparation and Crystallization Behavior of Oxygen Deficient Vitreous Silica," J. Amer. Ceram. Soc. 48, (7), 382-383 (1965).

20. Wagstaff, F. E., K. J. Richards, "Kinetics of Crystallization of Stoichiometric $SiO_2$ Glass in $H_2O$ Atmospheres," J. Amer. Ceram. Soc. 49, (3), 118-121 (1966).

21. Boland, Paul, Guidelines for the Establishment of Optimal Heat Treatment Process Parameters for Slip-Cast Fused Silica Components, Special Technical Report No. 3, Contract N00017-67-C-0053, Naval Ordnance Systems Command, prepared by Georgia Tech Engineering Experiment Station (1968).

22. Poulos, N. E., et al., High Temperature Ceramic Structures, p 81, Final Summary Report, Project No. A-212, Contract No. NOrd-15701, Georgia Institute of Technology (1962).

23. Harris, J. N. and J. D. Walton, Jr., Rain Erosion Sled Testing of Slip-Cast Fused Silica Radomes, p 49 Final Technical Report, Project No. A-925, Contract DA-01-021-AMC-14464(Z) Georgia Institute of Technology, March 1967, AD 813521.

24. "Slip-Cast Fused Silica Radome Assembly," p 78, Contract NOw-64-0505, General Dynamics, Pomona Division.

# CHAPTER IV

# SLIP-CAST FUSED SILICA PROPERTIES

## 4.1 Introduction

The thermal and electrical properties of sintered slip-cast fused silica are density dependent but may vary somewhat due to the type and size of pores present. The mechanical properties are generally density dependent but may vary more due to the degree of sintering. The degree of sintering is dependent on particle size distribution and solids content of the fused silica slip, impurity levels in the fused silica grain used to make the slip, other impurities picked up during processing of the slip and the slip-cast piece, sintering time and sintering temperature. Sintering, as discussed in Chapter III, is limited by the competing process of crystalline grain growth (cristobalite). The growth rate of cristobalite can be so rapid as to prevent optimum sintering (See 3.5); in this case, maximum densities and strengths will not be reached. Because the density of cristobalite is 2.36 gm/cc, relatively large quantities of cristobalite will increase the bulk density of the overall cast piece but the piece will have a large porosity and will have very little strength due to the inversion and volume change of cristobalite in cooling to room temperature.

Other major material factors that affect the strength values obtained for a given ceramic material are microstructure, surface finish, and specimen size. In addition certain external conditions also influence the strength value. The conditions which are most critical are test temperature and the various factors involved in processing the ceramic product. Finally, the test method used to obtain the strength data also influences the magnitude and reproductibility of the data.

## 4.2 Mechanical Properties

### 4.2.1 Room Temperature Properties

4.2.1.1 Elastic Modulus. The room temperature elastic modulus of slip-cast fused silica has been determined dynamically on hundreds of slip-cast fused silica specimens of both "high purity" and commercial grade. Static elastic modulus measurements have been made on a smaller number of samples, but these, in general, agree well with dynamic measurements and are usually within 5 to 8 per cent.

Elastic modulus is a function not only of density but also of how well the specimen is sintered. Figure 4-1 shows the room temperature dynamic elastic modulus with respect to bulk density for numerous "high-purity" and commercial grade specimens, and Figure 4-2 shows elastic modulus as a function of density for both slip-cast and foamed "high-purity" fused silica.

As-cast and dried "high-purity" slip-cast fused silica has a density of 113 to 115 $lb/ft^3$ and a dynamic elastic modulus of 4 to 5 x $10^5$ psi. Under initial sintering there is very little increase and, in some cases, a slight decrease in density while the elastic modulus is increasing rapidly to 1.8 to 2.0 x $10^6$ psi. As sintering continues bulk density begins to increase and elastic modulus continues to increase but at a decreasing rate. For high-purity slip-cast fused silica, the rate of increase with bulk density becomes logarithmic from about 124 $lb/ft^3$ to nearly theoretical density of 139 $lb/ft^3$. This portion of the curve can be described in terms of porosity by

$$E = (10.5 \times 10^6)e^{-3.2P} \qquad 4\text{-}1$$

where p = volume fraction pores.

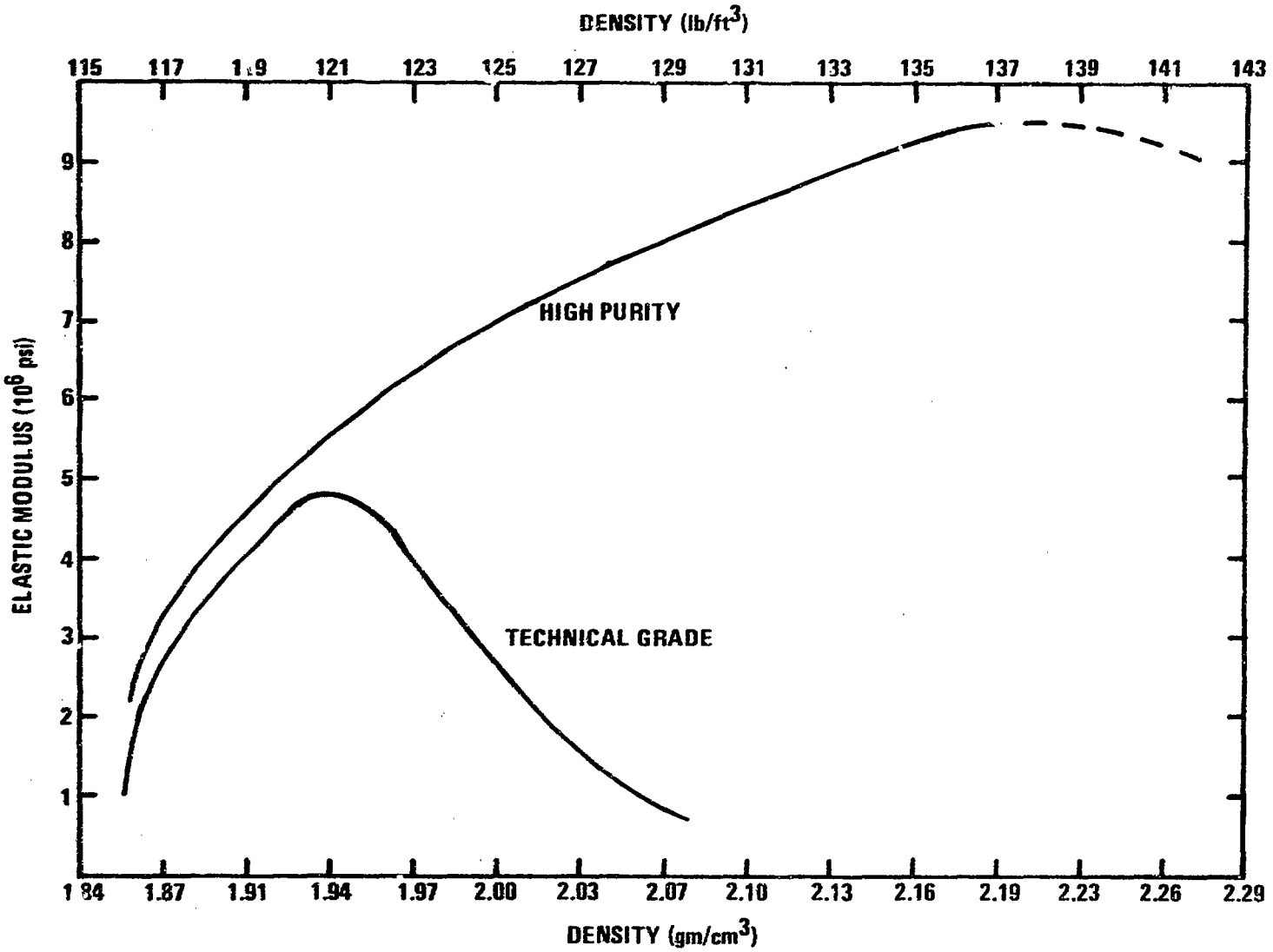


Figure 4-1. Elastic Modulus versus Density for High Purity and Technical Grade Slip-Cast Fused Silica.

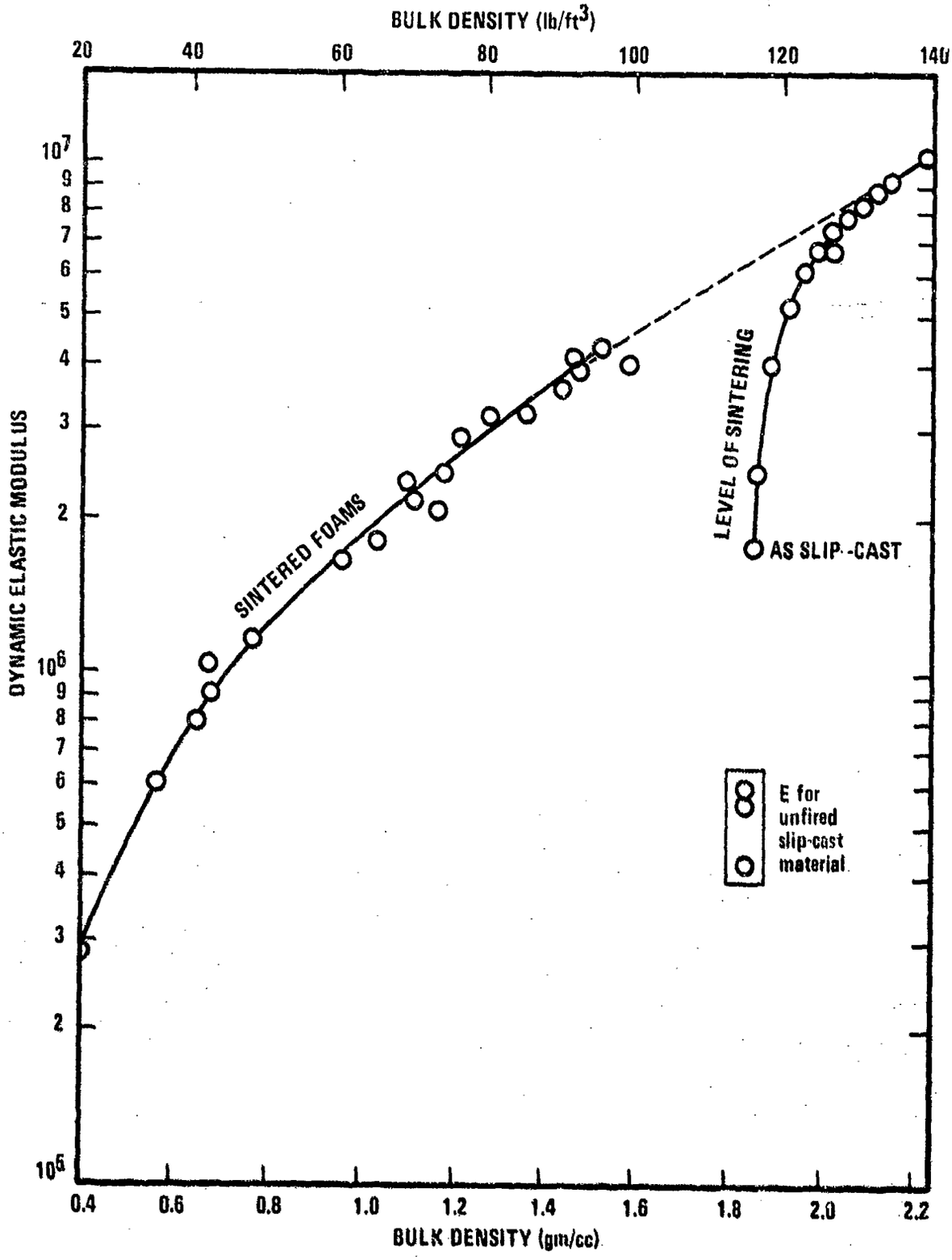


Figure 4-2. Elastic Modulus with Respect to Density for Slip-Cast Fused Silica from 30 to 130 lb/ft$^3$.

A straight line connecting the upper portions of the slip-cast and foam data in Figure 4-2 is also described by Equation (1). Walton 1/ suggests that the exponent for any ceramic should be in the range -4p to -7p and Gannon et al. 2/ used a value of -6.6p to describe the elastic modulus curve they obtained for technical grade silica. The exponent of -3.2p indicates a vast improvement in elastic modulus over previous work. By starting with a foam composition rather than slip-cast material it is possible to sinter "high-purity" rebonded fused silica to maximum modulus of elasticity at any density between 60 and 124 $lb/ft^3$.

The points plotted on Figure 4-1 are for sintering temperatures of 2100°, 2200°, 2250° and 2400° F for various sintering times. Elastic modulus versus sintering times for three "high-purity" slips is shown in Figure 3-12. The points in Figure 4-1 are for several slips of varying mean particle size. The significance of this is that the majority of "high-purity" slips, cast and sintered to the same density will vary only slightly in elastic modulus even though the two slips reach the same density at different times. A very coarse or very fine slip may vary somewhat at the lower densities, but should follow the curve shown in Figure 4-1 above 124 $lb/ft^3$.

The curve for the technical grade slip shown in Figure 4-1 reaches a maximum between 120 and 122 $lb/ft^3$ then falls off rapidly. This rapid drop in elastic modulus is attributed to the formation of large quantities of cristobalite. The drop appears to occur after the formation of approximately 25 volume per cent cristobalite. The large volume change accompanying the cristobalite inversion destroys the integrity of the test specimen causing the elastic modulus to show a decrease. The high-purity material does not show a decrease until after theoretical density of approximately 139 $lb/ft^3$ is reached.

Densities greater than 139 $lb/ft^3$ can be achieved because the density of cristobalite is approximately 147 $lb/ft^3$. At values above 139 $lb/ft^3$ elastic modulus drops rapidly.

4.2.1.2 Modulus of Rupture. The dynamic measurement of elastic modulus is rather insensitive to small surface and interior flaws, hence good agreement is obtained from sample to sample as long as density is constant and the specimens are well sintered. This is not the case with modulus of rupture or transverse strength. The values obtained for modulus of rupture are dependent on the type of test loading, surface condition, geometry and size (volume) of the test specimen.

A.S.T.M. Designation C674, "Flexural Properties of Ceramic Whiteware Materials," calls for the use of three-point loading in determining modulus of rupture of circular or rectangular cross-section specimens. However, experience has shown that three-point loading gives a higher mean strength and a larger deviation than does four-point loading. This occurs because of the small volume under maximum stress in three-point loading.

The calculation of modulus of rupture, whether three-point or four-point loading, is made by the use of the equation

$$\sigma_{MR} = \frac{MC}{I} \qquad (4\text{-}2)$$

$\sigma_{MR}$ = failure stress (modulus of rupture)

M = bending moment at failure point

c = distance from neutral axis to the failure surface

I = moment of inertia of the cross section under the bending moment.

The use of this equation assumes the transverse plane at the point of the calculation remains as a transverse plane after bending, e.g. the material is homogeneous, obeys Hooke's Law, and the stress field is linear as a function of distance from the neutral axis.

The above equation and assumptions are adequate for four point loading modulus of rupture determinations. However, when three point loading is used, a corrective factor must be applied to the basic equation to account for the "wedging" effect. As reported by Shook 3/ the following equations have application to this end

$$\sigma_{MR} = \frac{Mc}{I} \left(1 - \frac{4}{3\pi} \frac{h}{L}\right) \quad \text{(rectangular bar)} \qquad (4\text{-}3)$$

$$\sigma_{MR} = \frac{Mc}{I} \left(1 - \frac{3}{2\pi} \frac{d}{L}\right) \quad \text{(circular bar)} \qquad (4\text{-}4)$$

where

h = depth of bar in direction of load at failure point

d = diameter of bar at failure point

L = extreme support span distance

It is apparent from these equations that uncorrected three point loading modulus of rupture calculations will always yield strength values greater in magnitude than will four point loading modulus of rupture determinations on identical samples.

Because of the above reasons the majority of test data on both commercial grade and "high purity" slip-cast fused silica has been obtained on round test bars nominally 3/4-inch in diameter and 6 inches in length. These bars

were loaded to breaking using 1/4 point-four point loading with a 4-inch lower span and a 2-inch upper span. Loading rate was 6000 pounds per minute. Using this type of test there is still a large data spread as shown by the curve in Figure 4-3. The points shown are for various "high purity" fused silica slips. An even larger spread in data occurs with technical grade materials because of the variation in rate of cristobalite formation. Figure 4-4 shows modulus of rupture versus bulk density for a good technical grade slip (one that devitrifies slowly). The other individual points are the median values with 95 per cent confidence intervals for a number of different commercial slips. It should be noted that the main reason for this variation is the rate of devitrification. It is hypothesized that devitrification begins at the surface and proceeds inward with time. This hypothesis explains why the modulus of rupture (Figure 4-3) begins to drop in the high purity material above a density of 2.02 gm/cc while the elastic modulus (Figure 4-1) is still increasing. The small amount of cristobalite at the surface is insufficient to affect the elastic modulus but can cause micro-cracking of the surface, thus drastically reducing modulus of rupture. Cristobalite build up in the commercial material is so rapid that the elastic modulus begins to drop almost simultaneously with the drop in modulus of rupture.

The effect of cristobalite on modulus of rupture is related to density. Less dense material can tolerate considerably more cristobalite than dense material. A commercial material with a density in the range of 115 to 118 lb/ft$^3$ may in some few cases contain up to 25 volume per cent cristobalite before any effect on transverse strength is noted. Usually 12 to 15 per cent is regarded as the upper limit for satisfactory performance 4/. A slip-cast fused silica

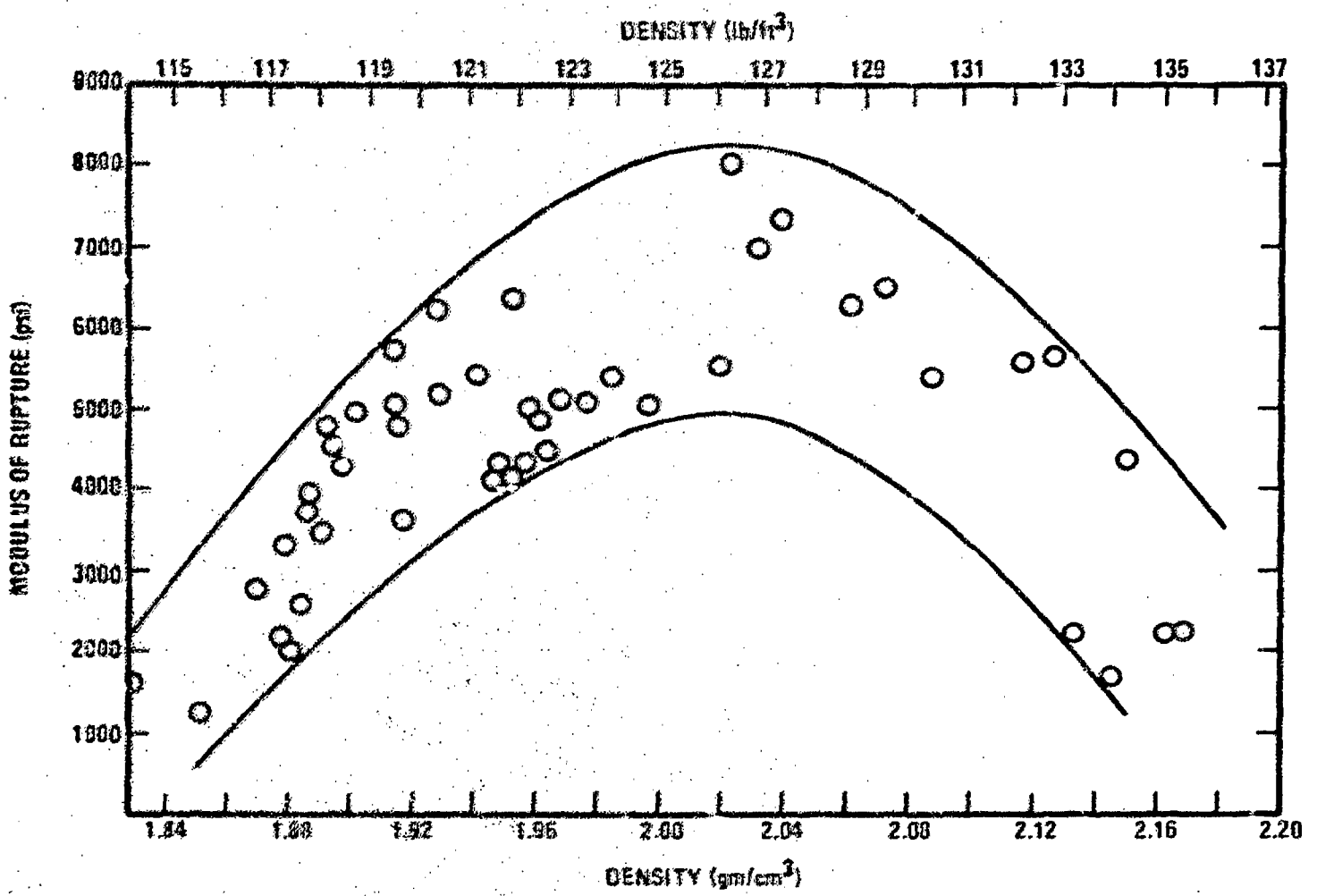


Figure 4-3. Modulus of Rupture versus Density for High Purity Slip-Cast Fused Silica. (Reference 5.)

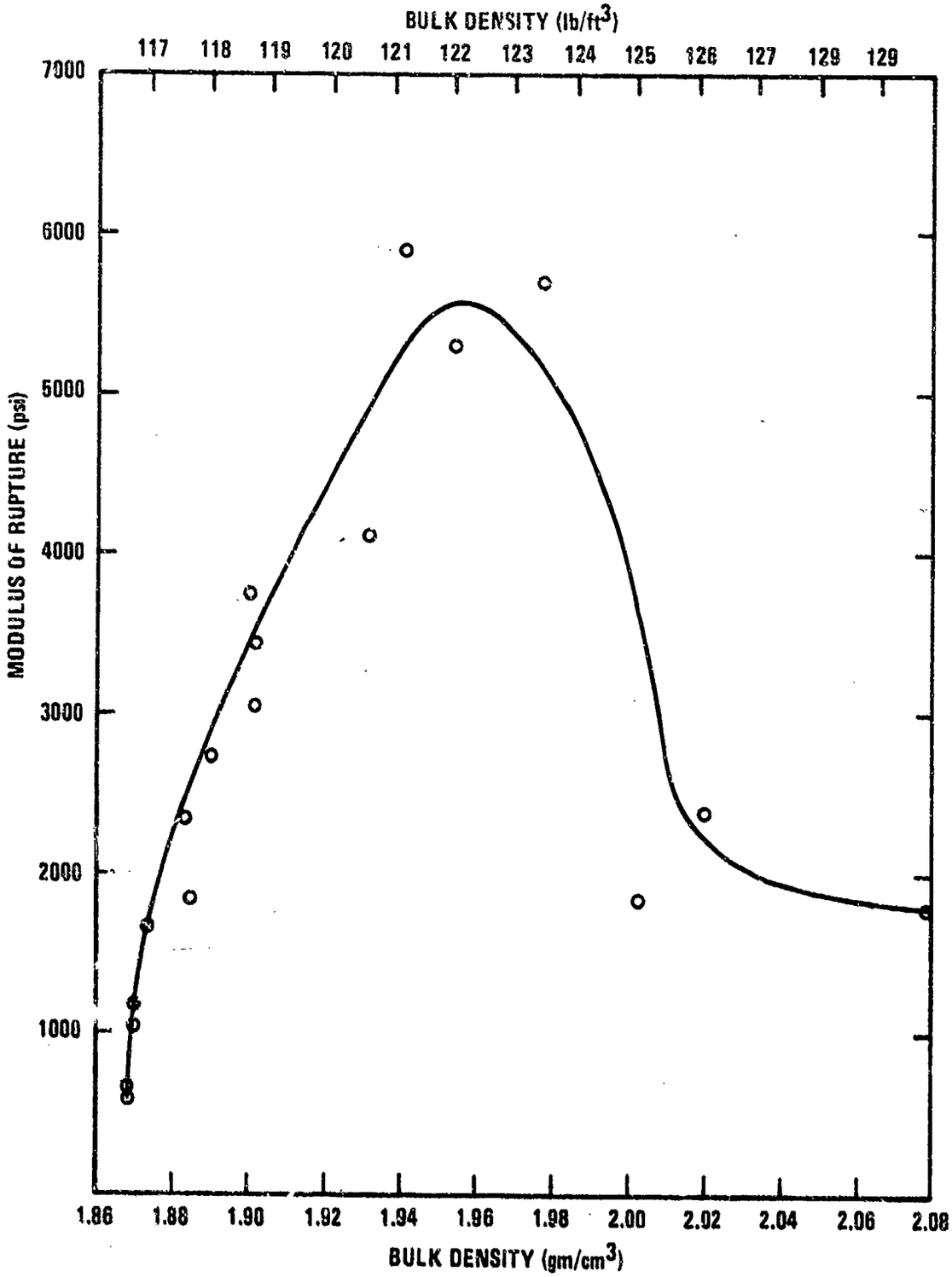


Figure 4-4. Modulus of Rupture versus Density for a Technical Grade Slip-Cast Fused Silica.

body with a density in the range of 122 to 128 $lb/ft^3$ may show deleterious effects on modulus of rupture with as little as one to two volume per cent cristobalite.

Removing the as-cast and fired surface layers from fused silica test specimens can cause a marked improvement in transverse strength. The improvement comes about not only from removing surface cristobalite but also from removing other imperfections on the as-cast surfaces. Reducing the total volume under maximum stress will also show an apparent increase in strength.

Table 4-1 shows the effect of machined surfaces and volume size on transverse strength for two different slip-cast fused silicas.

TABLE 4-1

SURFACE AND VOLUME EFFECTS ON
MODULUS OF RUPTURE OF SLIP-CAST FUSED SILICA

| Density | Specimen Geometry | Surface Finish | Size (inch) | Breaking Span Upper/Lower (inch)/(inch) | Modulus of Rupture |
|---|---|---|---|---|---|
| 2.06 | Round | As-cast | 3/4 D x 6 | 2/4 | 4597 ± 803 |
| 2.06 | Round | Ground & polished | 3/4 D x 6 | 2/4 | 5920 ± 249 |
| 1.96 | Round | As-cast | 3/4 D x 6 | 2/4 | 4860 ± 260 |
| 1.96 | Rectangular | Machined | 1/4 x 1/8 x 2-1/4 | 1/2 | 9330 ± 380 |

4.2.1.3 Compressive Strength. Fleming 5/ reported an average room temperature compressive strength of 23,000 psi for technical grade slip-cast fused silica. Southern Research Institute reported values ranging from

24,000 to 54,000 psi for technical grade material and 30,000 to 54,000 psi for "high-purity" slip-cast fused silica. Room temperature compressive strength is shown as a function of density for specimens of similar material tested at Georgia Tech 6/ and at Southern Research Institute 7/ in Figure 4-5.

4.2.1.4 Tensile Strength. Fleming 5/ reported a room temperature tensile strength of 4300 psi for technical grade slip-cast fused silica. Southern Research Institute reported values of 2500 to 4300 psi for the technical grade and 2200 to 4300 psi for the high-purity slip-cast fused silica 7/.

These specimens were all of the "dog bone" type and were loaded by a straight pull.

Using the hydrostatic ring tensile test developed by Sedlacek 8/, rings were fabricated with inside diameters of 5-3/4, 16-1/2 and 29-1/2 inches 9/. These rings were stressed to failure with the results shown in Table 4-2. All rings were prepared from the same fused silica slips and sintered as nearly as possible under the same conditions. The fracture strength of these rings showed a consistent variation with volume, becoming smaller as the volume increased. This is typical of brittle ceramic materials and indicates that slip-cast fused silica probably follows a Weibull statistical distribution law; however, additional data is required before reliable values of the statistical parameters can be established.

### 4.2.2 Elevated Temperature Properties

The strength of fused silica has long been known to show a substantial increase with temperature 10,11/. The reason for this increase

TABLE 4-2

VOLUME EFFECTS ON TENSILE STRENGTH
OF LARGE DIAMETER RINGS

| Ring Diameter (inch) | Ring Thickness (inch) | Ring Width (inch) | Volume ($inch^3$) | Tensile Strength (psi) |
|---|---|---|---|---|
| 5-3/4 | 1/4 | 1/2 | 2.2 | 3863 ± 201 |
| 16-1/2 | 1/2 | 3/4 | 21.3 | 3135 ± 150 |
| 29-1/2 | 1/2 | 3/4 | 38.9 | 2568 ± 470 |

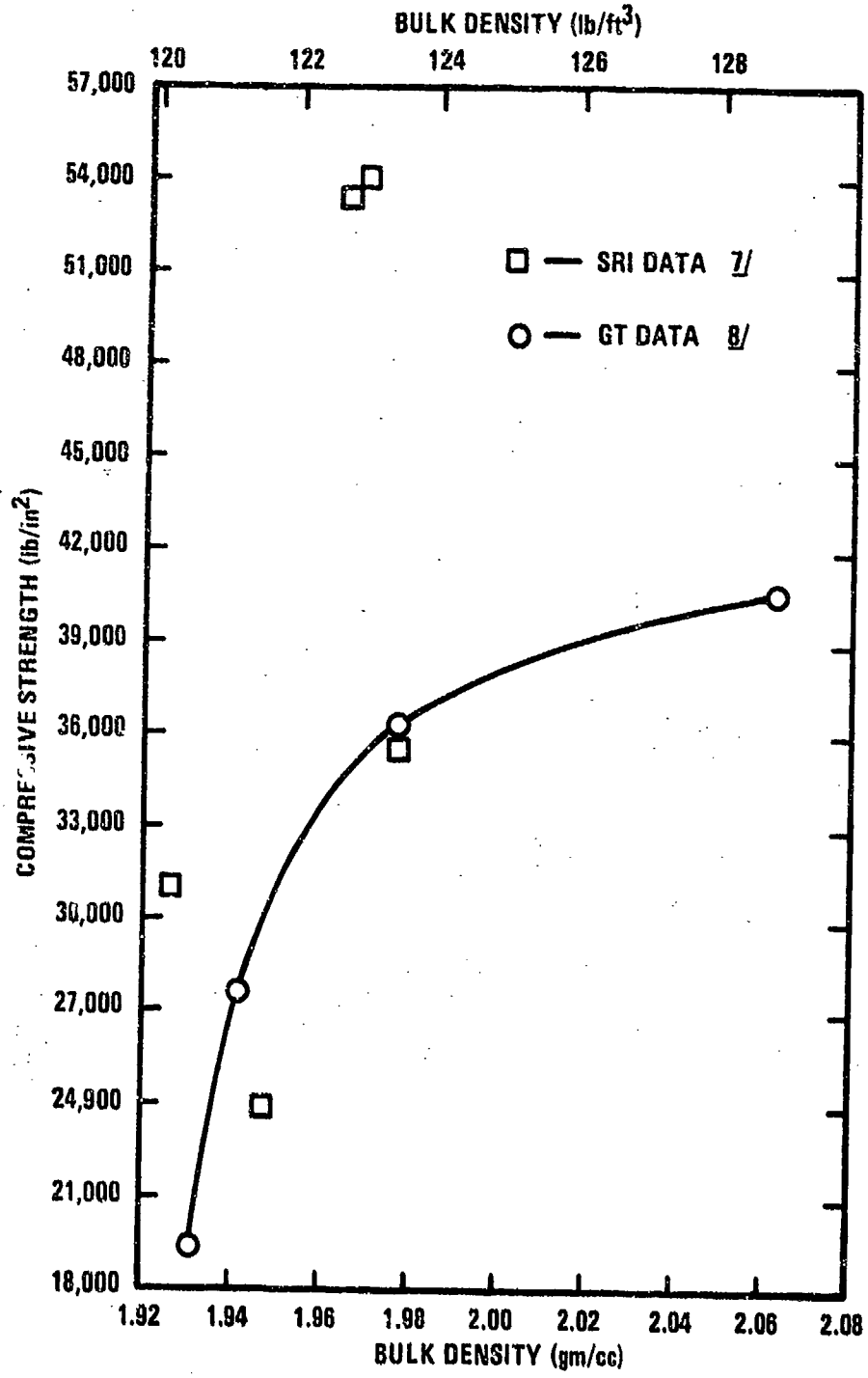


Figure 4-5. Compressive Strength of Slip-Cast Fused Silica with Respect to Bulk Density.

is not clear. Stress relief by plastic flow at highly stressed points near surface flaws is possible since plastic flow under deformation has been demonstrated even at room temperature 12,13/. Since the strength increases essentially constantly as the temperature is increased while the viscosity shows a very slow change 12/, this is unlikely to be a predominant mechanism. A structural rearrangement has also been suggested 14/. One mechanism, which has been suggested, is that surface flaws resulting from thermal shock of the cristobalite formed during fabrication become filled-in as the cristobalite expands on heating. As these flaws are filled by the expanding cristobalite, they become more mechanically stable and tend to act less as stress concentrators 15/.

4.2.2.1 Elastic Modulus. Data on the modulus of elasticity of slip-cast fused silica at elevated temperatures are very limited. However, moduli determined from static data appear to decrease with temperature while moduli measured from sonic resonance data appear to increase with temperature. Figure 4-6 gives values for static elastic modulus as a function of temperature.

4.2.2.2 Modulus of Rupture. The modulus of rupture versus temperature for technical grade and high-purity silica slips are shown in Figure 4-7.

4.2.2.3 Tensile Strength. The tensile strength of both technical grade and high-purity slip-cast fused silica is shown in Figure 4-8.

4.2.2.4 Compressive Strength. Values for compressive strength of both high-purity and technical grade material with respect to temperature are shown in Figure 4-9.

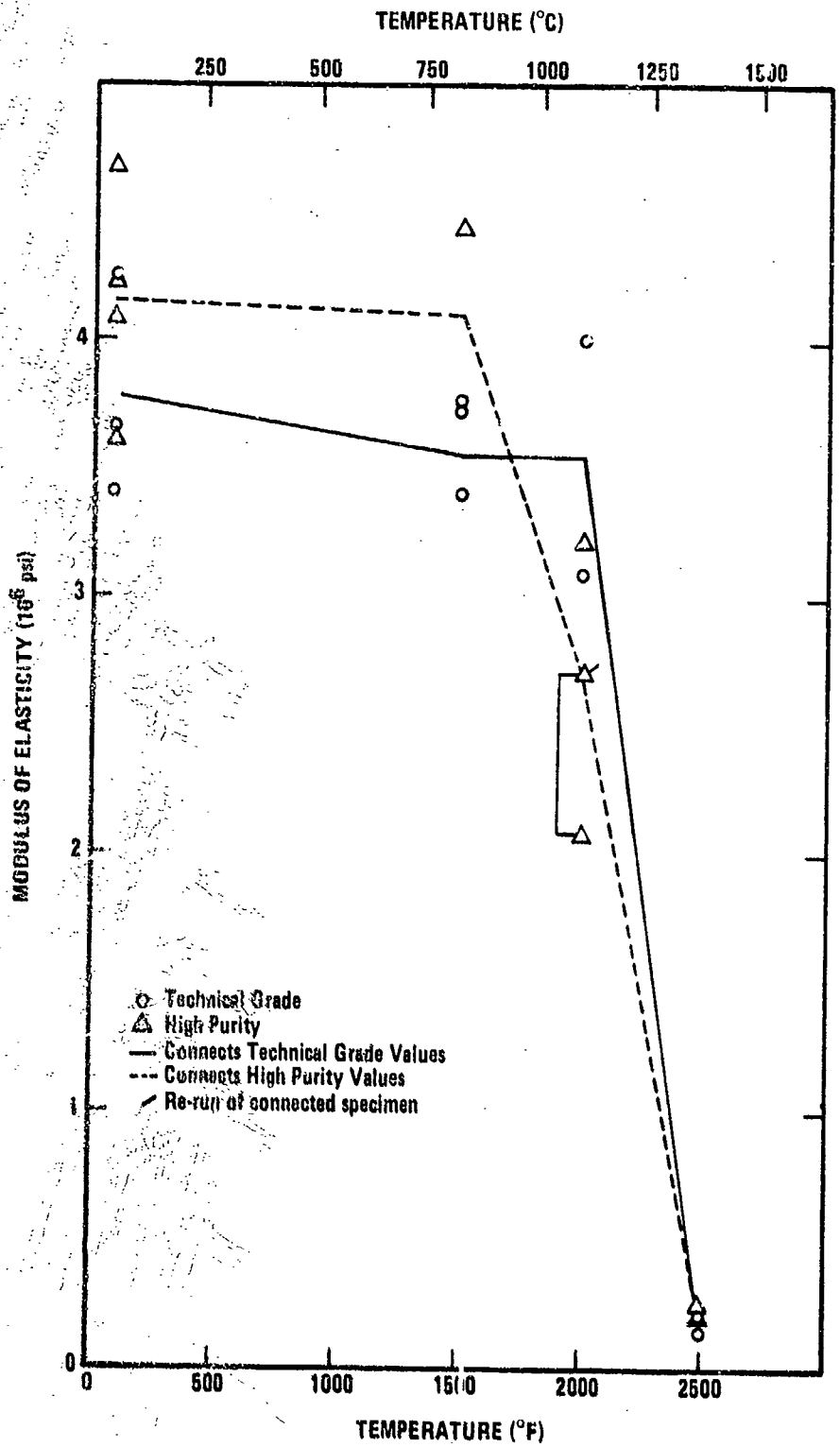


Figure 4-6. Flexural Modulus of Nlasticity versus Temperature for Slip-Cast Fused Silica. (Reference 7, page 48.)

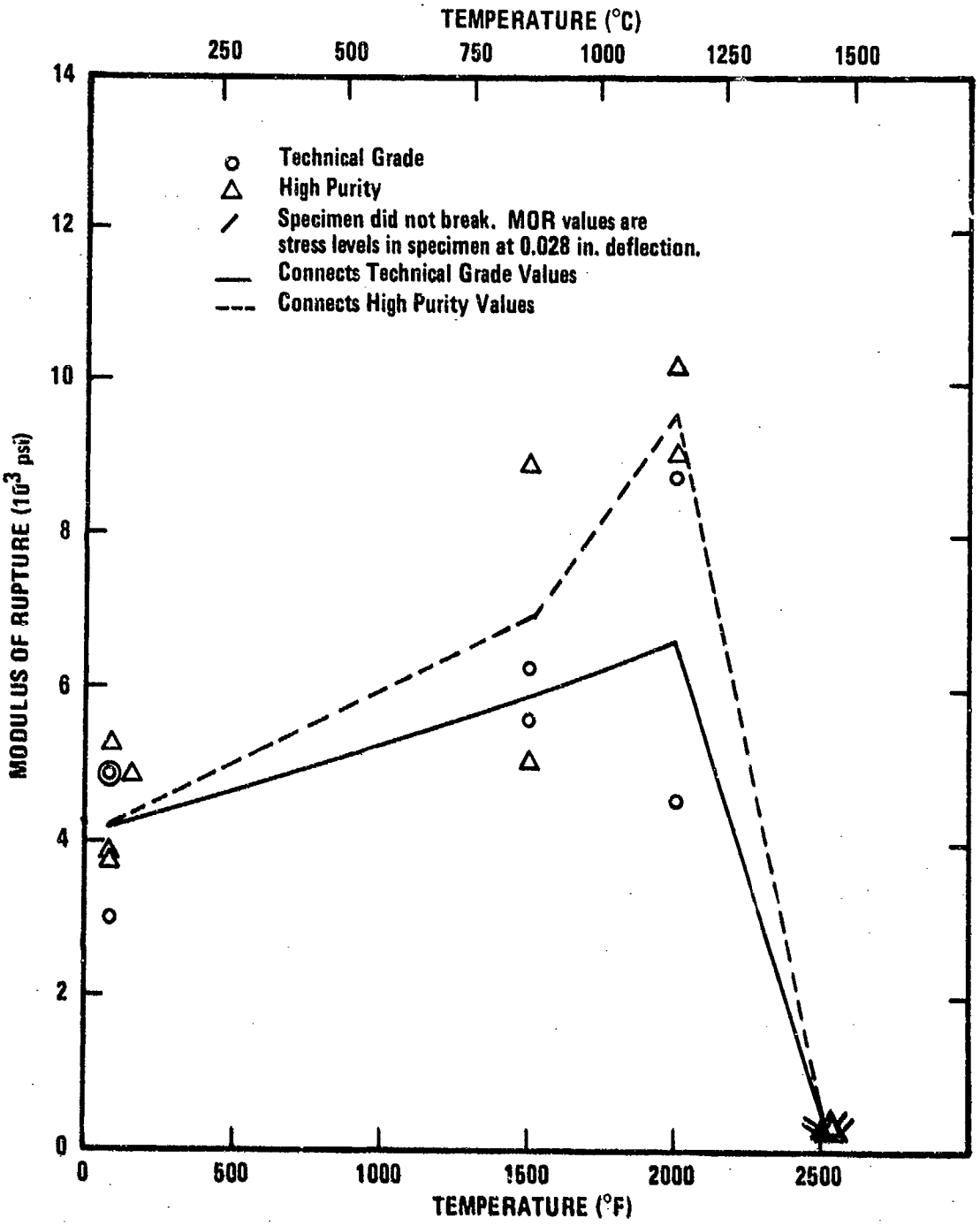


Figure 4-7. Modulus of Rupture versus Temperature for Slip-Cast Fused Silica. (Reference 7, page 47.)

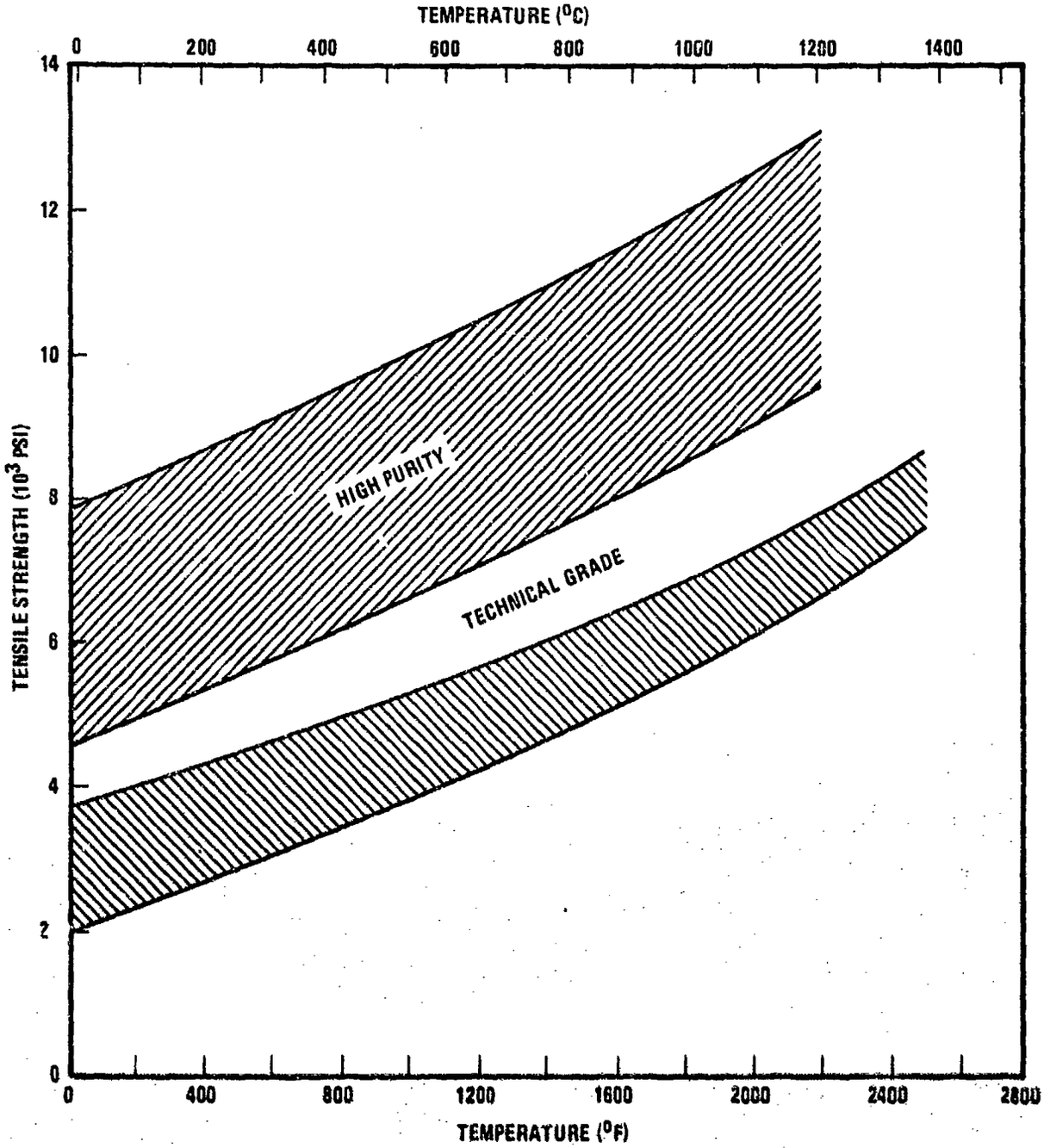


Figure 4-8. Tensile Strength versus Temperature for Slip-Cast Fused Silica. (Reference 7, page 33.)

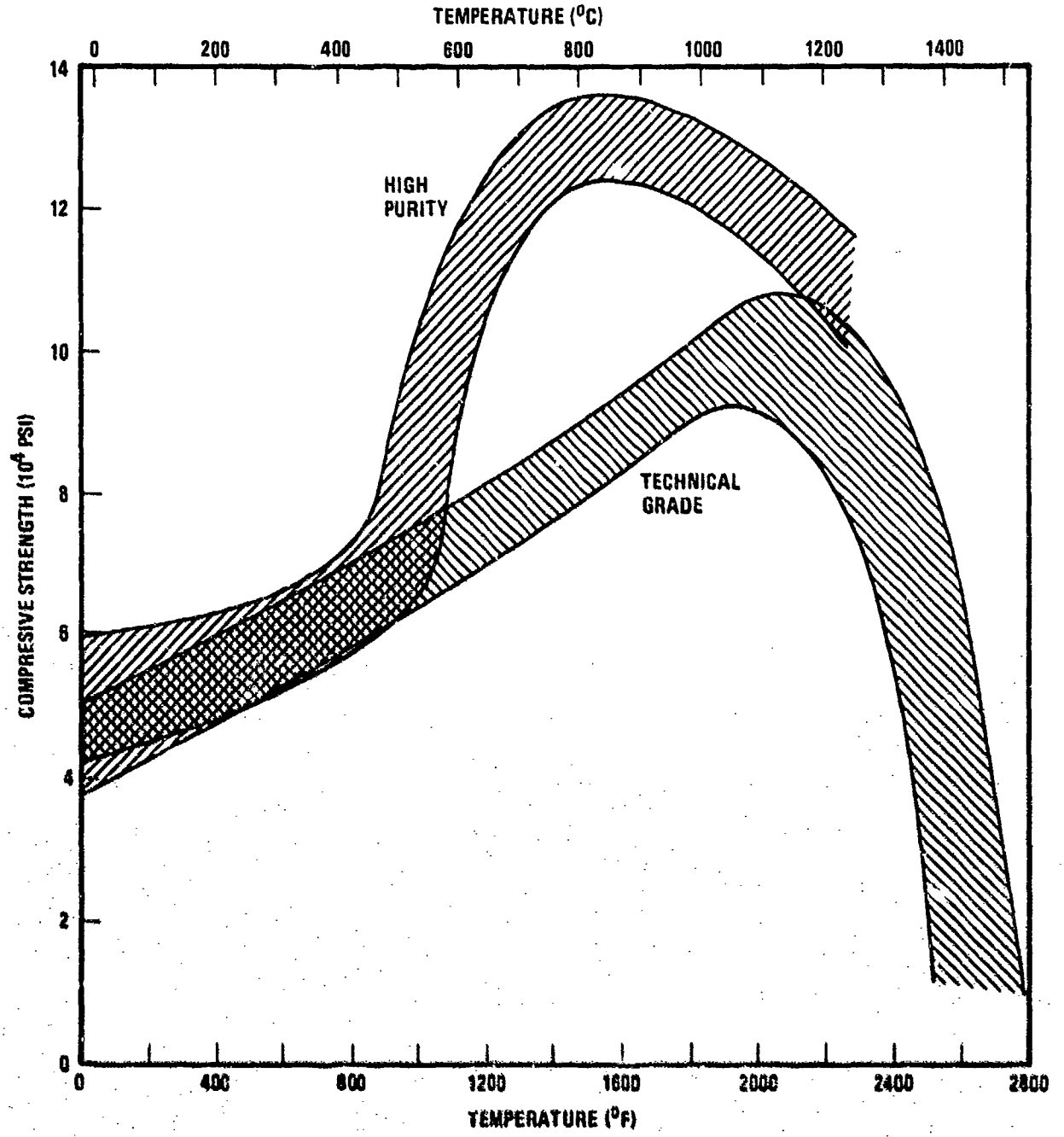


Figure 4-9. Compressive Strength versus Temperature for High Purity and Technical Grade Slip-Cast Fused Silica. (Reference 7.)

4.2.2.5 Poisson's Ratio. Poisson's ratio with respect to temperature is shown in Figure 4-10 for transparent and slip-cast fused silica. The Fleming and Corning data were taken from sonic resonance measurements. The broad band of values is based on optical strain measurements, and reflects the increasingly plastic nature of the material above its sintering temperature.

## 4.3 Physical Properties

### 4.3.1 Thermal Expansion

Fleming 5/ discussed thermal expansion of fused silica at some length and based differences in expansion on the equilibrium temperature. Figure 4-11 was presented in this discussion, and it was suggested that the equilibrium temperature for glass-worked silica, which this data represents, is in the neighborhood of 2300° F. Fleming further suggested that since the processing temperature of slip-cast fused silica is 2200° F for sufficient time to reach an equilibrium density, then the equilibrium temperature is near 2200° F and expansion data should fall slightly below the points in Figure 4-11. Actual measured data on slip-cast fused silica is also displayed in Figure 4-11. It can be seen that the data for technical grade slip-cast material falls below the glass-worked fused silica points. However, the data for the high-purity slip-cast material falls above the glass-worked fused silica points. The reason for this is not apparent but may be due to inaccuracies in measurement. Although the variation in coefficient of thermal expansion are quite small, in some cases the differences may be critical. In an analysis of thermal shock, for example, the stress could be different by a factor of two or more.

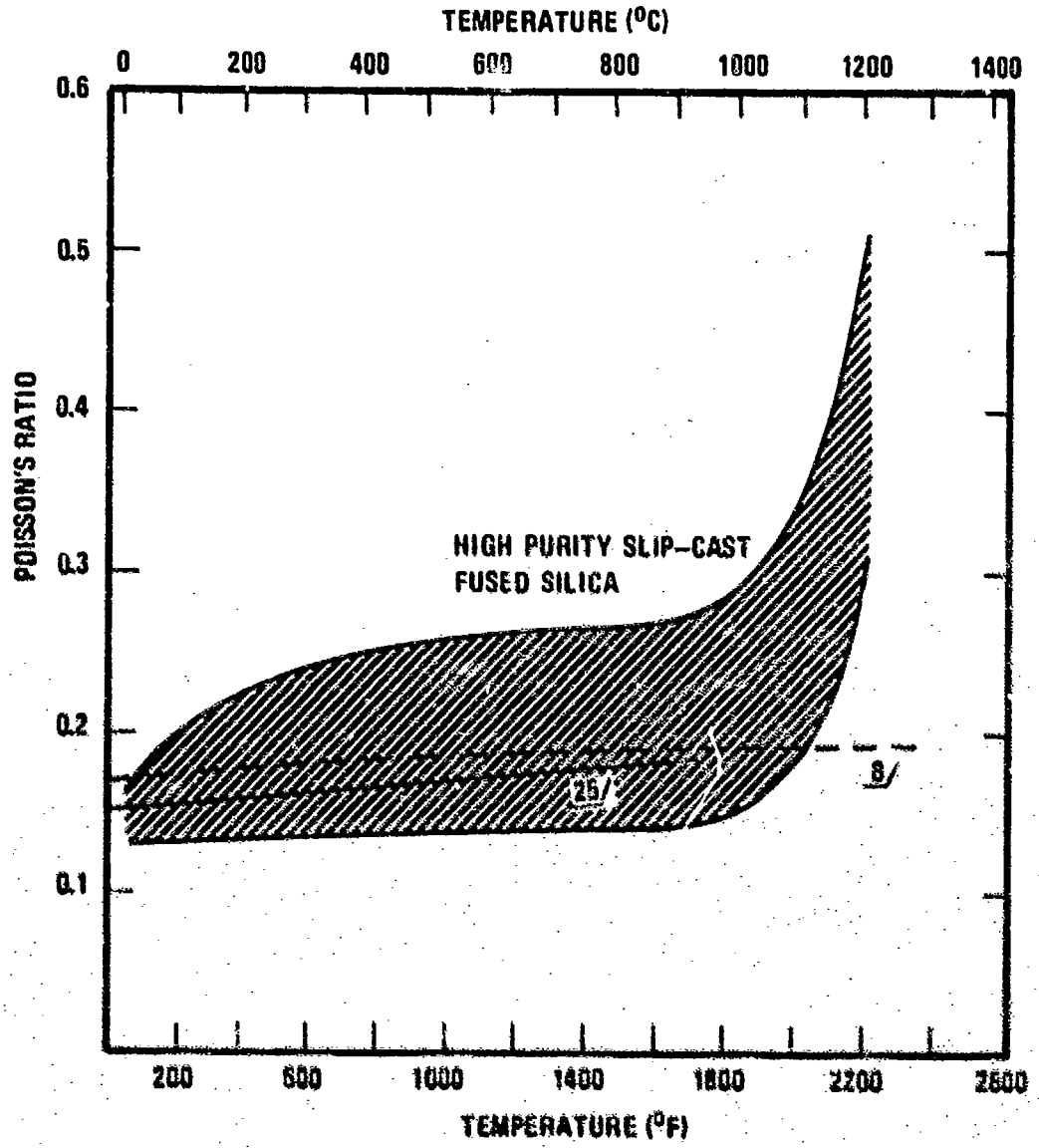


Figure 4-10. Poisson's Ratio of Slip-Cast Fused Silica.

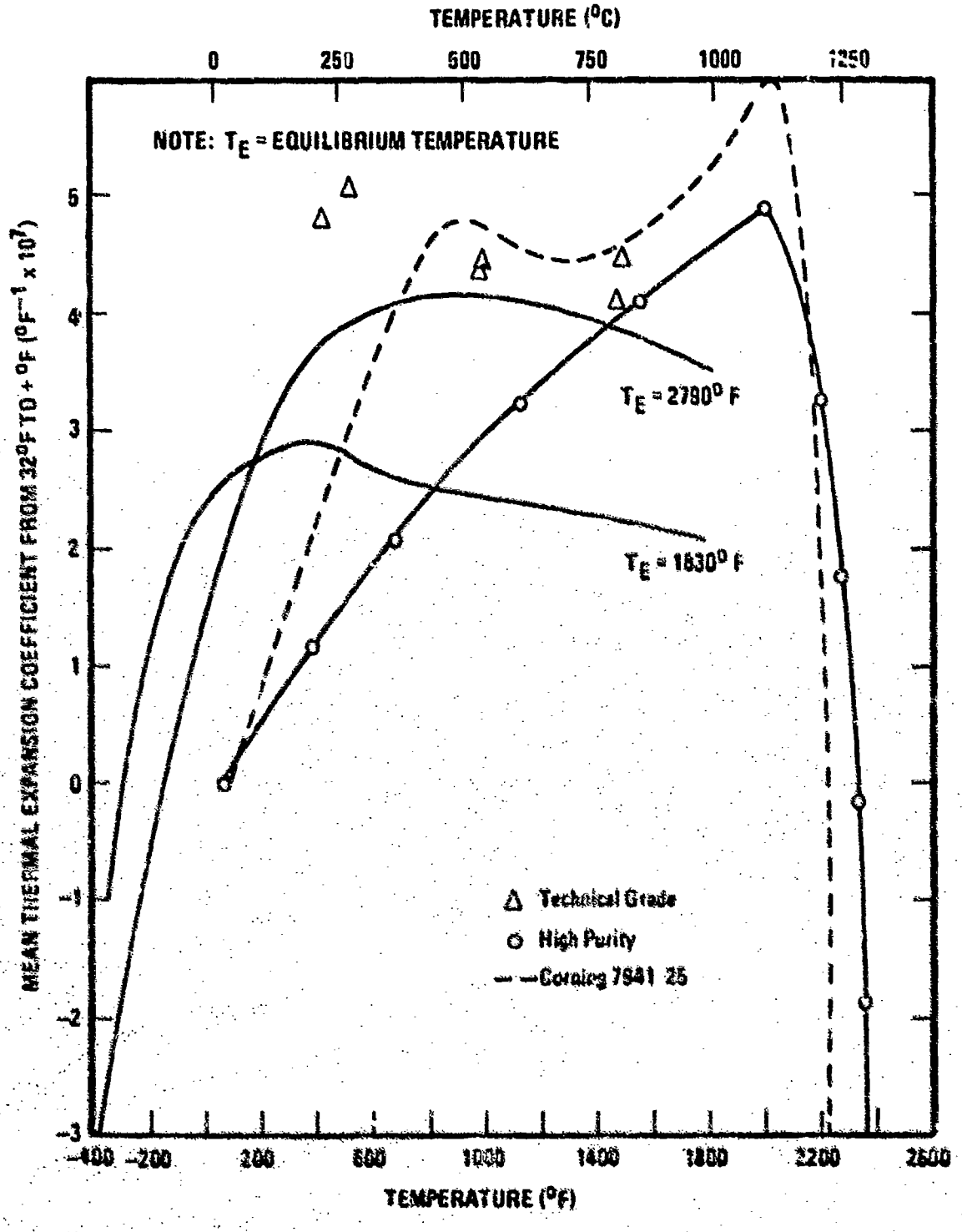


Figure 4-11. Expansion Coefficient of Fused Silica.
(Reference 8, page 85.)

The thermal expansion of slip-cast fused silica cannot be measured accurately at temperatures very much above the processing temperature of 2200° F. Figure 4-12 shows the thermal expansion of a technical grade and high-purity grade of slip-cast fused silica measured using a graphite dilatometer. At temperatures above 2200° F, thermal expansion appears to decrease rapidly; however, this is in reality further densification with permanent contraction of the test specimen.

### 4.3.2 Viscosity

Fleming 5/ produced the curve shown in Figure 1-1 for viscosity of fused silica with respect to temperature using a number of data sources. Murphy 17/ established viscosity curves with respect to time for high-purity and technical grade slip-cast fused silica. This data is shown in Figures 4-13 and 4-14. It can be seen by comparing these two figures with Fleming's data (Figure 1-1) that there is good agreement for short times at temperature. However, as time increases, particularly for temperature above 2200° F the viscosity increases. This increase in viscosity with time can be attributed to structural (crystalline) changes in the material. Cristobalite determinations for each temperature after testing are shown in Figure 4-15.

### 4.3.3 Thermal Conductivity

The thermal conductivity of fused silica is structure dependent. Since slip-cast fused silica is porous, it contains numerous air pockets which are small enough not to be subject to internal convection currents but numerous enough to have a significant effect in lowering the conductivity. As a result, the thermal conductivity of the slip-cast material is lower than that of the glass-worked material. At elevated temperatures, radiation

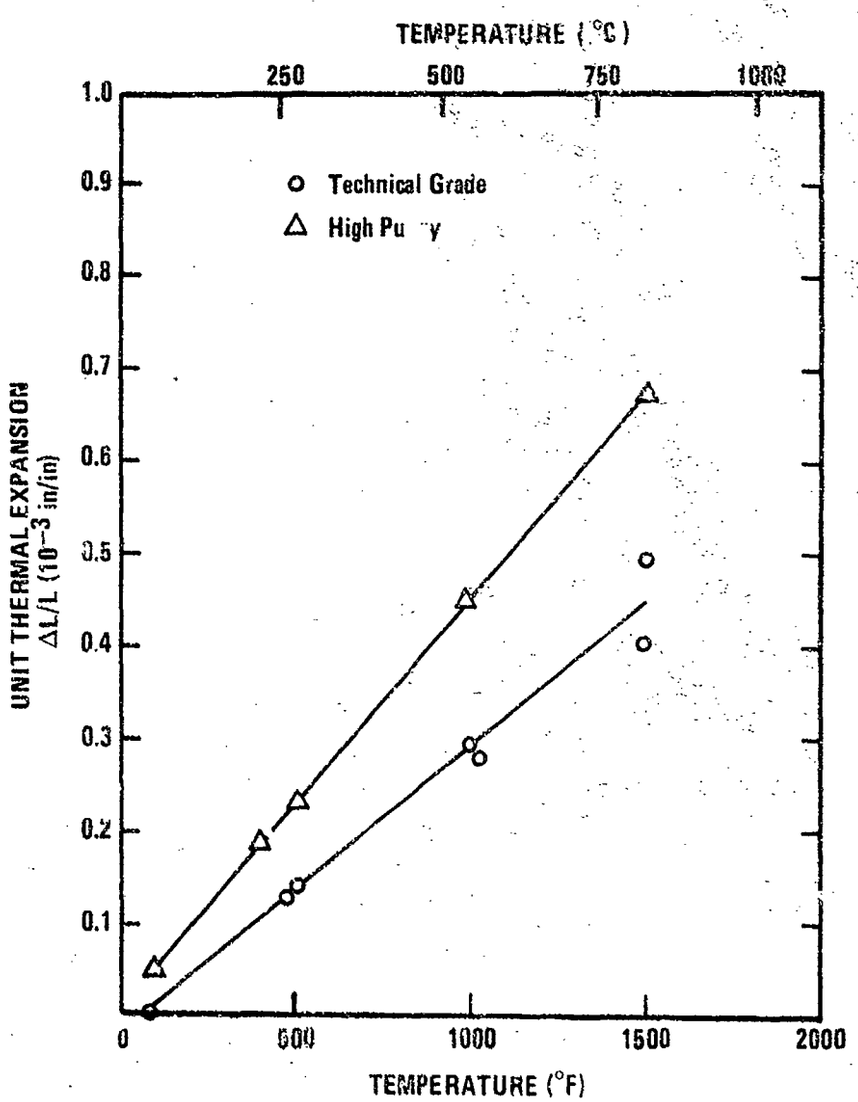


Figure 4-12. Thermal Expansion of Slip-Cast Fused Silica Determined in a Graphite Dilatometer. (Reference 7, page 23.)

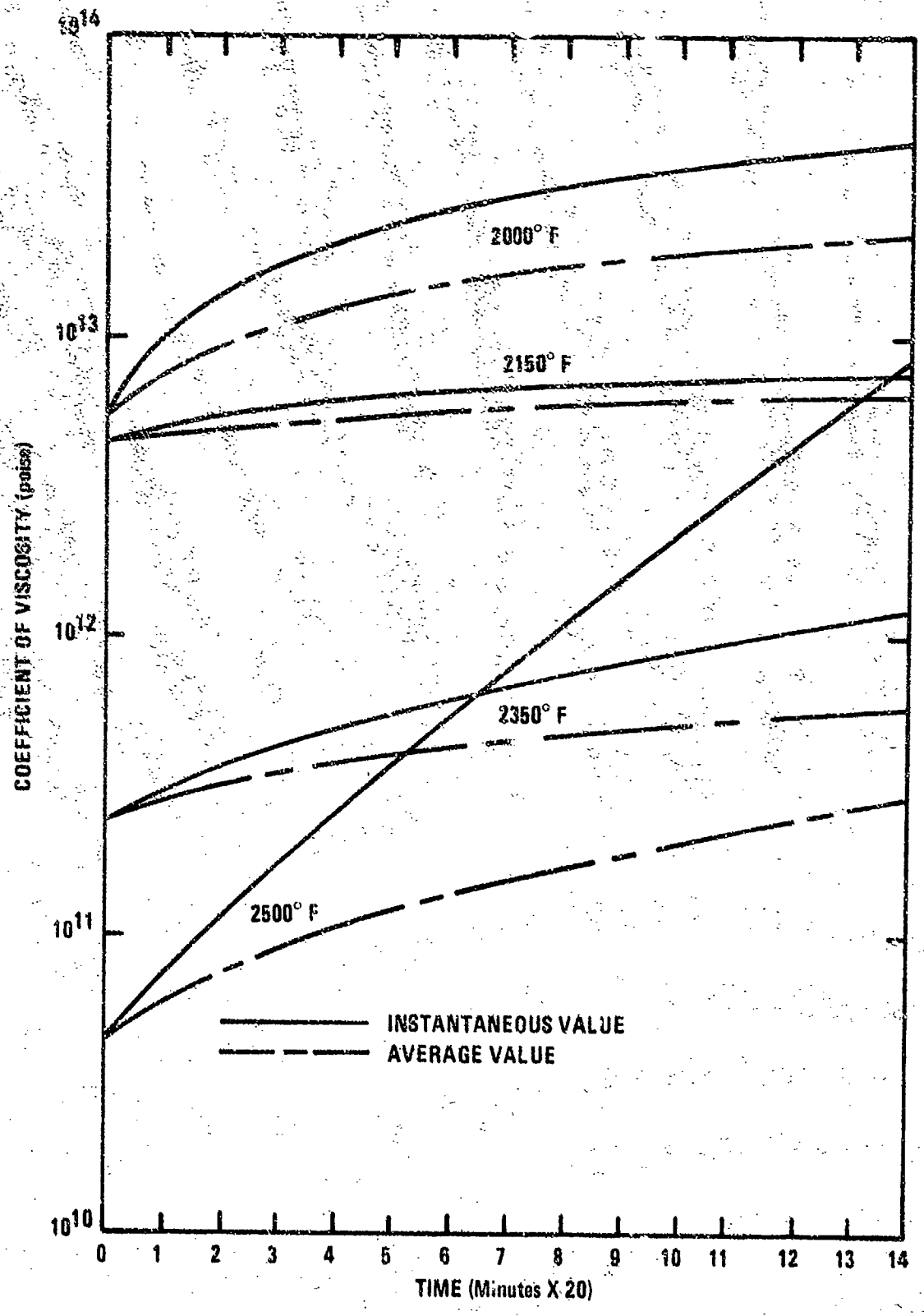


Figure 4-13. Variation of Viscosity with Time for Technical Grade Slip-Cast Fused Silica.

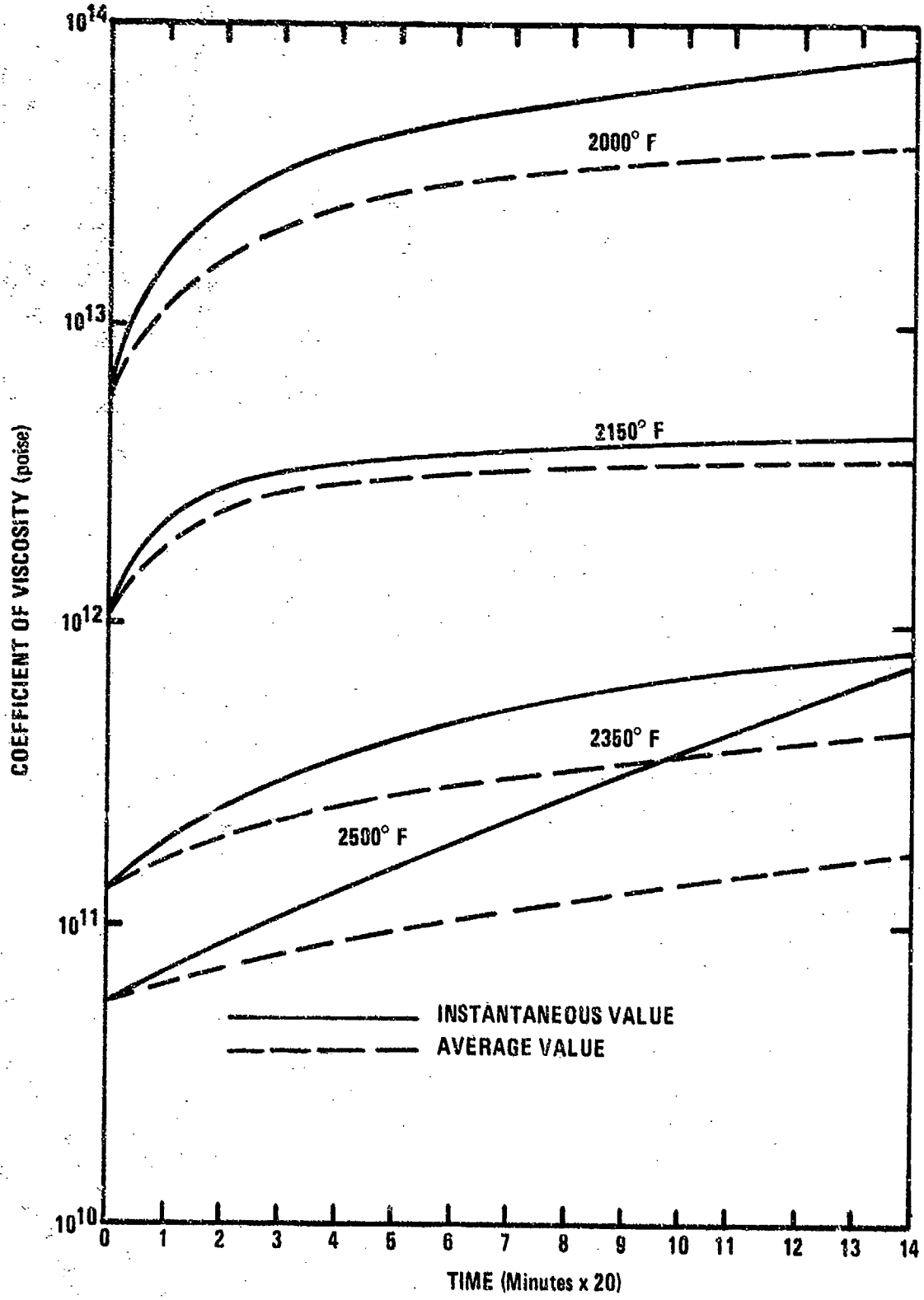


Figure 4-14. Variation of Viscosity with Time for High Purity Slip-Cast Fused Silica.

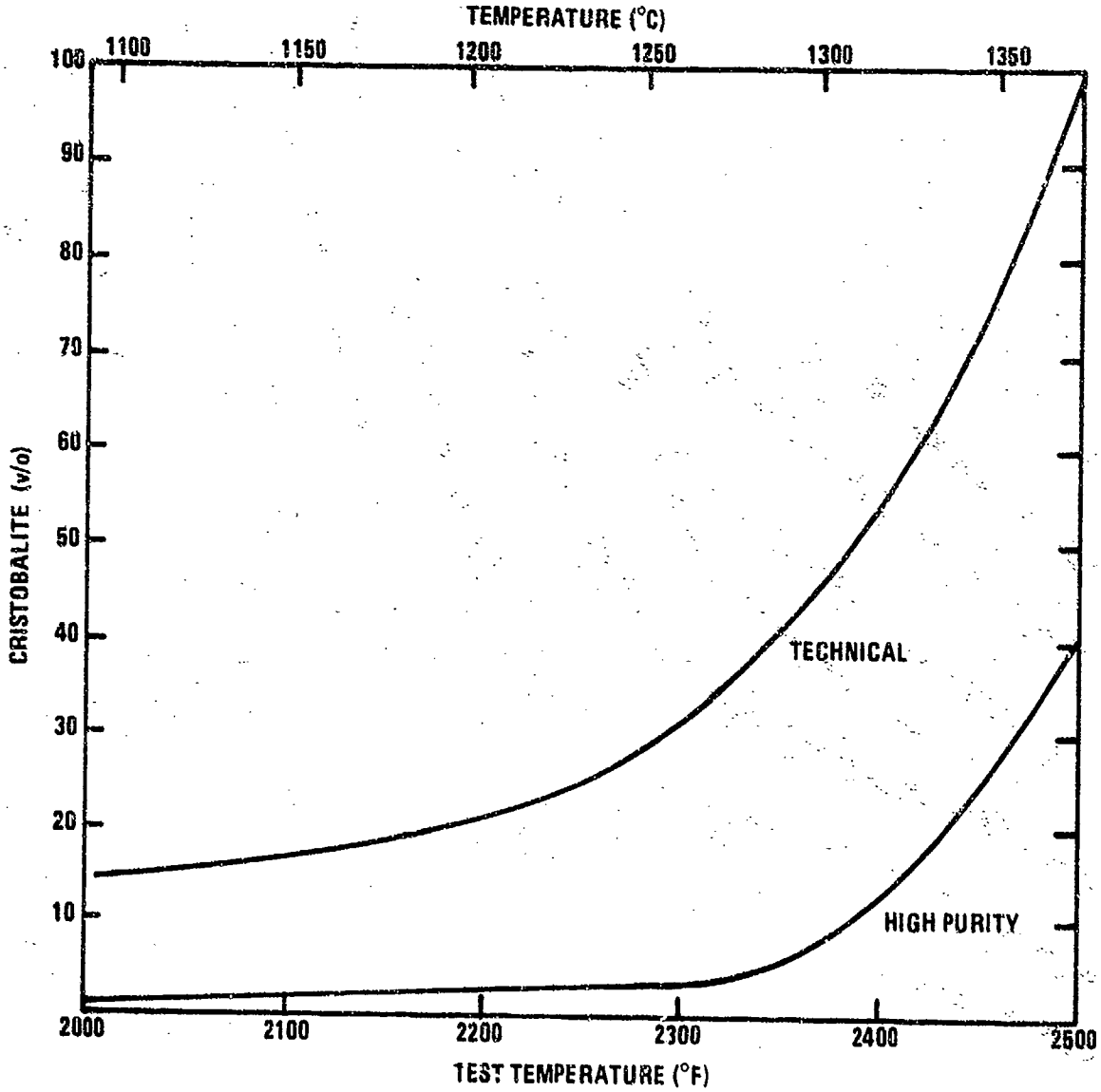


Figure 4-15. Cristobalite Levels in High Purity and Technical Grade Slip-Cast Fused Silicas after Viscosity Tests.

contributes essentially nothing to the thermal conductivity of the slip-cast material but contributes considerably in the case of the glass-worked material. As a result, the two classes of fused silica differ considerably in thermal conductivity above 1800° F. The thermal conductivity of the slip-cast material is primarily a function of density (porosity) and is shown with respect to temperature for several densities in Figure 4-16.

There is considerable interest in thermal conductivity data for slip-cast fused silica at temperatures above the normal processing temperature (2200° F) and even to temperatures approaching 4000° F. Most of this interest centers around aerospace applications, where atmospheric heating occurs on re-entry and for other hypersonic vehicles operating in the atmosphere. This heating at a high heat flux is usually over a small area of the radome or leading edge and lasts for only a few seconds. Thermal conductivity measurements on slip-cast fused silica above the processing temperature using conventional guarded hot plate thermal conductivity equipment would be meaningless. This type of equipment requires that equilibrium conditions be reached before each measurement. This requires that the sample be at temperature for a lengthy period. If the sample is above the processing temperature, two events are occurring simultaneously which render the data meaningless. First, the entire specimen is densifying due to further sintering, and secondly, crystallization (cristobalite) formation is occurring. The result is that such data is not representative of the material or conditions to be expected. A hypersonic radome would be densified to only a finite depth from the surface, depending on the heat flux and time of exposure. Bomar 19/ has developed equations and constants to predict thermal conductivity density and heat capacity. The experimental set-up by Bassett and Bomar 20/ to measure dielectric

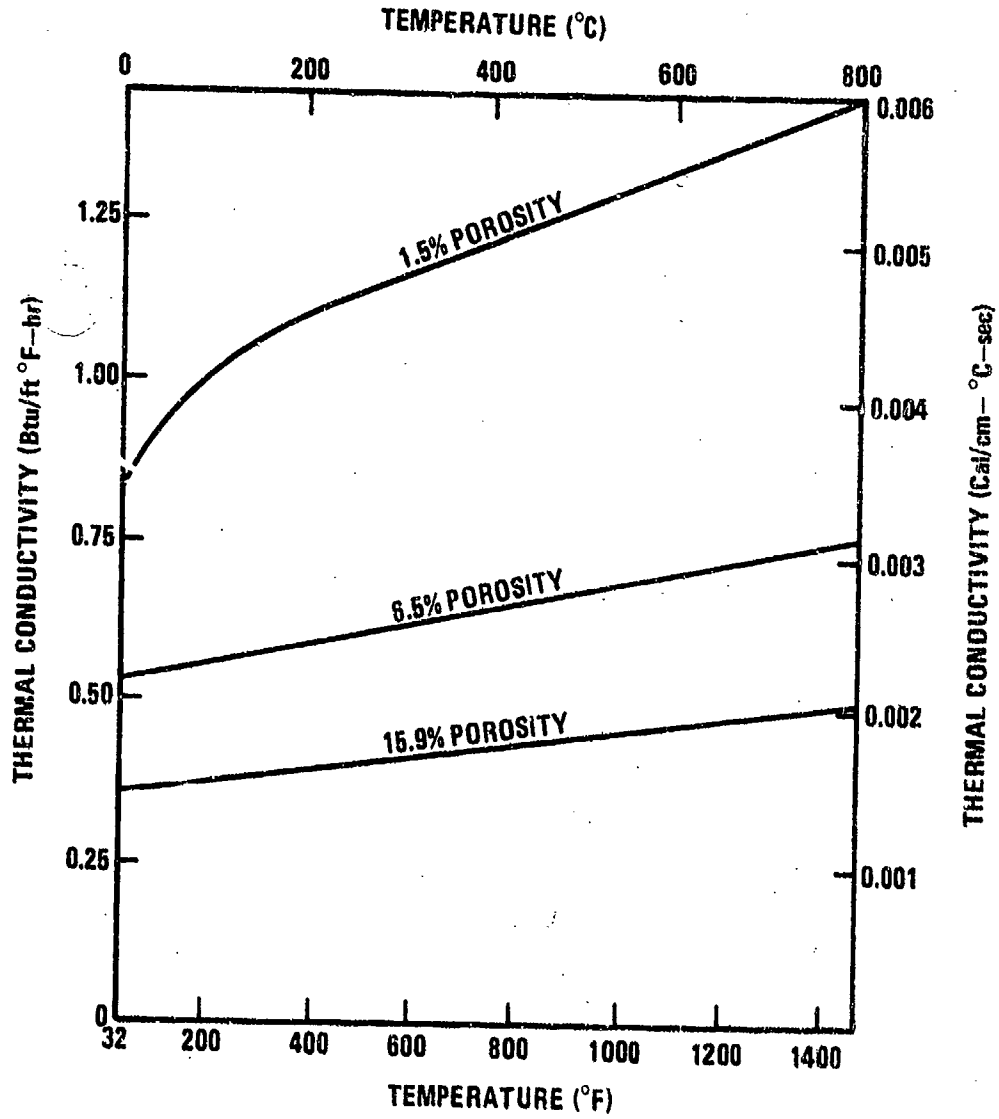


Figure 4-16. Thermal Conductivity of Slip-Cast Fused Silica at Various Porosity Levels 18/.

properties of ceramic materials is not unlike atmospheric heating of a radome. These utilize a high heat flux on a portion of one side of a rotating flat plate. Heating in this manner results in rapid densification of the surface being heated and also in a density and temperature gradient through the slab. While being heated, the plate is expanding due to thermal expansion and receding due to densification.

In order to calculate the temperature profiles and sample thickness, a solution to the two-dimensional transient heat conduction equation for a slab of finite thickness with time and temperature dependent properties and with a receding or expanding surface is required. This equation is developed from the energy equation in conjunction with the continuity and momentum equations as described in Bird, Stewart, and Lightfoot 21/. Because of the experimental method used to heat the sample, the heat fluxes in the radial and angular directions are assumed to be small and thus may be neglected. Further, if one assumes that for any incremental thickness ($\Delta z$) the corresponding change in radius ($\Delta r$) is very small, then a quasi one-dimensional heat conduction problem results where r becomes a function of z only. The physical situation, then, is represented by the following equation which is an appropriate modification to Bird et al. for a pure substance

$$\rho(T,t)\ Cp(T)\ \pi r^2 \frac{DT}{Dt} = -(\nabla \cdot \pi r^2 q) - T/\hat{V} \left(\frac{\partial \hat{V}}{\partial T}\right)_p \pi r^2 \left(\frac{DP}{Dt}\right) \qquad (4\text{-}5)$$

where T is temperature

t is time

r is radius of the local cross-sectional area at any z

a is thickness

$\rho$ is density

Cp is heat capacity

q is heat flux

V is specific volume, and

P is pressure.

Assuming that an expanding/contracting solid may be treated as a fluid at constant pressure, the quantity $\frac{DP}{Dt}$ is equal to zero. Further, if q is defined as $k(T,\rho)\ \frac{\partial T}{\partial z}$, then, with appropriate mathematical manipulation, Equation 4-5 reduces to

$$\rho(T,t)\ Cp(T)\ \left(\frac{\partial T}{\partial t} + v_z \frac{\partial T}{\partial z}\right) = k(T,\rho)\ \frac{\partial T}{\partial z}\ \left(\frac{1}{r^2}\frac{\partial r^2}{\partial r}\right) + \frac{\partial}{\partial z}\ (k(T,\rho)\ \frac{\partial T}{\partial z}). \quad (4\text{-}6)$$

Considering the group $k(T,\rho)\ \frac{\partial T}{\partial z}\ \left(\frac{1}{r^2}\frac{\partial r^2}{\partial r}\right.$ in Equation 4-6, if the thermal expansivity of a solid in the radial direction is defined as $\alpha_r = \frac{\partial r}{r}/\partial T$, and an appropriate variable change is made, then the group under consideration reduces as follows:

$$k(T,\rho)\ \frac{\partial T}{\partial z}\ \left(\frac{1}{r^2}\frac{\partial r^2}{\partial r}\right) = 2\ \alpha_r\ k(T,\rho)\ \left(\frac{\partial T}{\partial z}\right)^2, \quad (4\text{-}7)$$

and Equation (4-7) becomes

$$\rho(T,t)\ Cp(T)\ \left(\frac{\partial T}{\partial t} + v_z \frac{\partial T}{\partial z}\right) = 2\ \alpha_r\ k(T,\rho)\ \left(\frac{\partial T}{\partial z}\right)^2 + \frac{\partial}{\partial z}\left(k(T,\rho)\frac{\partial T}{\partial z}\right). \quad (4\text{-}8)$$

In order to consider the change in thickness due to a change in density, the continuity equation must be used. This equation is given in Bird et al. 21/ as follows:

$$\frac{\partial \rho}{\partial t} + \rho v = 0. \qquad (4\text{-}9)$$

This equation and Equation 4-8 provide the basis to obtain the thermal profiles and sample thickness as a function of time.

In order to solve the differential equations derived above, the time and temperature behavior of certain physical and transport properties of the samples must be known. Analytical forms for each of these properties are described in the following paragraphs.

The density of pure crystalline materials is a function of temperature and pressure only; however, the density of materials formed by ceramic-powder metallurgical techniques is affected by sintering. This is especially important for slip-cast fused silica. Because sintering is a function of time at a temperature, the density of the material is a function of time as well as temperature.

A general equation describing these phenomena is given by Bassett and Bomar 19/:

$$\rho = \rho_t \left(\frac{\varphi_1}{\varphi_1 + \varphi_2}\right) - (\rho_{t_o} - \rho_o) \exp(\theta - \varphi_1 t) + \rho_{t_o} \left(\frac{\varphi_2}{\varphi_1 + \varphi_2}\right) \exp(\theta - \varphi_1 t) \qquad (4\text{-}10)$$

where $\rho$ = density ($lb/ft^3$ or $gm/cm^3$)

$t$ = time (hr)

$\varphi_1$ = $k_o \exp(-\Delta E/RT)$

$\varphi_2$ = $(\alpha_z + 2d_r) \frac{\delta T}{\delta t}\Big|_t$

$\theta$ = $\int_{T_o}^{T} (\alpha_z(T) + 2\alpha_r(T))dT$

$k_o$ = particle size base constant ($hr^{-1}$)

$\Delta E$ = activation energy (Btu/lb-mole)

R = gas constant (Btu/lb-mole °R)

T = temperature (°R)

$\alpha_z(T) = \frac{1}{z}\frac{\delta z}{\delta T}$ = thermal expansion coefficient ($°R^{-1}$) = $a + bT + cT^2 + dT^3$

"t" = denotes theoretical properties

"o" = refers to ambient temperature.

Slip-cast fused silica can be assumed to be isotropic giving $\theta = -3\int\alpha(T)dT$. Also, for simplicity, $\varphi_2$ can be taken as 0 for no dependence upon a temperature gradient is shown in the data available. Finally, $\rho t$ can be expressed as

$$\rho t = \rho to \exp(\theta) \tag{4-11}$$

giving

$$\rho = \rho to \exp(\theta) - (\rho to - \rho o) \exp(\theta - \varphi_1 t). \tag{4-12}$$

The sintering rate of slip-cast fused silica has been obtained from experimental sintering data for certain high purity slips 22/. Values for the constants in Equation 4-12 are given in Table 4-3. The sintering curves shown in Figure 4-17 were calculated using Equation 4-12 and agree well with the experimental data at 2500° and 2700° F; no experimental data are available above 2700° F.

The thermal conductivity of amorphous or glassy materials has been reported by Jakob 23/ to be proportional to some power of the temperature. Jakob also showed that for non-metallic crystalline substances the thermal conductivity was inversely proportional to temperature. In addition,

TABLE 4-3

CONSTANTS FOR THE DENSITY FUNCTION FOR HIGH PURITY SCFS

| $\varphi_1$ | | $\alpha(T)$ | | | | | |
|---|---|---|---|---|---|---|---|
| $k_o$ | $\Delta E$ | a | b | c | d | $\rho_{to}$ | $\rho_o$ |
| $2.016(10^{12})$ | $1.634(10^{5})$ | $2.86(10^{-7})$ | 0 | 0 | 0 | 2.239 | 1.934 |

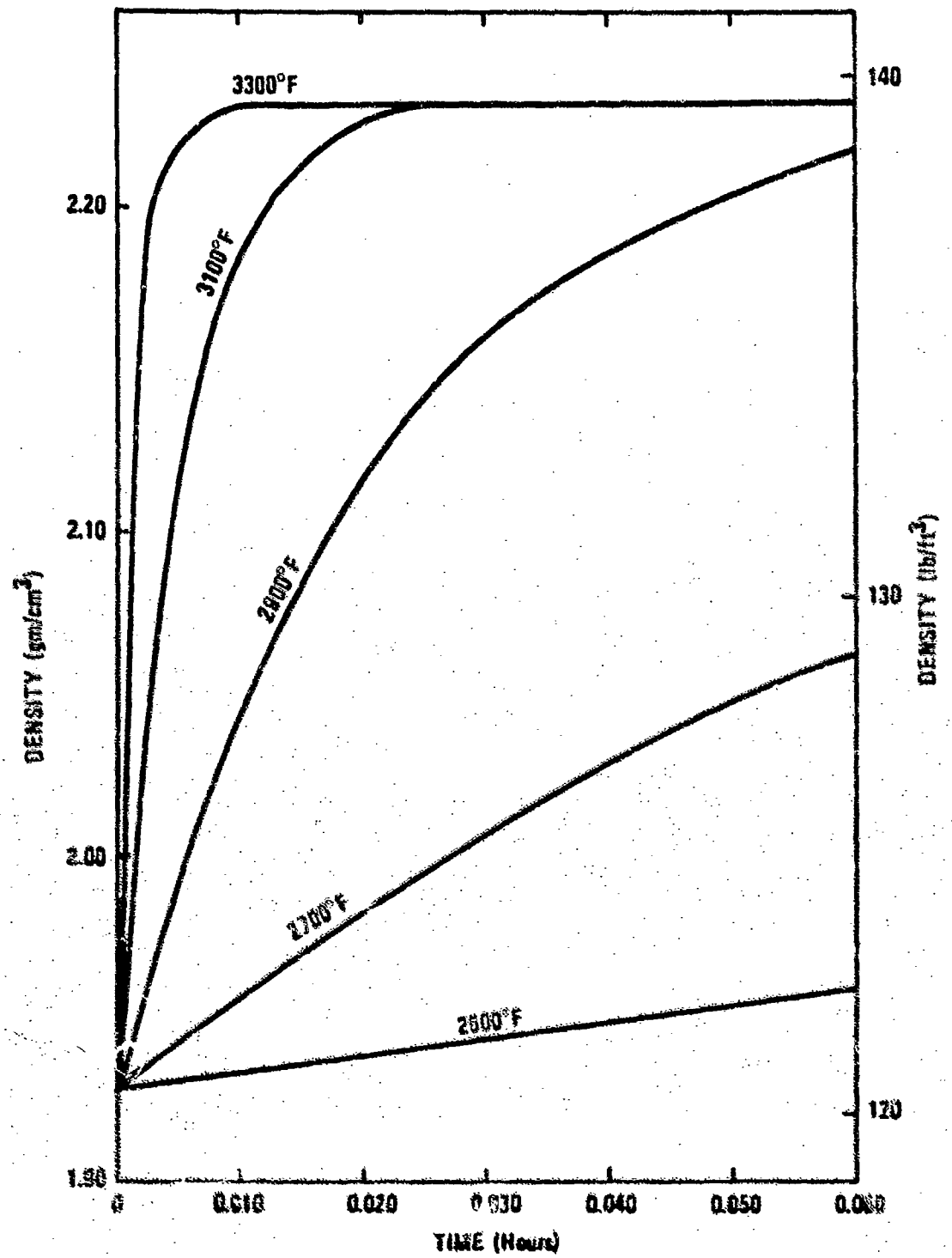


Figure 4-17. Density of Slip-Cast Fused Silica versus Time at Temperature. (Reference 19.)

there will be an effect on the thermal conductivity due to a change in density. At temperatures above about 3000° F, fused silica rapidly loses any porosity present and becomes transparent. Published data on the thermal conductivity of transparent silica at high temperatures shows exceedingly poor agreement so that an investigator has almost no idea which value he should use in heat transfer calculations above 3000° F.

Bassett and Bomar 19/ were required to calculate temperature profiles in slip-cast fused silica as part of their data reduction operation for obtaining high temperature dielectric properties. The most feasible approach to selecting the appropriate value of thermal conductivity above 3000° F was to include embedded thermocouples in their sample materials, then to choose values of conductivity which gave temperature profiles matching the thermocouple data.

Their data have been used to aid in establishing the thermal conductivity of slip-cast fused silica shown in Figure 4-18. This figure shows conductivity as a function of temperature and density. A typical radome will have an initial density on the order of 1.90 to 1.95 $gm/cm^3$. Above 2500° F this radome will densify rapidly until its conductivity approaches that of clear fused silica near 3300° F. The lower curve in Figure 4-18 applies when heating is sufficiently rapid that any particular layer of silica in the radome wall is in the temperature range 2500° to 3300° F for about 10 minutes or less. Slower heating rates would cause the lower curve to lie nearer to the upper curve at temperatures above 2500° F.

For radome calculations with relatively high heating rates, use of the lower curve in Figure 4-18 is recommended. These data are fitted by the following equations:

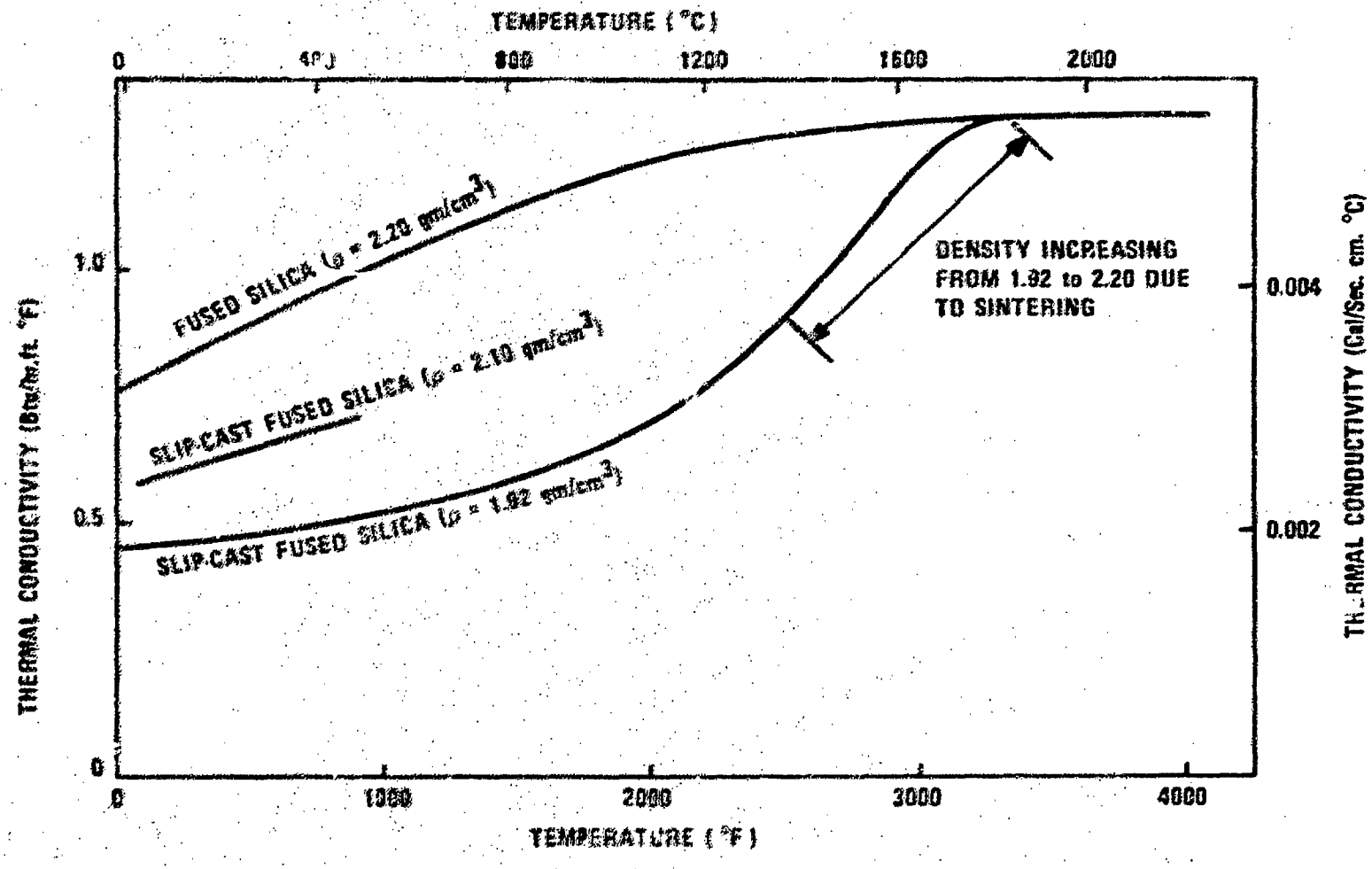


Figure [illegible]. Thermal Conductivity of Slip-Cast Fused Silica.

$$k = a + \frac{b}{T} + cT + dT^3 \quad (0°F \leq T \leq 3100° F) \qquad (4\text{-}13a)$$

$$k = 1.29 \quad (3100° F \leq T \leq 4000° F) \qquad (4\text{-}13b)$$

where a,b,c,d, are constants

k is thermal conductivity

T is temperature (°R)

Values of the constants are given in Table 4-4.

TABLE 4-4

CONSTANTS FOR THE THERMAL CONDUCTIVITY FUNCTION

| Material | a | b | c | d |
|---|---|---|---|---|
| SCFS | $4.767(10^{-1})$ | 0 | $-1.828(10^{-5})$ | $1.869(10^{-11})$ |

### 4.3.4 Heat Capacity

Equations developed by Bomar 19/ in his thermal analysis program can also be used to predict heat capacity.

The heat capacity of solids is a function of temperature and pressure only, provided the material does not experience a phase or structural change. The thermal history or time dependence, then, is of no consequence. Since the assumption has all ready been made that the pressure dependence of the solids is negligible, the heat capacity function may be represented by the following equation for a given temperature range:

$$Cp = a + bT + c/T^2 \qquad (4\text{-}14)$$

This equation results from consideration of the statistical thermodynamic description of a solid and is discussed in detail in many thermodynamic texts such as Lewis and Randall 24/. This equation was used to "fit" existing experimental data for slip-cast fused silica. Values for the constants are given in Table 4-5. Also included in this table is the reference for the data used. Considerable extension of the data from the literature to the temperature ranges required for this work was made by these authors.

TABLE 4-5

CONSTANTS FOR THE HEAT CAPACITY FUNCTION

| Material | a | b | c | Reference |
|---|---|---|---|---|
| SCFS | $2.45(10^{-1})$ | $1.418(10^{-5})$ | $-2.50(10^{4})$ | 7 |

A graphical representation of these data is shown in Figure 4-19. Since the heat capacity of fused silica varies little with form, it can be compared with Fleming's compilation of data for glass-worked silica also included in Figure 4-19 along with experimental data obtained at Southern Research Institute.

### 4.3.5 Enthalpy

Since heat capacity data are usually based on measurements of the change in enthalpy, enthalpy data will show the same agreement as heat capacity data. Fleming's 5/ compilation of data for glass-worked fused silica is compared with Southern Research Institute's 7/ data on technical and high-purity slip-cast fused silica in Figure 4-20.

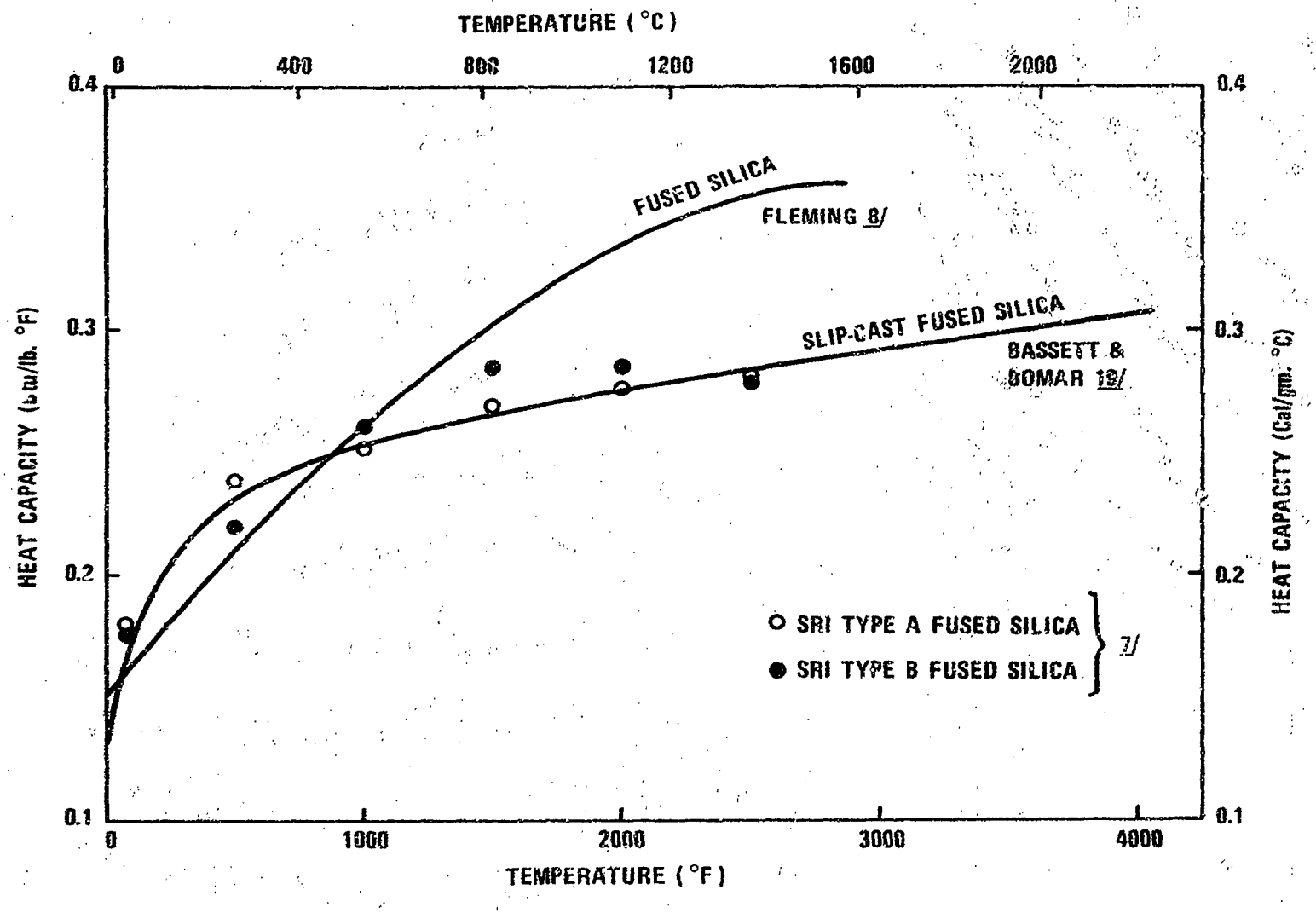


Figure 4-19. Heat Capacity of Fused Silica.

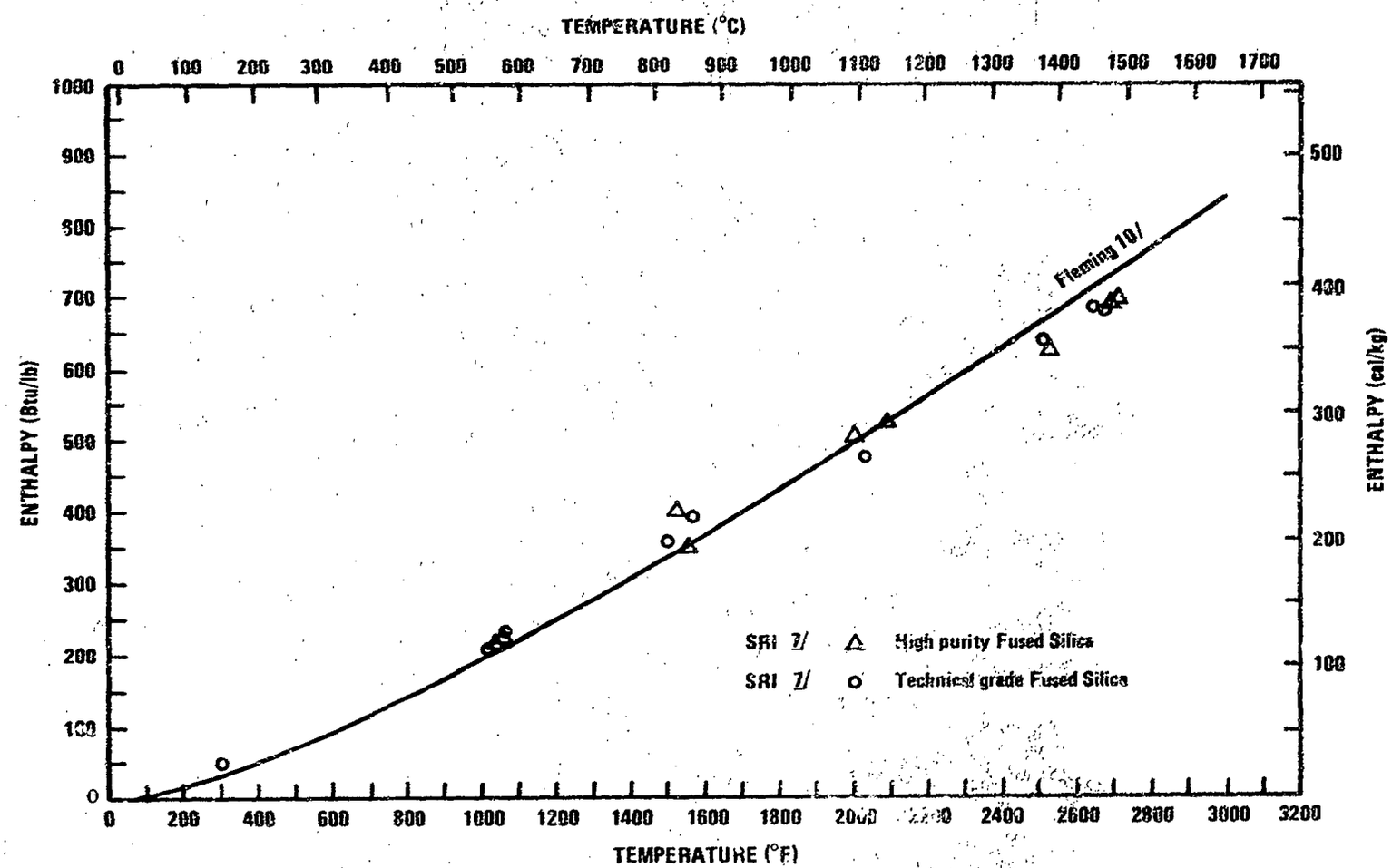


Figure 4-20. Enthalpy of Fused Silica.

### 4.3.6 Thermal Diffusivity

The thermal diffusivity for technical grade and high purity slip-cast fused silica is shown in Figure 4-21. The thermal diffusity for 30 and 50 $lb/ft^3$ fused silica foam is also shown on this figure.

## 4.4 Electrical Properties

### 4.4.1 Resistivity

Figure 4-22 shows the electrical resistivity of a technical grade slip-cast fused silica and for glass worked fused silica. The low value of resistance at room temperature is probably due to the presence of moisture in the pores. As the temperature is increased moisture is expelled and the resistance increases at high temperatures the resistivity of slip-cast fused silica is nearly that of the glass worked material.

### 4.4.2 Dielectric Constant and Loss Tangent

The dielectric constant of slip-cast fused silica is affected primarily by changes in density and temperature, although it does change very slightly with frequency. Impurities have little effect on the dielectric constant; hence, there is little difference in the dielectric constant and loss tangent of technical and high purity slip-cast fused silica of the same density.

The loss tangent is affected by moisture and impurities in the silica. At low temperatures moisture can result in a high loss tangent. At high temperatures the loss tangent increases more rapidly in impure material. Figure 4-23 is a plot of dielectric constant versus density for room temperature measurement at X-band (9.375 GHz). The author of this data suggested

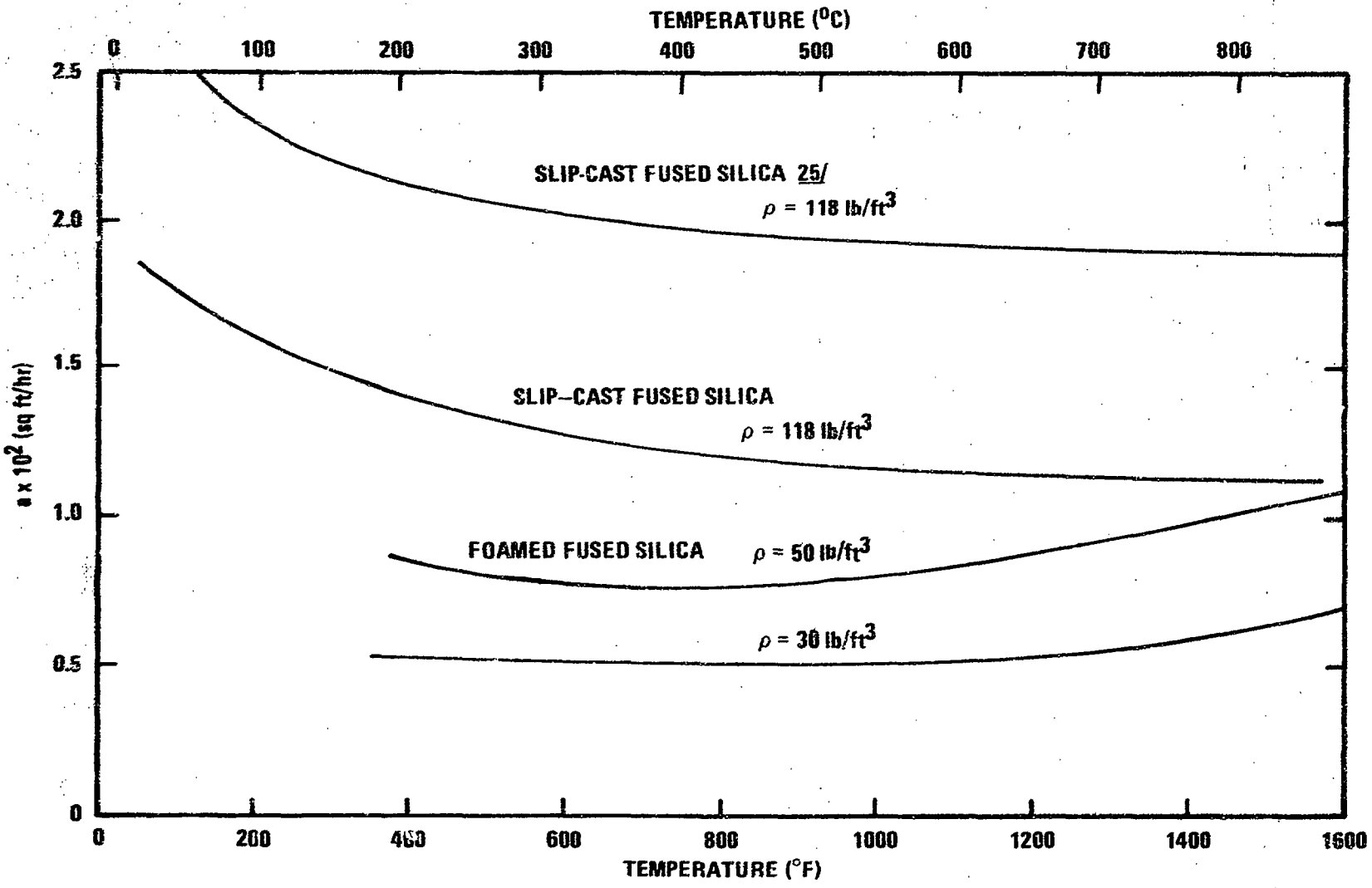


Figure 4-21. Thermal Diffusivity of Slip-Cast Fused Silica and Foamed Fused Silica. (Reference 8, page 35.)

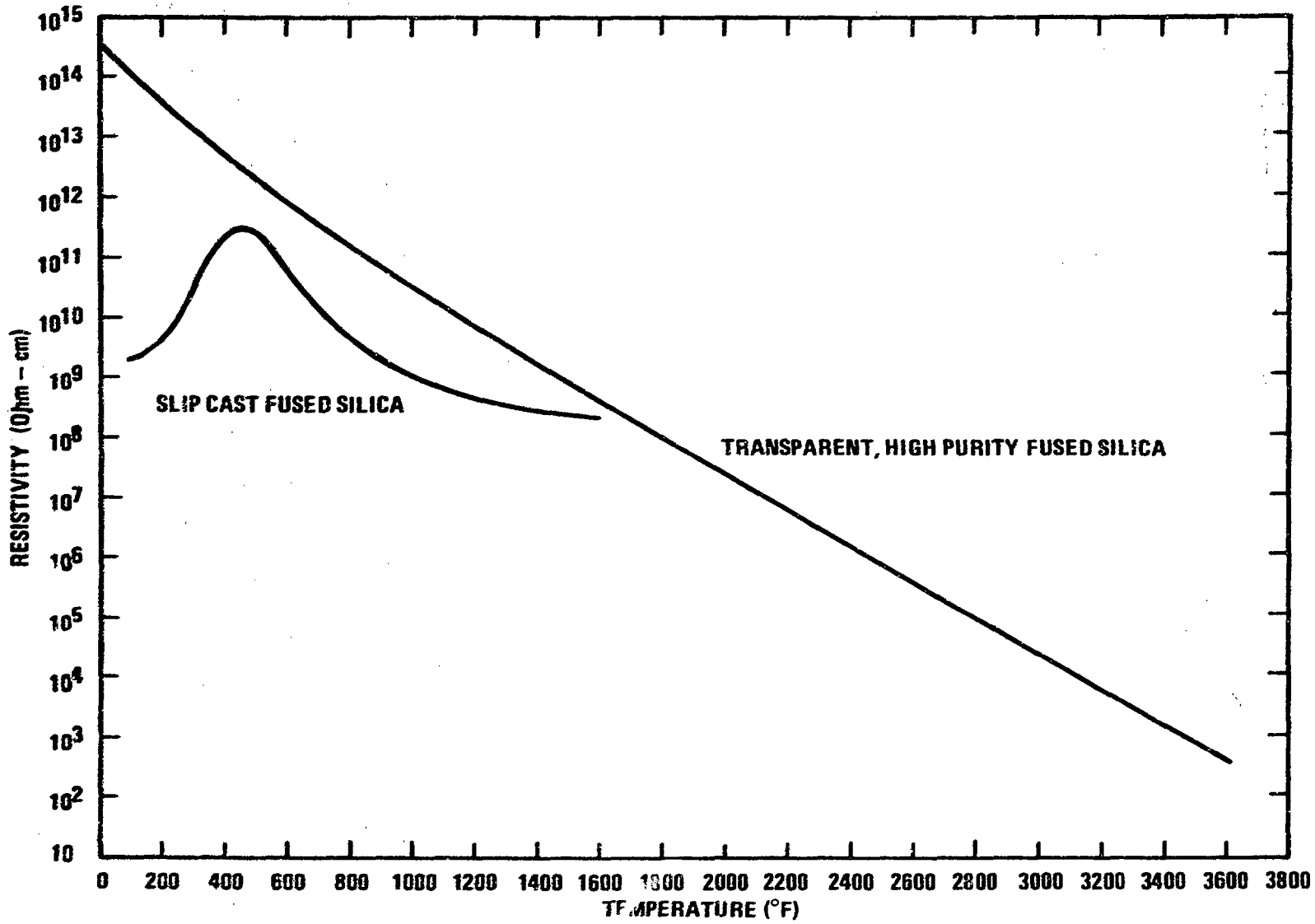


Figure 4-22. Electrical Resistivity of Fused Silica.

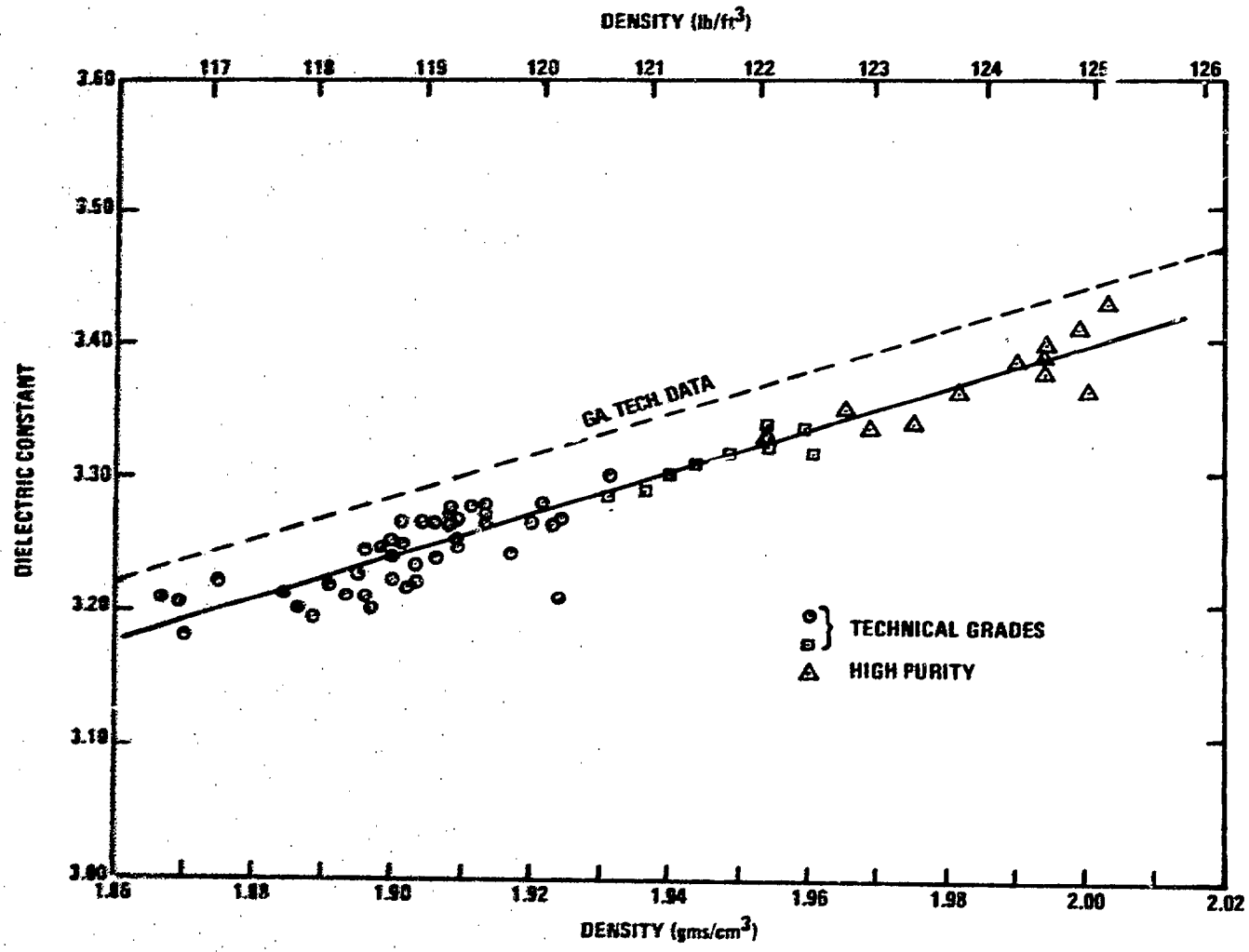


Figure 4-23. Dielectric Constant of Slip-Cast Fused Silica versus Density Measured at X-Band. (Reference 5.)

am empirical straight line curve fit which is valid over the narrow range of density presented 26/

$$K' = 1.61\ \rho + 0.183, \tag{4-15}$$

The upper dashed line provides a better fit to data collected both at Georgia Tech and is for the form

$$K' = 1.61\ \rho + 0.223 \tag{4-16}$$

Over a wider range of density values, the log mixture rule can be used:

$$\log K = \Sigma\ V_i \log k_i \tag{4-17}$$

where $k_i$ = dielectric constant phase i

$V_i$ = volume fraction of phase i.

If one assumes only two phases, $SiO_2$ and air, neglecting cristobalite and other impurities, the equation can be rewritten

$$K' = K'_{theo}\ (exp)\ \frac{\rho_a}{\rho_{theo}} \tag{4-18}$$

where $k'_{theo}$ = Dielectric constants of theoretically dense fused silica at any frequency

$\rho_a$ = bulk density of test specimen

$\rho_{theo}$ = Theoretical density of fused silica.

For theoretically dense fused silica measured at room temperature and X-band frequency the dielectric constant is 3.85. Using this value Equation 4-18 is reduced to

$$K' = 3.85 \text{ (exp) } \frac{\rho}{139} \qquad (4\text{-}19)$$

where $\rho$ = bulk density in $lb/ft^3$.

Since frequency causes only slight variation, this provides a method for estimating the room temperature dielectric constant of any density material. Figure 4-24 is a theoretical curve plotted from Equation 4-19 and shows individual points measured at frequencies of 7.5 to 50 GHz.

The effect of temperature is more pronounced. Figure 4-25 shows the dielectric constant with respect to temperature for several densities of slip-cast fused silica measured at 6 GHz frequency. Figure 4-26 shows dielectric constant and loss tangent data for two slip-cast fused silicas from different sources and with different densities, and for a glass-worked silica as well.

The majority of dielectric measurements have been limited to temperatures of 2500° F or below; however, Bassett and Bomar have developed a technique 5/ to measure dielectric properties of ceramic materials at temperatures of 4000° F and above. Figure 4-27 shows data for slip-cast fused silica to 4000° F. The rapid increase in dielectric constant and loss tangent between 2500° and 3700° F is due to densification due to rapid sintering at these temperatures.

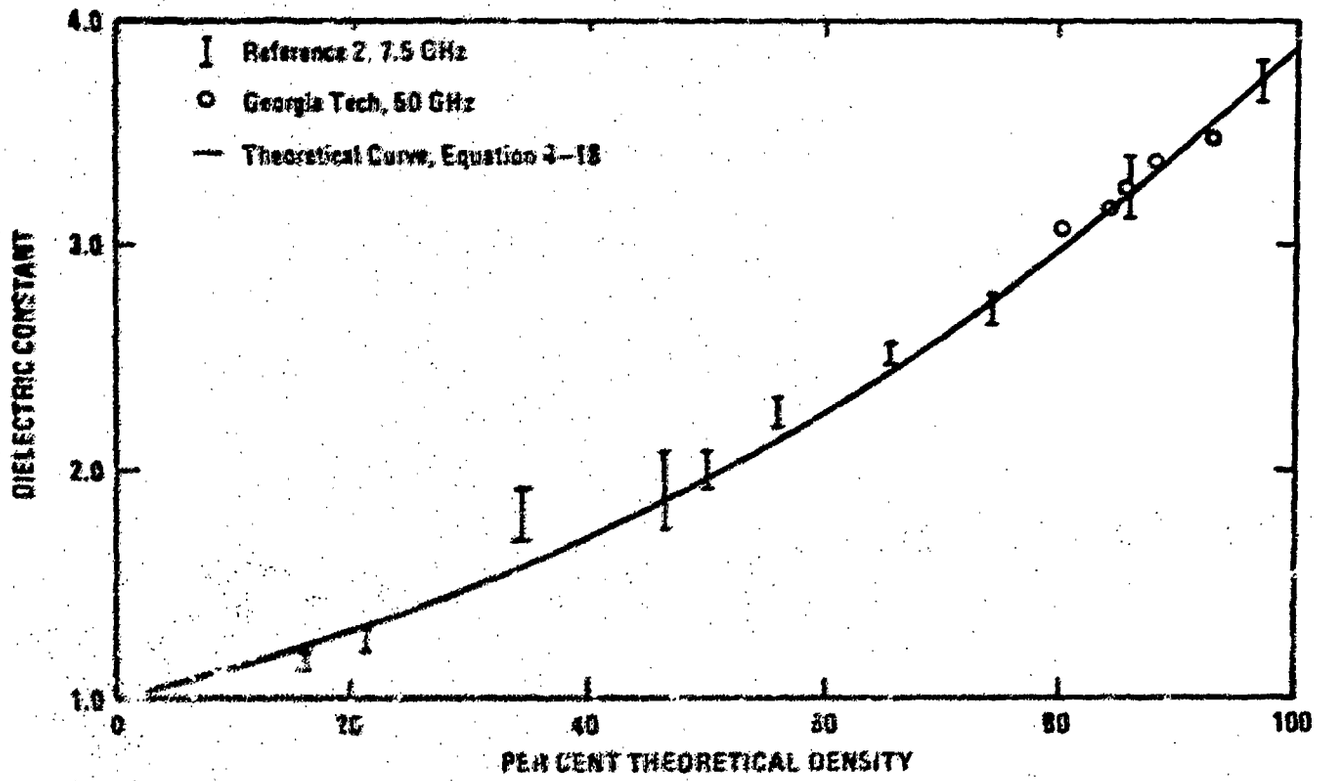


Figure 4-24. Dielectric Constant of Slip-Cast Fused Silica as a Function of Density.

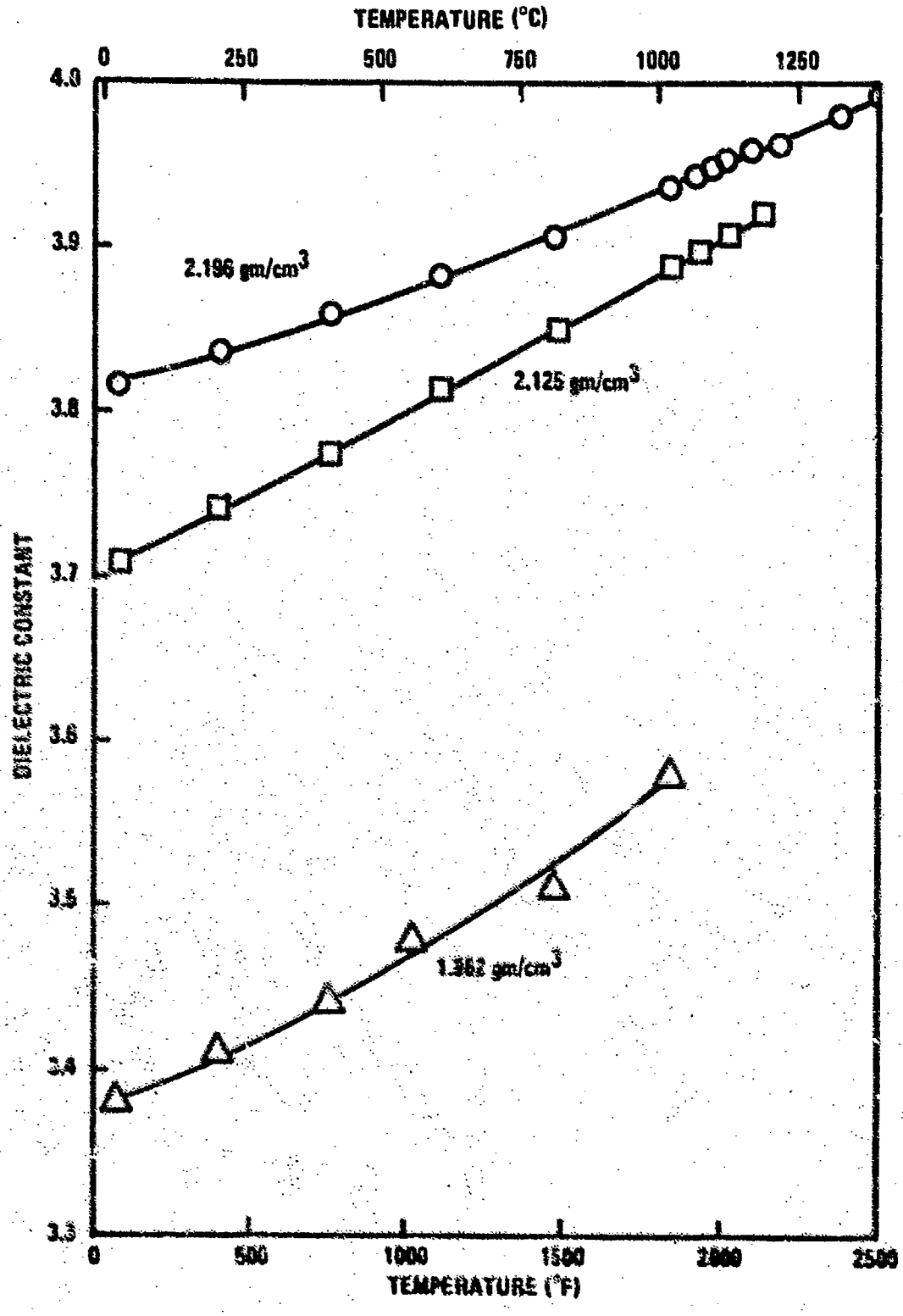


Figure 4-25. Dielectric Constant versus Temperature for Slip-Cast Fused Silica at 6 GHz.

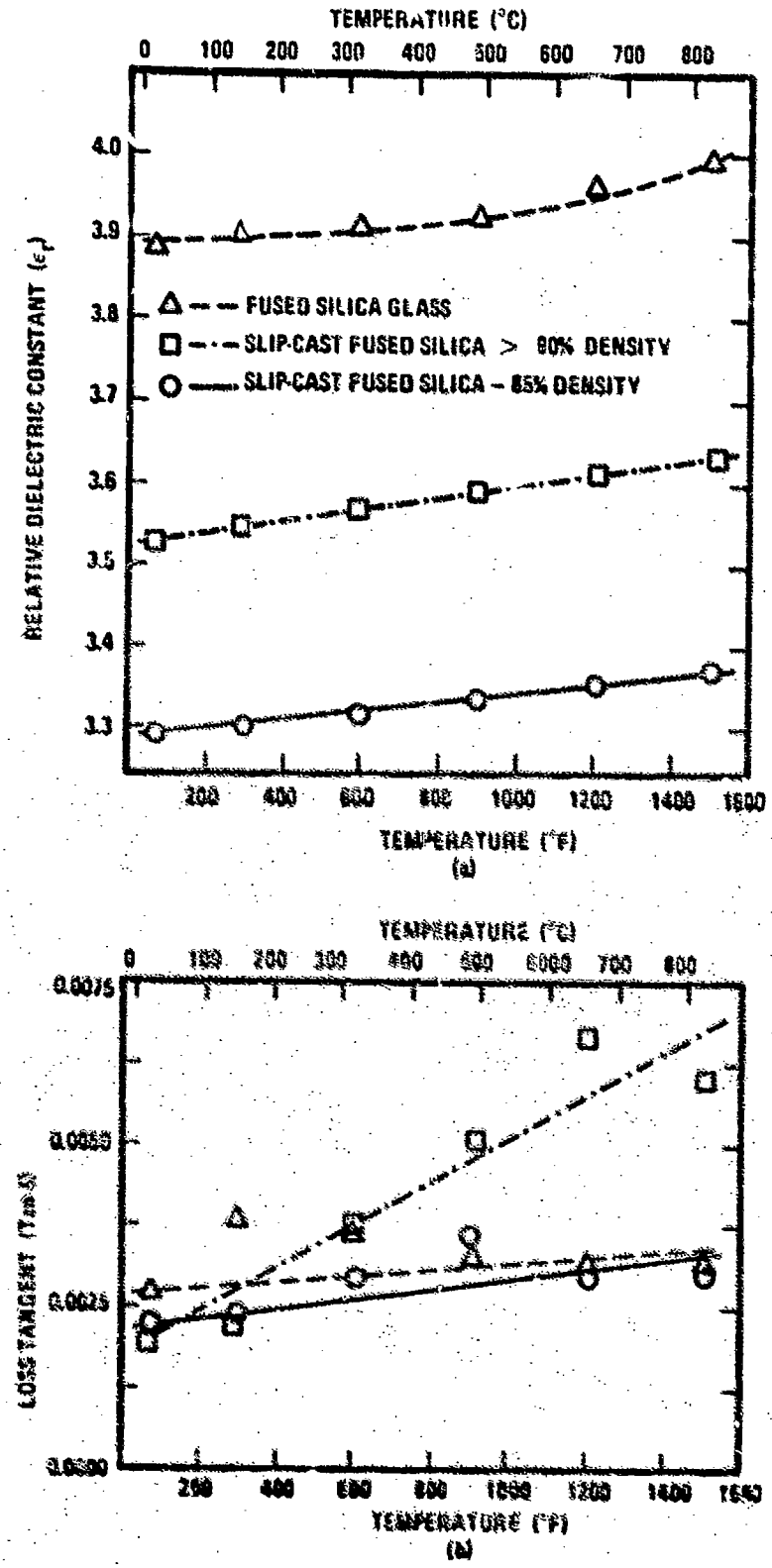


Figure 4-26. Dielectric Constant Loss Tangent for Fused Silica versus Temperature.

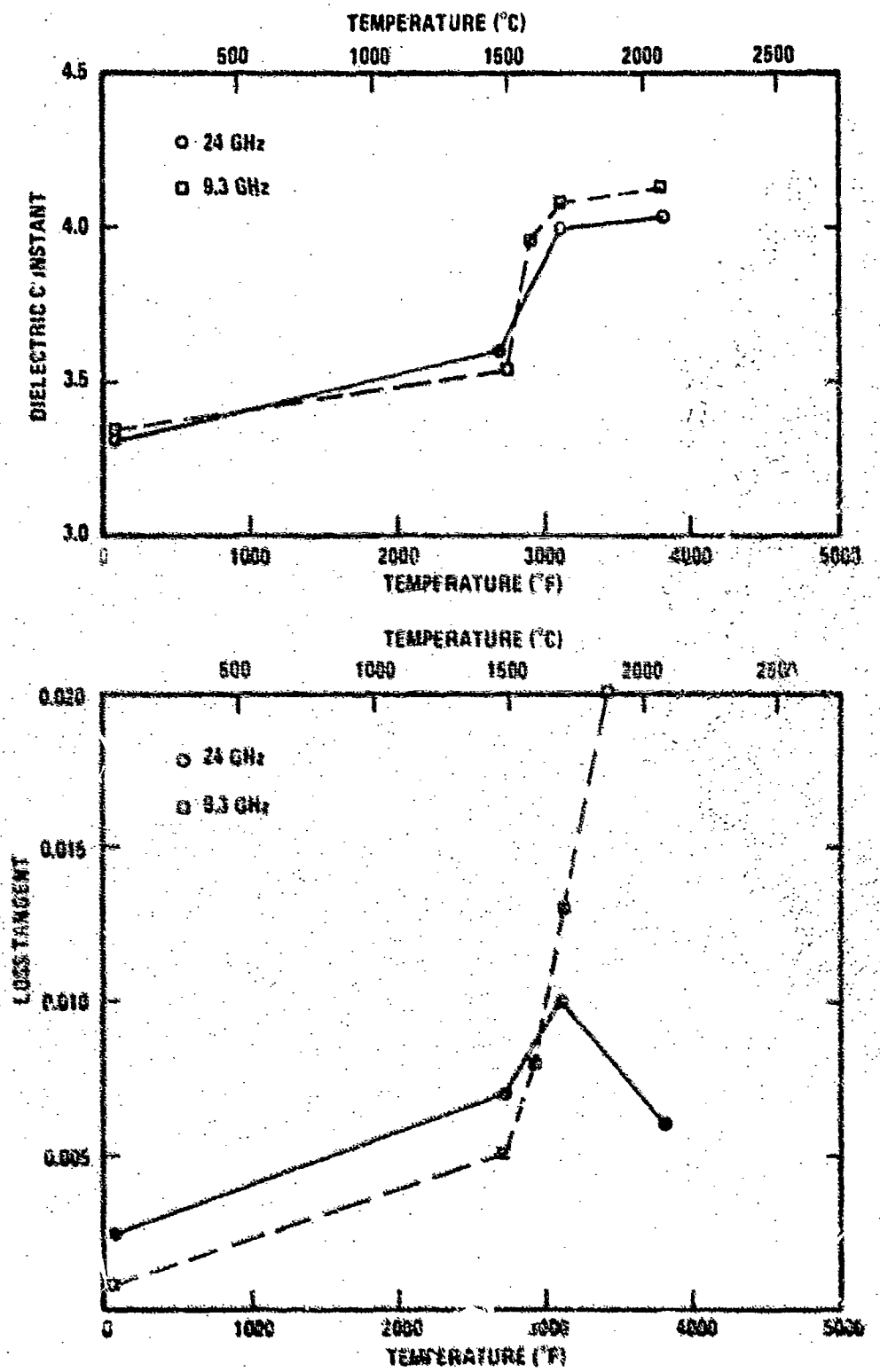


Figure 4-27. Dielectric Constant and Loss Tangent of High Purity Slip-Cast Fused Silica Measured with Focused Microwave Beam Apparatus. (Reference 19.)

## 4.5 References for Chapter IV


1. Walton, J. D., Jr., "Inorganic Radomes," Chapter 5, Radome Engineering Handbook, Design and Principles, Marcel Dekker, Inc., 1970.

2. Gannon, R. E., G. M. Harris and Thomas Vasilos, "Effect of Porosity on Mechanical, Thermal and Dielectric Properties of Fused Silica," Amer. Ceramic Soc. Bull. 44.

3. Shook, William B., Critical Survey of Mechanical Property Test Methods For Brittle Materials, Technical Documentary Report No. ASD-TDR-63-491, Contract No. AF 33(657)-8064 by the Engineering Experiment Station, Ohio State University, Columbus, Ohio, July 1963.

4. Murphy, C. A., Characterization of Fused Silica Slips, Contract N00017-67-C-0053, Dept. of the Navy, Naval Ordnance Systems Command by Georgia Institute of Technology, Engineering Experiment Station, Special Technical Report No. 2, April 1968.

5. Fleming, J. D., Fused Silica Manual, Engineering Experiment Station, Georgia Institute of Technology, Atlanta, Georgia, September 1964, U. S. Department of Commerce OTS No. 21312.

6. Harris, J. N. and E. A. Welsh, Improving Rain Erosion Resistance of Slip-Cast Fused Silica, Contract DA-AH01-67-C-247, U. S. Army Missile Command, Redstone Arsenal, Alabama, by the Engineering Experiment Station, Georgia Institute of Technology, Atlanta, Georgia, December 1967.

7. The Thermal and Mechanical Properties of Slip-Cast Fused Silica, Southern Research Institute, Birmingham, Alabama, November 1968.

8. Sedlacek, R. and F. H. Holden, "Method for Tensile Testing of Brittle Materials," The Review of Scientific Instruments 33 (3), March 1962, pp 298-300.

9. Harris, J. N., J. H. Murphy and E. A. Welsh, Ceramic Systems for Missile Structural Applications, Final Report Contract N00017-70-C-4438, Naval Ordnance Systems Command by the Engineering Experiment Station, Georgia Institute of Technology, Atlanta, Georgia, in process.

10. Dawihl W. and W. Rix, "Strength of Quartz Glass at Elevated Temperatures," Z. Tech Physik 19 (10) 294, 1938.

11. Dawihl W. and W. Rix, "Cause of Changes in Strength of Quartz Glass at Higher Temperatures," Glastech Ber 18 (10) 265 (1940).

12. Ainsworth, L., "Diamond Pyramid Hardness of Glass in Relation to the Strength and Structure of Glass: I, Investigation of the Diamond Pyramid Hardness Test Applied to Glass," J. Soc. Glass Technol. 38 479T (1954).

## 4.5 References for Chapter IV


13. Ryshkewitch, Eugene, "Are Ceramics Really Brittle?" Ceram Ind. 69 (6) 116 (1957).

14. Babcock, C. L., S. W. Barber and K. Fr ians, Ind Eng Chem 46, 161 (1959).

15. Chaklader, A. C. D. and A. L. Roberts, "Relationships Between Constitution and Properties of Silica Refractories: I, Effects of the Devitrifying of Silica Glass," Trans Brit Ceram Soc 56 331 (1957).

16. Corning Materials Handbook, Radome Department, Corning Glass Works, April 1963

17. Murphy, J. H. and J. N. Harris, Ceramic Systems for Missile Structural Applications, Quarterly Report No. 2, Contract N00017-70-C-4438, Naval Ordnance Systems Command.

18. Romashin, A. G. and Yu E. Pivinskii, "Properties of Fused Silica Ceramics," Refractories Russia 33 (9) 590-595, 1948.

19. Bassett, H. L. and S. H. Bomar, Jr., "High Temperature Complex Permittivity Measurements on Reentry Vehicle Antenna Window Materials, Contract F29601-70-C-0069, Air Force Weapons Laboratory, Kirtland AFB, N. M., by the Engineering Experiment Station, Georgia Institute of Technology, Atlanta, Georgia (ro be published).

20. Bassett, H. L. and S. H. Bomar, Jr., Dielectric Constant and Loss Tangent Measurement of High Temperature Electromagnetic Window Materials, AFWL TR-69-92, December 1969.

21. Bird, R. B., W. E. Stewart and F. N. Lightfoot, Transport Phenomena, John Wiley and Sons, New York, 1960, Chapter 11.

22. Gorton, C. W. and A. C. Merritt, "Densification of Slip-Cast Fused Silica," Paper presented at the 73rd Annual Meeting of the American Ceramic Society, Chicago, April 1971.

23. Jakob, M., Heat Transfer, Vol. I, John Wiley and Sons, New York, 1949.

24. Lewis, G. N. and M. Randall, Thermodynamics 2nd ed. Revised by Pitzer, K. S. and L. Brewer, McGraw-Hill Book Co., New York, N. Y., 1961, 723 pp.

25. Walton, J. D., Jr. and N. E. Poulos, Slip-Cast Fused Silica, ML-TDR-64-195, October 1964.

26. Fellows, B., "X-Band Dielectric Constant of Slip-Cast Fused Silica," The U. S. A. F. Avionics Laboratory-Georgia Institute of Technology Symposium On Electromagnetic Windows, AFAL-TR-68-07, Vol. I, June 1968.